

**MAXIMUM PENETRATION LEVEL OF SOLAR
PHOTOVOLTAIC TO THE ELECTRICAL GRID IN
PENINSULAR MALAYSIA**

CHUA KAE JUAN

**COLLEGE OF GRADUATE STUDIES
UNIVERSITI TENAGA NASIONAL**

2020

**MAXIMUM PENETRATION LEVEL OF SOLAR
PHOTOVOLTAIC TO THE ELECTRICAL GRID IN PENINSULAR
MALAYSIA**

CHUA KAE JUAN

**A Dissertation Submitted to the College of Graduate Studies,
Universiti Tenaga Nasional in Partial Fulfillment of the
Requirements for the Degree of**

Master of (Electrical Engineering)

FEBRUARY 2020

DECLARATION

I hereby declare that the thesis is my original work except for quotations and citations which have been duly acknowledged. I also declare that it has not been previously, and is not concurrently submitted for any other degree at Universiti Tenaga Nasional or at any other institutions. This thesis may be made available within the university library and may be photocopied and loaned to other libraries for the purpose of consultation.

CHUA KAE JUAN

Date :

ABSTRACT

Depletion of fossil fuel reserves and global warming are the two major challenges faced by the earth. Therefore, the need for sustainable source of energy such as renewable sources have become increasingly significant. In Malaysia, renewable energy (RE) was targeted to reach 30% by year 2030 in the Green Technology Master Plan, and the minister's aspiration was for RE to reach 50% of generation mix by year 2050 since Malaysia is located within the equatorial region. This dissertation analyses the impact of Large Scale Solar (LSS) to the generic grid of Peninsular Malaysia and determines the optimal penetration level of Large Scale Solar beyond which the grid stability is compromised. A complete process flow is proposed in the study starting from choosing the potential LSS power plant sites, selecting base case, developing study scenarios and conducting power system studies for scenarios with different solar penetration level. Load flow analysis is executed to study the impact of LSS to the transmission lines capacity, bus voltage and fault current level of the circuit breaker in the network. In addition, the impact of increased LSS penetration level during normal steady state condition as well as under disturbance conditions over timescales of a few seconds to 60 seconds have been analyzed. All the load flow and dynamic stability studies are studied by using Power System Simulator for Engineering (PSS/E) simulation software tool. The studies showed that the maximum penetration level of Large Scale Solar is 22% based on the system off-peak demand. The studies also showed that the Large Scale Solar is not detrimental to the grid in steady state and dynamic studies as long as it is within the maximum penetration limit. However, if the solar penetration is beyond the 22% maximum penetration limit, transmission grid will be unstable under system disturbance.

ACKNOWLEDGEMENT

First, I would like to express my appreciation to my project supervisor Prof. Ir. Dr. Vigna Kumaran A/L Ramachandaramurthy for giving me the opportunity to undertake the project that I am interested on and provide me the guidance and support to complete my project.

Next, I would like to thank my family for supporting me throughout my studies. The support and encouragement from my parents are very important for me to complete my project. Thank you for giving me the morale support and motivation to complete my dissertation.

Lastly, I would like to express my gratitude to my employer, Tenaga Nasional Berhad and my bosses for giving me the opportunity to present my project in CIGRE International Conference AORC Technical Meeting 2019 in Bali, Indonesia. It was a precious and valuable experience for me to present the paper in the international conference.

TABLE OF CONTENTS

	Page
DECLARATION	ii
ABSTRACT	iii
ACKNOWLEDGEMENT	iv
TABLE OF CONTENTS	v
LIST OF TABLES	viii
LIST OF FIGURES	x
LIST OF ABBREVIATIONS	xiv
LIST OF PUBLICATIONS	xv
CHAPTER 1 INTRODUCTION	1
1.1 Background	1
1.2 Project Overview	2
1.3 Problem Statement	3
1.4 Project Objectives	4
1.5 Scope of Research	4
1.6 Thesis Outline	4
CHAPTER 2 LITERATURE REVIEW	6
2.1 Introduction	6
2.2 Review of Related Research	6
2.3 Calculation of PV Penetration	8
2.4 Impact of High PV Penetration	8
2.5 Solution and Future Direction for High PV Penetration Challenges	12
2.6 Transmission System Reliability Standards (TSRS)	15
2.7 Summary of Chapter 2	19

CHAPTER 3	METHODOLOGY	20
3.1	Introduction	20
3.2	Overall Methodology	20
	Figure 3.1. Process Flow in Determining Maximum Solar Penetration Level.	22
3.3	Solar Penetration Formula	23
3.4	Power Flow Study and Analysis	24
	3.4.1 Power Flow Equation	25
3.5	Modelling of LSS for Power System Studies	26
3.6	Summary of Chapter 3	28
CHAPTER 4	RESULTS AND DISCUSSION	29
4.1	Introduction	29
4.2	Assumptions Used for the Case Study	30
4.3	Location of LSS Power Plant	31
	4.3.1 Solar Irradiance in Peninsular Malaysia	31
4.4	Analysis of Results for Base Case	39
	4.4.1 Overview of Base Case	39
	4.4.2 Base Case – Steady State Analysis	42
	4.4.3 Dynamic Analysis on Base Case	48
4.5	Scenario Development	55
	4.5.1 Scenario Studies – Steady State Analysis	56
	4.5.2 Scenario Studies – Dynamic Analysis	64
4.6	Discussion of Results	87
4.7	Summary of Chapter 4	89
CHAPTER 5	CONCLUSION AND RECOMMENDATIONS FOR FUTURE WORK	90
5.1	Introduction	90
5.2	Significant Contribution of project	91

5.3	Recommendation for Future Work	92
	REFERENCES	93
	APPENDICES	

LIST OF TABLES

Table 2.1	Six Classification of Challenges due to High PV Penetration.	10
Table 2.2	Solutions for High PV Penetration Challenges.	12
Table 2.3	Voltage Limits for Pre and Post-Disturbances for Planning Study.	15
Table 2.4	Short Circuit Ratings for Different System Voltage.	16
Table 2.5	Thermal Loading Limits of Transmission Equipment.	17
Table 2.6	Maximum Fault Clearance Times for Difference System Voltages.	17
Table 2.7	System Performance Requirements for Different Category Events.	18
Table 2.8	Frequency Range for Different System Conditions.	19
Table 3.1	Modules in Standard PV Dynamic Model.	28
Table 4.1	List of Identified 132kV Substations for LSS Connection in PSSE.	38
Table 4.2	List of Allocated States at Regions in Peninsular Malaysia.	40
Table 4.3	Percentage of Generation Mixed in the Base Case.	41
Table 4.4	Critical Fault Current Clearing Times for Base Case.	49
Table 4.5	Base Case - Impact of Losing 1000 MW Generating Unit.	51
Table 4.6	Base Case - Impact of Losing DC Perak to Central Tie-Lines.	53
Table 4.7	Base Case - Impact of Losing DC Southern to Central Tie-Lines.	54
Table 4.8	Base Case - Impact of Losing DC Perak to Northern Tie-Lines.	54
Table 4.9	Base Case - Impact of Losing 500 kV Northern Generator Substation.	55
Table 4.10	Base Case - Impact of Losing 500 kV Central Generator Substation.	55

Table 4.11	Base Case - Impact of Losing 500 kV Southern Generator Substation.	55
Table 4.12	Solar Penetration Level for Each Scenarios.	56
Table 4.13	Critical Fault Clearing Times for Base Case and Scenarios.	65
Table 4.14	Scenario A & B - Impact of Losing 1000 MW Generating Units.	69
Table 4.15	Scenario C - Impact of Losing 1000 MW Generating Units.	73
Table 4.16	Impact of Losing Double Circuit 500 kV Perak – Central Inter-Area Tie-Lines.	74
Table 4.17	Impact of Losing Double Circuit 275 kV Perak – Central Inter-Area Tie-Lines.	75
Table 4.18	Impact of Losing Double Circuit 500 kV Southern – Central Inter-Area Tie-Lines.	75
Table 4.19	Impact of Losing Double Circuit 275 kV Southern – Central Inter-Area Tie-Lines.	76
Table 4.20	Scenario A, B & C - Impact of Losing 500 kV Central Generator Substation.	77
Table 4.21	Scenario A, B & C - Impact of Losing 500 kV Southern Generator Substation.	81
Table 4.22	Scenario A, B & C - Impact of Losing 500 kV Perak Generator Substation.	85
Table 4.23	Summary of Steady State Results for Base Case and Scenarios A, B and C.	88
Table 4.24	Summary of Dynamic Results for Base Case and Scenarios A, B and C.	88

LIST OF FIGURES

Figure 3.1	Process Flow in Determining Maximum Solar Penetration Level.	22
Figure 3.2	Typical Weekday and Weekend Load Profile.	24
Figure 3.3	Layout of Grid Connected PV.	27
Figure 3.4	Connectivity Diagram for Solar PV Model.	28
Figure 4.1	Global Horizontal Irradiation (GHI) at Peninsular Malaysia.	32
Figure 4.2	Potential Power for Solar PV Plant in Peninsular Malaysia.	33
Figure 4.3	Proposed 42 number of LSS Locations at Peninsular Malaysia.	34
Figure 4.4	Proposed LSS Locations at Kedah & Perlis States.	35
Figure 4.5	Proposed LSS Locations at Perak State.	35
Figure 4.6	Proposed LSS Locations at Negeri Sembilan State.	36
Figure 4.7	Proposed LSS Locations at Malacca & Johor States.	36
Figure 4.8	Proposed LSS Locations at Pahang State.	37
Figure 4.9	Proposed LSS Locations at Kelantan & Terengganu States.	37
Figure 4.10	Total Generation and Load in the Base Case.	40
Figure 4.11	Inter-Area Power Flow in the Base Case.	41
Figure 4.12	Voltage Profile for 132 kV – 500 kV Northern Substation.	43
Figure 4.13	Voltage Profile for 132 kV – 500 kV Perak Substation.	43
Figure 4.14	Voltage Profile for 132 kV – 500 kV Central Substation.	44
Figure 4.15	Voltage Profile for 132 kV – 500 kV Southern Substation.	44
Figure 4.16	Voltage Profile for 132 kV – 500 kV Eastern Substation.	45

Figure 4.17	Fault Current for 132 kV Substations in Base Case.	46
Figure 4.18	Fault Current for 275 kV Substations in Base Case.	46
Figure 4.19	No Contingency Results for Base Case.	47
Figure 4.20	N-1 Contingency Results for Base Case.	47
Figure 4.21	Base Case – Machine Rotor Angle Under CFCT Test	49
Figure 4.22	Base Case Generator Rotor Angle During 60 Seconds No Fault.	50
Figure 4.23	Base Case (Loss of 1000 MW Generation) - System Frequency.	51
Figure 4.24	Base Case (Loss of 1000 MW Generation) – Rotor Angle.	51
Figure 4.25	Base Case (Loss of 1000 MW Generation) - System Voltage.	52
Figure 4.26	Northern Voltage Comparison for 132 kV - 500 kV Substations.	58
Figure 4.27	Perak Voltage Comparison for 132 kV - 500 kV Substations.	58
Figure 4.28	Central Voltage Comparison for 132 kV - 500 kV Substations.	59
Figure 4.29	Southern Voltage Comparison for 132 kV - 500 kV Substations.	59
Figure 4.30	Eastern Voltage Comparison for 132 kV - 500 kV Substations.	60
Figure 4.31	Comparison of Fault Current for 132 kV Substations between Base Case and Scenarios.	61
Figure 4.32	Comparison of Fault Current for 275 kV Substations between Base Case and Scenarios.	62
Figure 4.33	Branch / Transformer No Contingency Loading for Scenarios A, B & C.	62
Figure 4.34	Comparison of N-1 Contingency Loading for 132 kV Substation between Base Case and Scenarios.	63
Figure 4.35	Scenario A – 1000 MW Machine Rotor Angle During the Fault.	65

Figure 4.36	Scenario A – Generator Rotor Angle During 60 Seconds No Fault.	66
Figure 4.37	Scenario B – Generator Rotor Angle During 60 Seconds No Fault.	67
Figure 4.38	Scenario C – Generator Rotor Angle During 60 Seconds No Fault.	67
Figure 4.39	Scenario A – System Frequency during Loss of 1000 MW Generation.	70
Figure 4.40	Scenario B – System Frequency during Loss of 1000 MW Generation.	70
Figure 4.41	Scenario A – Rotor Angle during Loss of 1000 MW Generation.	71
Figure 4.42	Scenario B – Rotor Angle during Loss of 1000 MW Generation.	71
Figure 4.43	Scenario A – System Voltage during Loss of 1000 MW Generation.	72
Figure 4.44	Scenario B – System Voltage during Loss of 1000 MW Generation.	72
Figure 4.45	Scenario C – System Frequency during Loss of 1000 MW Generation.	73
Figure 4.46	Scenario A – System Frequency during Loss of 500 kW Central Generator Substation.	78
Figure 4.47	Scenario B – System Frequency during Loss of 500 kW Central Generator Substation.	78
Figure 4.48	Scenario A – Rotor Angle during Loss of 500 kW Central Generator Substation.	79
Figure 4.49	Scenario B – Rotor Angle during Loss of 500 kW Central Generator Substation.	79
Figure 4.50	Scenario A – System Voltage during Loss of 500 kW Central Generator Substation.	80

Figure 4.51	Scenario B – System Voltage during Loss of 500 kV Central Generator Substation.	80
Figure 4.52	Scenario A – System Frequency during Loss of 500 kV Southern Generator Substation.	82
Figure 4.53	Scenario B – System Frequency during Loss of 500 kV Southern Generator Substation.	82
Figure 4.54	Scenario A – Rotor Angle during Loss of 500 kV Southern Generator Substation.	83
Figure 4.55	Scenario B – Rotor Angle during Loss of 500 kV Southern Generator Substation.	83
Figure 4.56	Scenario A – System Voltage during Loss of 500 kV Southern Generator Substation.	84
Figure 4.57	Scenario B – System Voltage during Loss of 500 kV Southern Generator Substation.	84
Figure 4.58	Scenario A – System Frequency during Loss of 500 kV Perak Generator Substation.	86
Figure 4.59	Scenario A – Rotor during Loss of 500 kV Perak Generator Substation.	86
Figure 4.60	Scenario A – System Voltage during Loss of 500 kV Perak Generator Substation.	87

LIST OF ABBREVIATIONS

DC	Double Circuit
GHI	Global Horizontal Irradiation
MESTECC	Ministry of Energy, Science, Technology, Environment and Climate Change
LSS	Large Scale Solar – means any solar photovoltaic plant with minimum size of 30 MWac connected to the Transmission Network.
PSS/E	Power System Simulator for Engineering
PV	Photovoltaic
RE	Renewable Energy
SEDA	Sustainable Energy Development Authority
TSRS	Transmission System Reliability Standards

LIST OF PUBLICATIONS

1. Sim, S.F., T.Y. Ling, S. Lau, and M.Z. Jaafar, A novel computer-aided multivariate water quality index. *Environ Monit Assess*, 2015. 187(4): p. 181.
2. Yatim, N.N.M., Z.M. Zain, M.Z. Jaafar, Z. Md Yusof, A.R. Laili, M.H. Laili, and M.H. Hisham. Noninvasive glucose level determination using diffuse reflectance near infrared spectroscopy and chemometrics analysis based on in vitro sample and human skin. in *Systems, Process and Control (ICSPC), 2014 IEEE Conference on*. 2014.

CHAPTER 1

INTRODUCTION

1.1 Background

Depletion of fossil fuel reserves and global warming are the two major challenges faced by the earth. Reduction on fossil fuel dependency through switching to renewable energy (RE) can reduce the green-house gases emission and secure future energy [1]. Therefore, the need for renewable energies has become increasingly significant in the past decade, and has gained considerable interest of the Electricity Regulators and governments [2][3][4].

RE represents energy from an undepleted source such as wind and solar photovoltaic (PV) [1]. Wind and solar PV are gaining huge interest among all forms of energy resources. They are expected to be the main contributor for power generation in future power systems, and are expected to reach at least 27% RE in final energy consumption at European level by year 2030 [5].

In Malaysia, Sustainable Energy Development Authority (SEDA) is a statutory body that reports to the Ministry of Energy, Science, Technology, Environment & Climate Change (MESTECC). SEDA is the driver to enhance RE in power generation mix in Malaysia, thus propelling the nation's electricity sector towards enhanced electricity supply security and sustainable social-economic development [6].

According to Dr. Chen Wei Nee, Chief Corporate Officer of SEDA Malaysia, the energy mix target of 53% coal, 29% gas, 15% large hydro, and 3% RE were cited in the 11th Malaysia Plan (2016-2020) [6]. Following that, RE was targeted to reach 30% by year 2030 in the Green Technology Master Plan. Since Malaysia is located within the equatorial region, solar PV is preferred as compared to wind energy.

The high cost of solar PV panel has been the main hindrance to its expansion until a few years ago. However, in order to encourage the solar PV installations, SEDA Malaysia had amended the country policies and regulations, to provide support in terms

of incentive and tax exemption to the solar PV developer [6]. Also, with the recent innovations in solar PV panel research and development, the price of the solar PV panel is reducing tremendously, with about 80% over the last seven years [1]. Hence, solar PV has the commercial potential in Malaysia.

From the power system point of view, installing solar PV close to the load can reduce power flows from high voltage lines to low voltage loads and thus, help reduce the capacity loading of the transmission lines, cables and transformers. Subsequently, besides saving the environment, power utility can benefit by reducing the investment cost of new transmission lines and transformers.

Conversely, solar PV is an intermittent and unreliable source of energy due to its uncontrollable output power [6]. Besides, installation of huge amount of solar PV at the load level will cause reverse power flow from the load level towards the transmission system, and solar PV has limited contribution for reactive power generation [7]. Also, unlike the conventional thermal power plant, solar PV do not contribute to system electrical grid inertia as they are asynchronously integrated into the grid through inverter. Hence, solar PV cannot help in the inertia response during frequency control like conventional synchronous generators [8].

Besides, solar PV plant output generally depends on the weather condition. This will not be an issue if the solar PV plant capacity is less but when the plant capacity is large, such PV plant output variations will impact the grid [9]. Solar PV plant impacts to the power system are discussed in [10-15]. The large penetration of these intermittent energies in the power system will vary the power flow patterns, and consequently have steady state and dynamic impacts to the power system [16]. Therefore, it is essential to analyse the impact of increased solar PV penetration into the power system, which is presently being dominated by conventional generation.

1.2 Project Overview

This dissertation investigates the optimum penetration level of LSS into the electrical grid and the steady state and dynamic impact of high LSS penetration.

The LSS is aggregated and modelled at 132 kV transmission buses with increasing generation capacity in order to determine the maximum LSS penetration level that the network can take. Other than steady state analysis, the effect of transients on the generic Peninsular Malaysia network is studied by using Power System Simulator for Engineering (PSS/E) software tool.

1.3 Problem Statement

Solar PV generation is growing at a fast pace and is expected to reach 50% of global energy mix by year 2050 [9]. This makes us to believe that integrating solar PV into power system networks is not a difficult task. However, when solar PV penetration level increased, power utilities started to face new non-traditional issues primarily due to the intermittent nature of solar energy. For instance, fast moving clouds could result in rapid fluctuations in solar PV output power, causing the change in daily demand profile in ways that make the grid system operators nervous to deal with not only uncontrollable demand but also uncontrollable generation in the network [17].

Solar PV makes the power system even more complicated especially when the penetration level is high [18]. When the solar PV generation is high, a significant amount of conventional generation are replaced with solar PV. Hence, low level of rotational inertia is found in the power system, as solar PV does not provide any rotational inertia.

When the electrical grid is subjected to any disturbances during low level of rotational inertia, frequency dynamics tend to become faster and the traditional frequency control schemes available in the conventional generation become too slow to prevent large frequency deviations. The loss of rotational inertia lead to new frequency instability phenomena in high solar PV penetration system, causing the frequency and power system instability [8]. Therefore, it is imperative to know the limit of solar PV penetration in the electrical grid before the grid reaches the instability point.

1.4 Project Objectives

The objectives of the project are:

- I. To study the impact of Large Scale Solar (LSS) to the transmission grid of Peninsular Malaysia during normal steady state and under disturbance conditions by using PSS/E simulation software.
- II. To determine the maximum penetration level of Large Scale Solar (LSS) to the transmission grid in Peninsular Malaysia without compromising the frequency and power system stability.

1.5 Scope of Research

The studies is based on the Peninsular Malaysia electrical network. Only large scale solar PVs that are connected to the 132 kV transmission substations are considered in this study. In the Peninsular Malaysia electrical network, voltage levels of 132 kV, 275 kV and 500 kV are considered transmission level.

The study is focused on steady state and dynamic analysis by using Power System Simulator for Engineering (PSS/E) software tool. The maximum penetration level of solar is obtained when the penetration level of LSS is about to breach the stability limit, without the need for system reinforcement.

Daytime trough load case is used for the studies. This provides the worst-case scenario where the LSS penetration level is high. The study considers only one snapshot, which is the worst-case scenario. Thus, there is limitation in getting the accurate data as compared to the quasi-dynamic power flow study with half hourly schedules of a study year with multiple generation dispatch patterns.

1.6 Thesis Outline

This thesis comprises of five main chapters.

Chapter 2 discusses the power system study and related projects done by the previous researchers to have better understanding on the project objectives.

Chapter 3 discusses the methodology and approaches to conduct the research. Complete process flow is discussed in a detailed flow chart and power flow equations that used in steady state studies are explained in details. Besides, dynamic models of solar in PSS/E simulation software are also presented in this chapter.

Chapter 4 discusses the result and analysis of the study. Power flow and dynamic stability study results for Base Case and Scenario studies are discussed in this chapter. Base case result is used as reference for comparison with the scenario study results to study the impact of solar penetration to the Peninsular Malaysia network. At the end of this chapter, maximum LSS penetration level is determined.

Chapter 5 concludes the study results and proposes recommendation for future work.

CHAPTER 2

LITERATURE REVIEW

2.1 Introduction

This chapter discusses the steady state and dynamic impact of grid connected solar PV done by researchers. In addition, the comprehensive preview of Transmission System Reliability Standards (TSRS) adopted by Grid Division of Tenaga National Berhad (TNB) will be discussed in this chapter.

2.2 Review of Related Research

The installation of large scale solar and wind plants into the grid is no longer a new concern in most of the developed countries like United States, Germany and China. According to the International Energy Agency (IEA), China and United States have 20 utility-scale plants with over 100 MW capacities [4].

With more solar PV connected into the system, high solar PV penetration has attracted the attention of the global researchers. Among the studies, authors in [10] studied the impact of increased solar PV penetration on the static performance and transient stability of the transmission system in Western United State. The calculation of the PV penetration percentage in the study was based on the total available generation in the base case. Researchers from the National Renewable Energy Laboratory (NREL) calculated the PV penetration based on the system peak load.

Authors in [4] presented the impact of connecting large scale PV and wind power plants to the national grid of Jordan. The impact on voltage stability due to increasing penetration level of PV and wind power plants had also been analysed with the DIgSILENT simulation software. P-V curves had been developed in the study in order to determine the maximum RE generation that could be connected to the grid before reaching the voltage instability limit. The result also showed that by introducing voltage and reactive power control capability for the RE power plants, the maximum RE generation size could be doubled.

Researchers in [16] analysed the impact of different large-scale solar penetration levels to the transmission grid. The research considered the solar power plant converter employed with synchronous power controller that allowed the solar plant to provide frequency and voltage regulations. Small-signal and transient stability were studied and the results showed that with synchronous power controller, solar plant could provide positive impact to the system by limiting the frequency deviations and reducing the oscillation damping and stress to other conventional generators.

Studies that analysed the impact of PV penetration to the transmission grid was discussed in [20-22]. Authors in [20] studied the impact of dynamic behaviour of PV plants to the short-term voltage stability of the transmission system, and authors in [21] studied the impact of high PV penetration to the grid stability, voltage regulation, power quality, protection and power flows coordination, in which the penetration level is greater than 15% of the maximum daytime feeder demand. Authors in [22] presented the dynamic impact of different ambient conditions on PV array to the change in voltage, frequency and power in the weak system. Several other studies on the impact of high PV penetration to the system voltage, frequency and power are shown in [23] and [24].

Authors in [25] studied the impact of redispatch and displacement of generation in the high PV penetration system, by using regression techniques and Chebyshev's inequality methods. This allows the authors to calculate the dispatch and displacement ratios of conventional generation for optimal power flow and transient stability studies.

Unlike the aforementioned works, this dissertation explores the maximum penetration level of solar by investigating the power flow and dynamic impacts of different solar penetration level to the electrical grid of Peninsular Malaysia. Besides, location of the PV plants were determined based on the high irradiation points in Peninsular Malaysia and the assumptions for PV plant injection point are described in details. In order to determine the optimal penetration of the PV plant, the conventional generations were dispatched optimally according to the merit order of the plants.

2.3 Calculation of PV Penetration

Solar PV penetration percentages that was used in [19] was based on the following equation:

$$\text{PV Penetration (\%)} = \frac{\text{Total PV Generation (MW)}}{\text{System Peak Load (MW)}} \times 100\% \quad (\text{Equation 2.1})$$

The calculation for the PV penetration percentage was based on the system peak load [19]. Other possible method includes calculating the PV penetration based upon the total available generation in the system or by the amount of energy served [10]. However, this method was not considered in this study.

2.4 Impact of High PV Penetration

Various researchers defined different percentage values as high PV penetration. Authors of [34] recommended 20% of total generation as high PV penetration whereas authors in [35-36] are in the opinion that high PV penetration is up to 15% and 50% respectively. Since there is no literary standard stated the percentage of high PV penetration. Therefore, as a rule of thumb, [37-38] suggested that 15% as high PV penetration as the challenges of high PV penetration become noticeable when PV penetration reached 15%.

High solar PV penetration in the power system would cause steady state and dynamic impact to the system. In steady state study, impacts on power flow and voltage support are discussed whereas for dynamic study, most of the authors focus on the impacts of system inertia, frequency and voltage stability of the system.

In power flow study, the properties of Large Scale Solar (LSS) generation is just like the conventional generation in terms of providing active power and reactive power support to the system. However, Solar PV generation is still an intermittent and unreliable power source [6]. With solar generation plant-up at the load level, the existing conventional generation and power flow patterns in the system will start to change [16].

Solar output power is highly dependent on the weather condition. Therefore, bidirectional power flows are expected in the system with high solar penetration. For instance, during sunny day time, huge amount of solar energy is generating at the load level will cause reverse power flow from the load level into transmission system. However, when sunlight is not available, power flows from the transmission system to the load level.

Traditionally, electrical power were generated by thermal power plants, hydro plants, and fossil or nuclear fuels. These power plants were fully controllable in term of the output power dispatch and had rotating synchronous generators. With the plant's stored kinetic energy, rotational inertia feature was made available for the rotating synchronous machines [8]. The contribution of rotational inertia was critical to sustain frequency dynamics and stability

However, inverter-connected solar PV generation does not provide any inertia support to the system. When more and more solar PV were introduced into the system, a significant amount of conventional generation units were required to shut down and replaced by LSS plant [10]. At this moment of time, the power system will have a very low level of rotational inertia.

When rotational inertia in the system is critically low, frequency dynamics become faster causing the existing frequency control schemes of the conventional generation to react too slowly. Hence, they are unable to prevent the large system frequency deviations from happening. Low or loss of rotational inertia will speed up system frequency instability. At last, the system is unable to withstand any disturbances as the system is too weak and system stability could be lost at any moment [8].

The intermittent nature of the solar PV generation, bidirectional power flows of the distribution network and lacking of inertia support [39-41] in the system cause various challenges to the system with increasing PV penetration level.

Many researchers had done plenty of the studies to determine the impacts and challenges due to high PV penetration into the system. Among all the research works

from past decade until recently [42-56], all the challenges are summarized and categorized into six classification as shown in Table 2.1 depend on the areas of impact.

Table 2.1. Six Classification of Challenges due to High PV Penetration [42-56].

Classification	Challenges
Big Data	Astronomical increase in the volume of data which includes consumer energy utilization pattern data, data for managing, control and maintenance of devices, data from generation, transmission and distribution networks and operational data [42]. These data conforms to the seven big data characteristics as discussed in [42-46], which includes volume, velocity, variety, veracity, volatility, validity and value.
Communication	Massive data intrusion because of high PV penetration could affect the Quality of Service (impacted by latency and bandwidth). Therefore, it is a big challenge to achieve low latency (time delay in data transmission) and to have adequate bandwidth while maintaining adequate efficiency and reliability [47-48].
Cybersecurity	Deployment of communication infrastructures for large data transmission and acquisition across the network could create vulnerabilities for cyber-attacks to attack on the both measurement and control signals [49-53], which could lead to the grid stability problem.
Feeder Issues	With more solar generation, power can flow in bidirectional direction. However, most of the distribution systems were not designed to accommodate bidirectional flow of power, which could increase the potential of damage to the utility grid and affects the utility customers who served by the same distribution circuit [54].

Whereas, for large scale solar which located far from the urban city, long transmission lines are required to transmit the solar PV output to the load centre which result in high “line losses” as some of the energy are converter into heat and lost during the transportation.

Besides, high PV penetration system also experience power quality problems range from voltage and frequency to other areas such as harmonics. Harmonics issue is mainly come from power inverters used in converting generated DC voltage into AC, which cause equipment to not operate as intended [55].

Control

PV generation does not result in inertia power generation, which has proven to be a challenging problem with high PV penetration into the grid system. The lack of system inertia in the grid could result in high rate of change of frequency and will speed up system frequency instability when subjected to system disturbance [8].

Regulation Issues

Another big challenge to the grid system operator is solar intermittency. The amount of solar generation is highly depend on the weather condition. Both under-generation and over-generation could result in grid instability [56].

In conjunction with the solar intermittency, grid-connected voltage quality issues must also be considered. Just like other conventional power plant, solar plants must be able to ride through various level of voltage sags in order to continue operate without outage [55].

2.5 Solution and Future Direction for High PV Penetration Challenges

With increasing high PV penetration into the system, many of the challenges as mentioned earlier in Table 2.1 would become more aggravated. More advance and smart protection systems and integrated technology are required in high PV penetration system to improve system reliability and grid resilience. Author in [57] recommended solutions for the future challenges as tabulated in Table 2.2.

Table 2.2. Solutions for High PV Penetration Challenges [57].

Challenges	System With High PV Penetration Level	Recommended Solutions
Reverse Power Flow	Expect to increase.	Minimum load ensured on feeders. Minimum Import Relay (MIR), Reverse Power Flow Relay (RPFR), Smart Inverter + Distribution Supervisory Control and Data Acquisition (SI+D-SCADA), Advanced Metering Infrastructure (AMI).
Voltage Instability Issues	Expect to increase.	Smart Transformers (ST), Dynamic and Composite Energy Storage System (DCESS), On Load Tap Changer (OLTC), Static Compensation (STATCOM), SI+D-SCADA with Fault Ride Through (FRT), Geographic Information System (GS) with PV Fleet management.

Complexity in Protection Coordination	Increase bidirectional flow of current and fault current levels, line to ground voltage increase due to more single phase prosumers, possible desensitization the substation relays, unwanted blowing of fuses, mal-operation of auto-reclose and bus section.	Advance short circuit analysis with high PV penetration, Smart Inverter (SI) with fault current monitoring and control capabilities Advanced Relay Communication and Protection Coordination (ARCPC).
Power Factor Problem	Expect to increase.	Use of SI with dynamic reactive power control for both utilities and prosumers, SI+D-SCARA, Optimal Energy Routing (OER).
Harmonics	Expect to increase.	SI+DLHC capabilities and use of STATCOMs.
Frequency Instability	Expect to increase.	GS with PV aggregation for utility scale PV system, SI+FRT, OER.
Feeder Losses	Possible to increase	Robust optimal PV placement algorithms, OER on the distribution losses.
Thermal Limit of the Grid	Expect to increase.	Optimal placement of utility scale and small scale aggregated PV system.
Security of Supply	Threatened.	Accurate estimation methods of prediction (of security of supply) should include future

market analysis consideration of the intermittent nature of PV system as well as the development of other dispatchable energy sources.

<p>Communication within Distributed Energy Resources (DER) and Substation, Cybersecurity</p>	<p>Reliable and well defined communication and control protocols needed.</p>	<p>Robust IEEE 2030 standards and adoption by all PV systems. Fast computing and communication architecture.</p>
<p>Dynamic Modeling of the High Penetration PV</p>	<p>System modelling with PHEVs, and proliferation of prosumers would be required. Energy routing modelling for IoT enabled TE would be required. More detailed studies on solar eclipse impacts would be needed.</p>	<p>Dynamic models PV systems should be developed for Geographic Information system (GIS)-based Distribution management System (DMS) and GIS-based Energy Management Systems (EMS) for remote monitoring and control.</p>
<p>Forecasting</p>	<p>Accuracy will be key to adequate planning, unit commitment and dispatch.</p>	<p>Hybrid-forecasting (nowcasting + forecasting), more accurate prediction models using multiple forecasting methods.</p>
<p>Dispatch and</p>	<p>Increase on PV penetration in transactive environment will require the implementation of</p>	<p>Optimal Smart Inverter Dispatch (OSID). Optimal set point for storage systems.</p>

Scheduling Problem	optimal power flow and optimal dispatch with high PV penetration mandatory.	Mitigation techniques for forecast and communication errors in OSID.
--------------------	---	--

2.6 Transmission System Reliability Standards (TSRS)

Transmission System Reliability Standards (TSRS) in [26] stated the general technical requirements that governing the planning and operation criteria in the transmission system. Besides, all the generators that are planned to be connected to the transmission system will also be required to comply with the TSRS requirements. The TSRS was also reflected in the Grid Code for Peninsular Malaysia [27].

The standards described in TSRS are divided into two, which are steady state and transient dynamic performance criteria. For steady state study, voltage level, short circuit and thermal loading limits are the main elements for the study. Whereas, for transient dynamic study, fault clearing times, frequency and stability limits are important to be determined.

A) Voltage

The voltage limits for pre-disturbance and post-disturbance in planning study are shown in Table 2.3. Pre-disturbance means during normal operation and all the elements in the power system remain intact. Whereas, post-disturbance is when fault is cleared and the transmission element may be lost from the system after the fault is cleared.

Table 2.3. Voltage Limits for Pre and Post-Disturbances for Planning Study [26].

Nominal Voltages	Pre-Disturbance		Post-Disturbance	
	Maximum	Minimum	Maximum	Minimum
500 kV	1.05 p.u	1.00 pu	1.05 p.u	0.95 pu
275 kV	1.05 p.u	1.00 pu	1.05 p.u	0.90 pu
132 kV	1.05 p.u	1.00 pu	1.05 p.u	0.95 pu
< 132 kV	1.05 p.u	1.00 pu	1.05 p.u	1.00 pu

Table 2.3 shows that the pre-disturbance maximum and minimum voltage limits for all the voltage levels are within the range of 1.00 pu – 1.05 pu. Whereas for post-disturbance 132 kV voltage levels, minimum of 0.95 pu is required to be achieved.

B) Short-Circuit Limits

The maximum three-phase symmetrical fault and single-phase asymmetrical fault should not exceed the short circuit ratings of the switching equipment, in order to keep the safety of the equipment and people at site. The standards for circuit breaker short circuit ratings is shown in Table 2.4.

Table 2.4. Short Circuit Ratings for Different System Voltage [26].

System Voltage	Short Circuit Rating of Circuit Breaker
500 kV	50 kA, 1 second
275 kV	40 kA, 3 seconds
132 kV	31.5 kA, 3 seconds
33 kV	25 kA, 3 seconds

Short circuit ratings in Table 2.4 were just a guidelines for new substation as most of the old circuit breakers were not up to the standard short circuit ratings in Table 2.4. Therefore, when doing the studies, it is important to know the actual short circuit rating of the switching equipment so that the maximum three-phase or single-phase fault currents do not exceed the actual short circuit rating of the switching equipment that available at site.

C) Thermal loading Limits

The thermal loading limits of transmission equipment that used for the studies were showed in Table 2.5. In the studies, the thermal loading for all the transmission equipment during no contingency and N-1 contingency should not exceed 100% loading.

Table 2.5. Thermal Loading Limits of Transmission Equipment [26].

Category	Contingency Elements	Thermal Loading Limits
No Contingency	All facilities in service	No thermal overloading is allowed
N-1 Contingency	Loss of a single element such as generator, transmission circuit, or transformer	No thermal overloading is allowed

D) Fault Clearing Times

Fault clearance times are the total times that required for the protection equipment operates to clear the fault and disconnect the faulted item from the system. Maximum fault clearance times are expecting more than the time required by Main Protection equipment to operate.

Usually for 132 kV system, 150 ms fault clearance times are using for the studies, and for 500 kV and 275 kV are 100 ms. Table 2.6 showed the maximum fault clearing times for 132 kV to 500 kV system.

Table 2.6. Maximum Fault Clearance Times for Difference System Voltages [26].

System Voltage (kV)	Fault Location	Fault Clearance Time (ms)
500 & 275	Substation / Lines / Cables	100
132	Substation / Lines / Cables	150

E) System Performance Requirements

Table 2.7 summarised the four categories of contingencies and the expected performance for each categories. All the categories will be tested in the transient and dynamic stability studies.

Table 2.7. System Performance Requirements for Different Category Events [26].

Category	Contingencies	System Limits or Impacts		
		System Stable	Load Loss	Cascading Outages
A				
No Contingencies	All facilities in service	Yes	No	No
B				
Loss of a Single Element	Three-phase or single-phase fault with normal clearing times resulting in the loss of a single generator / transmission circuit / transformer	Yes	No	No
C				
Loss of two elements	Three-phase or single-phase fault with normal clearing times resulting in the loss of two generators / transmission circuits / transformers.	Yes	Planned/ Controlled	No
D				
Loss of two or more elements or Cascading out of service	Three-phase fault with delayed clearing or with normal clearing resulting in the loss of a substation / all generating units at a station / tower with three or more circuits.	Yes	Yes	Yes

F) Frequency Limits

During normal operations, the system frequency should maintain within $\pm 1\%$ deviation from the nominal frequency of 50 Hz, which is between 49.5 Hz to 50.5 Hz. However,

for exceptional circumstances, the system frequency could reach 47 Hz to 52 Hz. The detailed of frequency limits are listed in Table 2.8.

Table 2.8. Frequency Range for Different System Conditions [26].

System Conditions	Frequency Range
Continuous Operation	47.5 – 52.0 Hz
Operation for at least 10 seconds is required for Frequency below 47.5 Hz	47.0 – 47.5 Hz

G) Stability Limits

To maintain the system stability, the relative rotor angle between any of the two generating units should not exceed 180 degrees at all the times. Other than that, the Damping Ratio of power, angle or voltage oscillation following any disturbance should more than 5%.

2.7 Summary of Chapter 2

The previous work done by the global researcher as discussed above are referred and used as the basic in this study to determine the optimal LSS penetration level. Besides, the standards and criteria listed in the Transmission System Reliability Standards (TSRS) is used as the guidelines to analyse the impact of high LSS penetration level into the generic electric grid in Peninsular Malaysia.

Taking into consideration that the various challenges can be arise due to high PV penetration as discussed earlier in Table 2.1, where the impact for high PV penetration is not only limited to the system stability, it also expanded up to the communication and cyber-security area of interest. Nevertheless, this dissertation only covers impact of high PV penetration to system stability by determined the impact at different LSS penetration level and to determine the maximum LSS penetration level that the system can withstand before the system goes into unstable zone of operation.

CHAPTER 3

METHODOLOGY

3.1 Introduction

In this chapter, the method that helps to acquire the maximum solar penetration level in this study are discussed. Besides, modelling of LSS generation and the electrical grid in PSS/E simulation software are also discussed in this chapter.

3.2 Overall Methodology

The methodology to determine the maximum solar penetration level requires the following steps: a) Determining the LSS plants location and injection nodes b) Setting up the base case c) Determining studies scenarios, d) Comprehensive steady state and dynamic stability studies with PSS/E Simulation software. The complete process flow that describes the methodology used in this study is shown in Figure 3.1.

The generic electrical grid of Peninsular Malaysia is used as the study case for this research. From the study case, the 275 kV and 500 kV networks represent the backbone in the system. The LSS generation is connected only to 132 kV substation as shown in Figure 3.1.

Based on the geographical location of Peninsular Malaysia, the generic grid is divided into five main regions, which are Northern, Perak, Central, Southern and Eastern. Thus, LSS plant up location and 132 kV injection substation will be categorised amongst of these five main regions.

The selection for LSS plants up location in the Peninsular Malaysia is referred to the solar irradiance profile from Solargis database to determine the feasible location to plant up LSS plants. Next, 132 kV substations around the identified feasible locations are listed down to connect the LSS plants.

Selection of Base Case for the study is also important. For high LSS penetration case, the worst-case condition which is the low load condition usually occurs during

daytime, typically on weekends at 12pm. If the study case with high LSS penetration level can remain stable in the worst condition, the identified percentage of the LSS penetration level will be used as the final result in this study. Therefore, the Base Case is selected as daytime with low load condition.

The steady state and dynamic stability studies on the Base Case are carried out by using PSS/E simulation software. The steady state study is focused on the steady state voltage, fault level, no contingency and N-1 contingency. For dynamic stability study, the focus will be on maximum fault clearing times, and Categories A, B, C and D. The definition for Categories A, B, C and D are summarized in Table 2.5.

LSS penetration levels of 22%, 23% and 30% based on system off-peak demand are applied to the Base Case, with the main objectives to determine the maximum LSS penetration level and to study the impacts of high LSS penetration into the grid. The studies were first performed for all possible penetration level and 22% was identified as the maximum penetration level. Whereas, 23% and 30% LSS penetration level are for the purpose of demonstrating the impact of high LSS penetration level when the LSS penetration exceeded the maximum penetration limit.

Steady state and dynamic stability studies are performed on Scenario A, B and C, where Scenario A is 22% LSS penetration level, Scenario B is 23% and Scenario C is 30% LSS penetration level. The steady state and dynamic impacts in all the scenarios are tabulated and compared with the Base Case. Scenario which passes in the steady state and dynamic stability analysis without any violation will be considered as the maximum solar penetration level. Else, the process cycle in Figure 3.1 is repeated until the maximum solar penetration level is obtained.

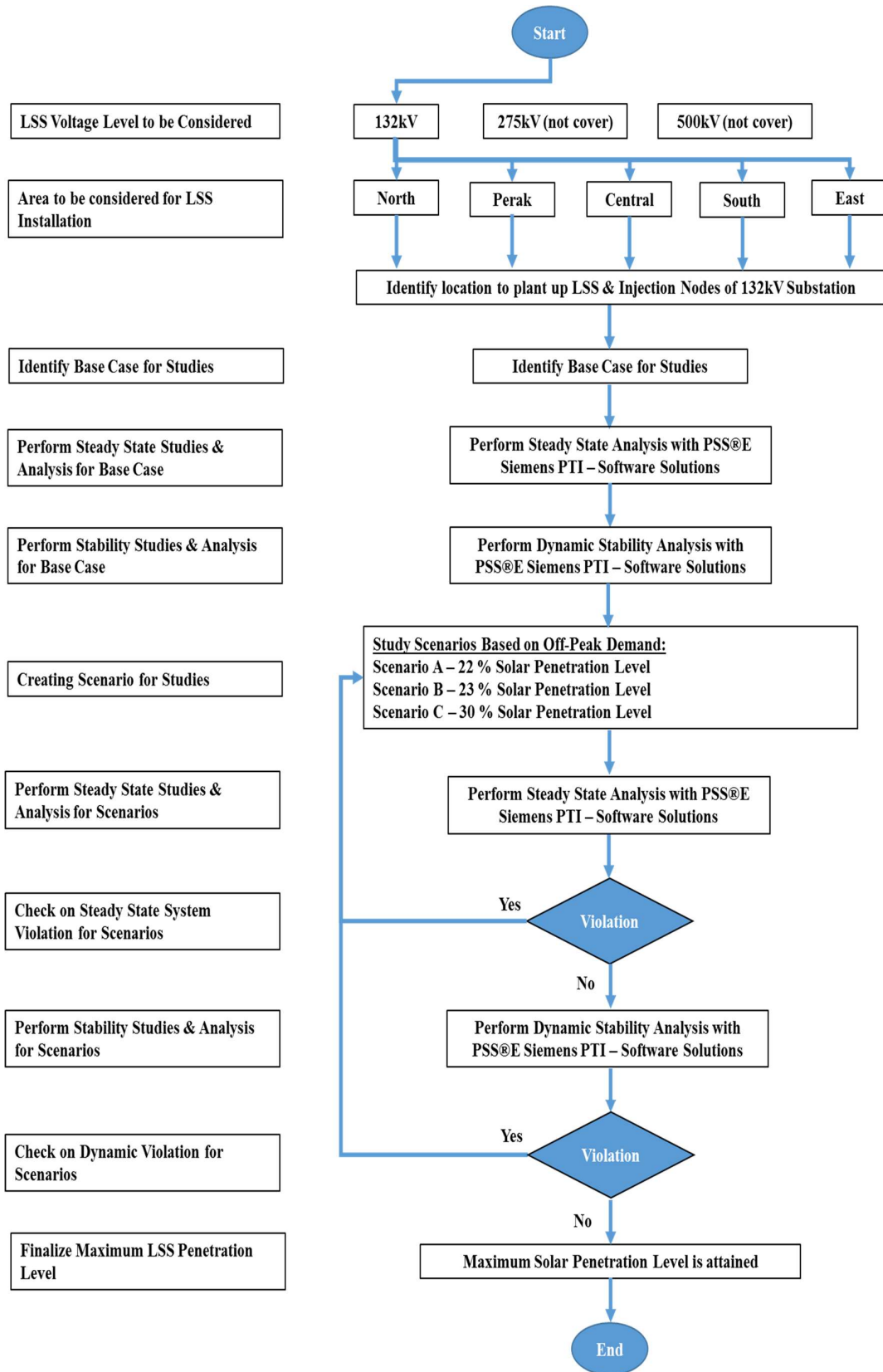


Figure 3.1. Process Flow in Determining Maximum Solar Penetration Level.

3.3 Solar Penetration Formula

According to the authors in [19], percentage of LSS penetration is based on system peak load, where the total LSS generation (MW) was divided by the system peak load (MW) as shown in Equation 3.1. System peak load in Equation 3.1 is referred to the highest load demand during weekday, which is usually happened in the evening.

$$LSS\ Penetration_{Peak\ Load}\ (%) = \frac{Total\ LSS\ Generation\ (MW)}{System\ Peak\ Load\ (MW)} \times 100\% \quad (3.1)$$

However, this study takes the consideration that the daytime low load is the worst-case condition. Therefore, the system peak load is not suitable to be adopted in this study. Hence, for the purpose of this study, LSS penetration level is developed based on the system off peak load as showed in Equation 3.2, by replacing the system peak load in Equation 3.1 to system off peak load value. System off peak load is referred to the highest load demand that happens during weekend noon.

$$LSS\ Penetration_{Off\ Peak\ Load}\ (%) = \frac{Total\ LSS\ Generation\ (MW)}{System\ Off\ Peak\ Load\ (MW)} \times 100\% \quad (3.2)$$

Equation 3.2 will be used throughout this study by taking the Total LSS Generation (MW) divided by System Off Peak Load (MW). Alternatively, the reverse of this formula as shown in Equation 3.3 is used to calculate Total LSS generation (MW) for each scenarios by considering the proposed LSS penetration level. By identifying the desired percentage of LSS penetration level, the amount of total LSS generation to be planted up in the study cases can be calculated through Equation 3.3.

$$Total\ LSS\ Generation\ (MW) = \frac{LSS\ Penetration_{off\ peak\ load}\ (%) \times System_{off\ peak\ load}\ (MW)}{100\%} \quad (3.3)$$

Figure 3.2 shows the typical weekday and weekend load profile of Peninsular Malaysia. The load profile is extracted from Tenaga Nasional Berhad (TNB) metering. From the load profile in Figure 3.2, weekday highest system demand occurs at 2.30 pm, which is around 18,566 MW. Whereas, weekend highest system demand occurs at 12 pm noon, which is around 12,996 MW, is 70% of the weekday demand. Therefore, assumption is made by considered system off peak load as 70% of system peak load.

By using Equation 3.4, system peak load (MW) can be obtained from the system off peak load (MW), by divided the off peak load with the factor of 0.7.

$$\text{System Peak Load (MW)} = \frac{\text{System Off Peak Load (MW)}}{0.7} \quad (3.4)$$

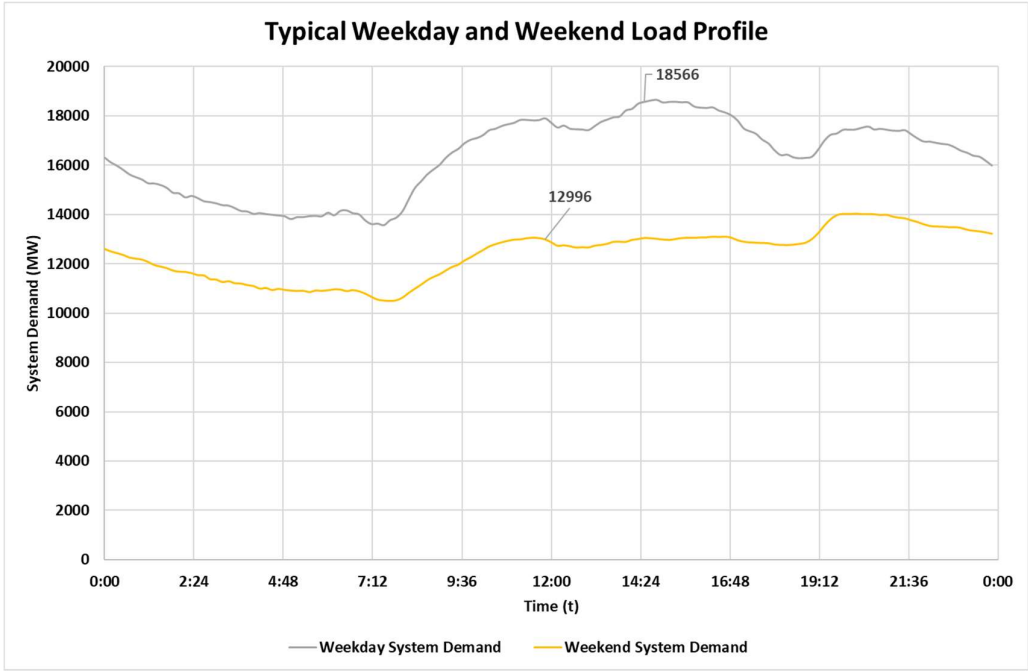


Figure 3.2. Typical Weekday and Weekend Load Profile.

3.4 Power Flow Study and Analysis

Power flow study, which is also known as load flows or steady state analysis, are important to determine the electrical grid conditions under the steady state and contingencies condition. This will enable the authors to understand the behaviour of the grid particularly on the steady state voltage, fault level and thermal loading of the transmission equipment.

In this study, power flow analysis is carried out to study the steady state impacts of the LSS generation to the generic grid of Peninsular Malaysia. Power flow equation is always nonlinear. It is therefore solved with the iterative methods such as Gauss-Seidel and Newton Raphson methods.

3.4.1 Power Flow Equation

During power flow studies, the values for voltage magnitude $|V|$, phase angle δ , real power P, and reactive power Q for each buses are determined. According to Hadi Saadat in [29], the network buses can be classified into slack bus, load buses and regulated buses. The same network buses are also applied in PSS/E simulation software [28].

i. Slack Bus

Swing bus in PSS/E is known as slack bus and it helps to make up the unbalance power between the load and generation in the power flow simulation. Generally, only one slack bus is available in a system and the bus type code for the swing bus is 3 – Swing Bus in PSS/E.

ii. Load Bus

Load Bus is also known as P-Q bus. There can be more than one load bus in a network. The bus type code for the load bus is 1 – Non-Generator Bus in PSS/E.

iii. Regulated Bus

Regulated bus is the generator bus or the voltage controlled bus. Just like the load bus, more than one generator can be found in a network. The bus type code for the load bus is 2 – Generator Bus in PSS/E.

According to Kirchhoff Current Law (KCL), current that enters a particular junction is equal to the current that leaving the same junction. In PSS/E, current at a particular bus, i is determined via KCL as shown in Equation 3.5 [29]. The system network impedances are converted to per unit admittances on common MVA base to calculate the power flow equation.

$$I_i = V_i \sum_{j=0}^n Y_{ij} - \sum_{j=1}^n y_{ij} V_j \quad j \neq i \quad (3.5)$$

where,

y_{ij} = Admittance of line connecting Bus i and Bus j

Understand that $P = VI$, Equation 3.6 is developed. Next, from Equation 3.7, current at bus i can be determined from the known active power, reactive power and voltage values at bus i [29].

$$P_i + jQ_i = V_i I_i^* \quad (3.6)$$

$$I_i = \frac{P_i - jQ_i}{V_i^*} \quad (3.7)$$

By substituting Equation 3.7 into Equation 3.5, an algebraic nonlinear equation as shown in Equation 3.8 is developed and can be solved iteratively by using Gauss-Seidel or Newton-Raphson method [29].

$$\frac{P_i - jQ_i}{V_i^*} = V_i \sum_{j=0}^n y_{ij} - \sum_{j=1}^n y_{ij} V_j \quad j \neq i \quad (3.8)$$

After obtaining the iterative solution for the bus voltages, the line current I_{ij} can be determined by using Equation 3.9 [29], where I_l is the current flowing in the line between bus i and bus j , I_{i0} is current flowing from bus i to ground and y_{i0} is the admittance in between bus i and ground.

$$I_{ij} = I_l + I_{i0} = y_{ij}(V_i - V_j) + y_{i0}V_i \quad (3.9)$$

3.5 Modelling of LSS for Power System Studies

Solar PV generation converts solar energy from the sun directly from solar radiant into a direct current (d.c) power. Power is generated by the solar cells, where the solar cell connectivity will give influence on the voltage and current output. For instance, solar cells connect in series will generate high voltage while solar cells connect in parallel will generate high current output [58].

Solar PV array consists of modules that connect in series-parallel arrangement to generate higher voltage, current and power output [58]. Figure 3.3 shows the arrangement of solar PV array which connects directly to the grid via d.c to alternating current (a.c) inverter, to convert d.c current from solar PV array to a.c and supply into the grid.

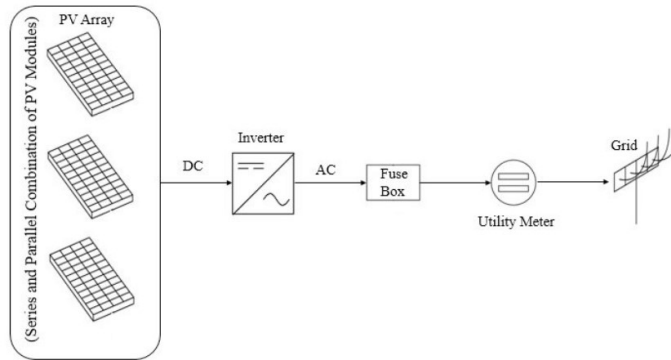


Figure 3.3. Layout of Grid Connected PV.

In PSS/E power flow case, LSS is modelled just like the other conventional generators, as regulated bus with bus type code 2 – Generator Bus [29]. The properties of LSS generator in steady state analysis is therefore similar with the conventional generator where they are capable of providing active power and reactive power according to the maximum and minimum active power and reactive power limits set in the PSS/E power flow case [10].

Reactive power output in steady state studies can be controlled by adjusting generator remote bus voltage. However, source reactance of LSS generator, X_{source} is set to 99999 [29], which is very large to make the rotor angle of LSS generator stable in dynamic simulation studies.

On the other hand, for PSS/E dynamic simulation study case, dynamic data of generators are prepared for dynamic simulation study. However, dynamic data of LSS is modelled differently from the conventional generators. With reference to PSS/E 32 Program Application Guide Volume 2 in [29], LSS generator is modelled as PSS/E standard PV dynamic model to simulate performance of solar PV employing generator connected to the grid with the power converter.

Standard LSS dynamic model will only provide fixed active power output to the system with fixed solar irradiance disregard of system frequency variation, but will provide reactive power support depend on the system voltage variation during dynamic stability studies.

In dynamic stability studies, the standard PV dynamic model comprises of the modules as shown in Table 3.1 while Figure 3.4 shows the interaction between the irradiation module, panel module and converter models.

Table 3.1. Modules in Standard PV Dynamic Model [29].

Model	Modules
PVGU	Generator / Converter Module
PVEU	Electrical Control Module
PANEL	Mechanical Module
IRRAD	Pitch Module

Solar PV dynamic models are designed conventionally as follows: generic PV modules with generator / converter module as PVGU, electrical control module as PVEU, mechanical module as PANEL, and pitch module as IRRAD. PVGU helps to calculate the injection current based on the active and reactive power commands from PVEU [29]. Detailed dynamic data of standard PV model is shown in Appendix A to Appendix D.

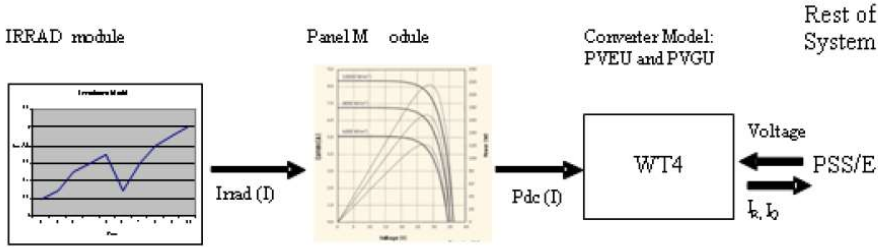


Figure 3.4. Connectivity Diagram for Solar PV Model [29].

3.6 Summary of Chapter 3

The methodology discussed in this chapter will provide the guidance to obtain the results in Chapter 4. Therefore, it is important to understand the overall process flow as discussed in paragraph 3.2 and to master the modelling of the solar dynamic models in the simulation software that is used for the simulation study. Besides, choosing the suitable LSS penetration formula to be adopted in the study is also important to help us identify the suitable LSS penetration level.

CHAPTER 4

RESULTS AND DISCUSSION

4.1 Introduction

At the end of this chapter, the maximum penetration level of LSS plant into the transmission grid of Peninsular Malaysia will be determined based on the ability of the transmission network in absorbing the maximum solar power without causing system instability. The impact of increasing LSS penetration into transmission grid will also be discussed in detailed in this chapter.

Identification of the assumptions on the LSS plant for connection to the transmission grid of Peninsular Malaysia is one of the key aspects that should not be overlook. The assumptions are explained in section 4.2 and will be used as the reference for the studies to determine the maximum LSS penetration level that the system is capable of managing.

The location of LSS plant connected to the transmission grid of Peninsular Malaysia is identified based on the geographical area, land availability, solar irradiance level, and substation configuration. The outcome will be used as the inputs to connect the proposed LSS plant to the identified substation in PSS/E software for the simulation studies.

Next, the selected network is analysed to understand the network condition and limitation during steady state and dynamic studies for benchmarking purposes. Then, the LSS plant will be connected to the identified substation for the steady state and dynamic studies.

Subsequently, study will be carried out at different solar penetration level to study the impact of increasing solar power plant generation in the system. The transmission grid condition will be monitored continuously for different solar penetration level. Lastly, maximum solar penetration level in the transmission network will be determined from

the maximum solar generation that the system can absorb while remain in stable condition.

4.2 Assumptions Used for the Case Study

The following are the assumptions adopted for the study.

- i. Referring to the Guidelines on Large Scale Solar Photovoltaic Plant for Connection to Electricity Network in [59], LSS which connects to Transmission network must generate more than 30 MW_{ac}. Therefore, Large Scale Solar (LSS) power plant, which generates power greater than 30 MW_{ac} is considered in the study.
- ii. LSS plants are installed at high solar irradiance location and rural area. Besides, the LSS plants shall be located near to the 132 kV transmission substations, which have double busbar configuration.
- iii. LSS connectivity to the transmission grid is through direct connection to the 132 kV transmission substation.
- iv. During daytime low load, with high solar irradiance and low system load, less conventional generators are operated and caused system rotational inertia low. In the event of system disturbance, the impact will be severe in low system inertia study case. Hence, Daytime Off-Peak study case is considered as the worst-case scenario and therefore will be used as the study case.
- v. Referring to the typical weekday and weekend load profile of Peninsular Malaysia in Figure 3.2, weekend system demand is around 70 percent of weekday system demand. Since off-peak usually happens during weekend while peak usually happens during weekday. Hence, assumption is made by considered Daytime Off-Peak load as 70 percent of the system Peak load.
- vi. LSS Penetration Level is based upon the system Peak load.
- vii. Spinning reserve for dynamic study is set to 1200 MW.
- viii. All the simulation results for voltage level, short circuit and thermal loading limits in steady state study, and fault clearing time, frequency and stability limits in transient dynamic study must fulfill the requirements stated in Transmission System Reliability Standard (TSRS), which had been discussed earlier in Chapter 2.6.

4.3 Location of LSS Power Plant

One of the difficult task is to determine the location of LSS power plant and the connection point to the identified 132 kV transmission substation. The location is imperative as it determines the solar irradiance.

4.3.1 Solar Irradiance in Peninsular Malaysia

Solargis database is one of the free solar irradiance database websites that can be used as the standard reference to identify LSS plants up location. Since the database website is free, solar irradiation and potential power output data are provided by the database website up to Year 2015, which is not the recent data.

For the purpose of determine the potential LSS plants up location, solar irradiance profile for Peninsular Malaysia which obtained from Solargis database is referred and is shown in Figure 4.1. Figure 4.1 shows that the red colour areas in Peninsular Malaysia are having the high GHI of more than 1899 kWh/m² per annum. Hence, the red colour areas, which located on the Northern side of Peninsular Malaysia, are the best location to install LSS PV plants.

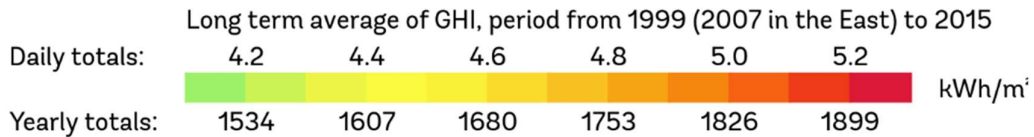


Figure 4.1. Global Horizontal Irradiation (GHI) at Peninsular Malaysia.

Apart from the Global Horizontal Irradiation (GHI) map, Solargis database also provides the potential power map for Solar PV plant in Peninsular Malaysia as shown in Figure 4.2. With the high GHI as shown in Figure 4.1, the installed solar PV plant in the high irradiation location will generate high power. Figure 4.2 shows the potential power generation for solar PV installed at different GHI in Peninsular Malaysia.

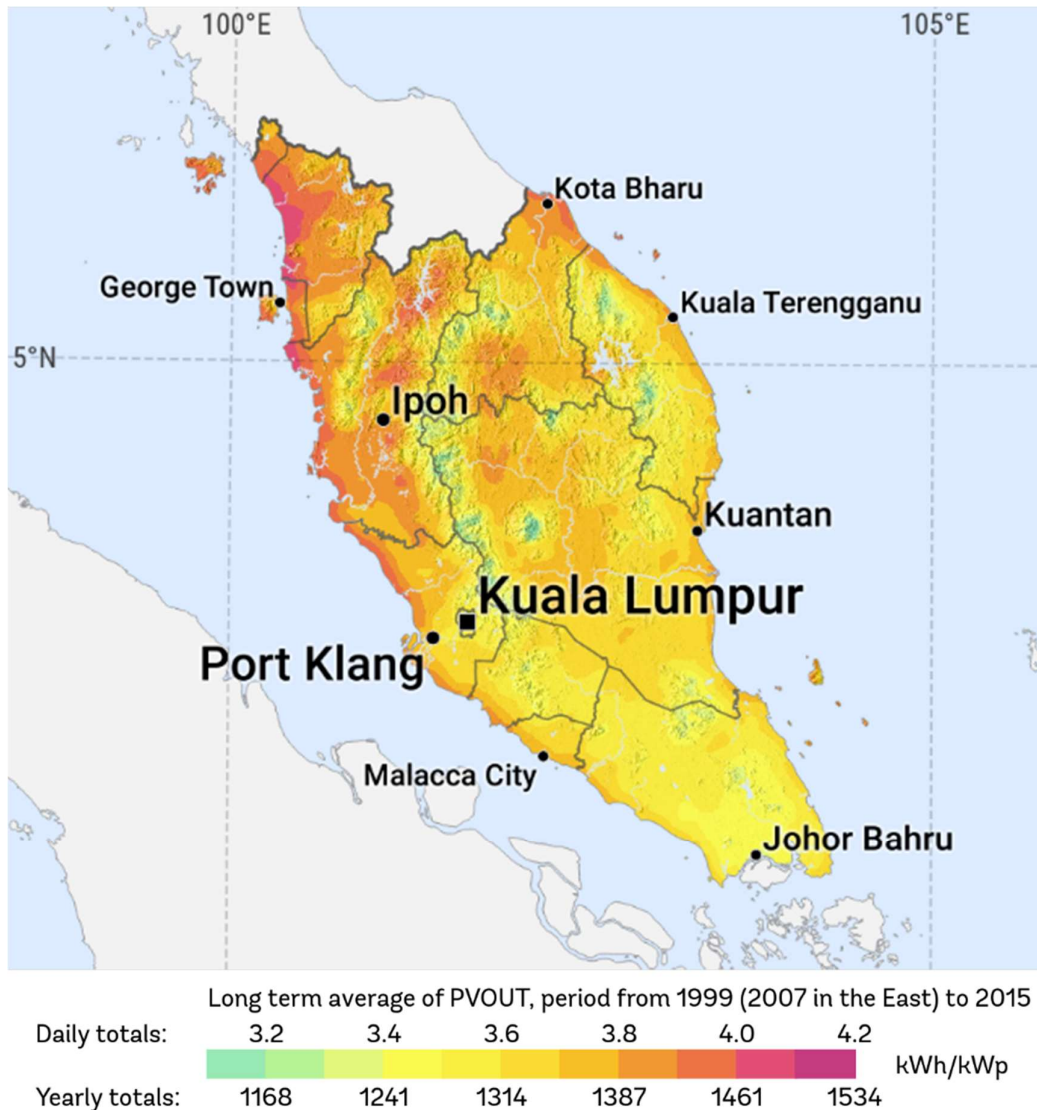


Figure 4.2. Potential Power for Solar PV Plant in Peninsular Malaysia.

With reference to the GHI map in Figure 4.1 and after filtering all the 132 kV transmission substation to obtain the double busbar substation, a total of 42 locations were proposed for the installation of LSS power plants in Peninsular Malaysia. The location of the 42 sites for solar PV installation is shown in Figure 4.3.



Figure 4.3. Proposed 42 number of LSS Locations at Peninsular Malaysia.

Figure 4.3 shows the proposed 42 number of LSS plants up locations which located at the high solar irradiance area and rural area. Besides that, these 42 LSS locations are near to the identified 132 kV transmission substations with double busbar configuration. Therefore, these 42 number of LSS power plant locations will be used in the simulation studies. Figure 4.4 to Figure 4.9 show the detailed plant up of these 42 number of LSS locations in difference states of Peninsular Malaysia.

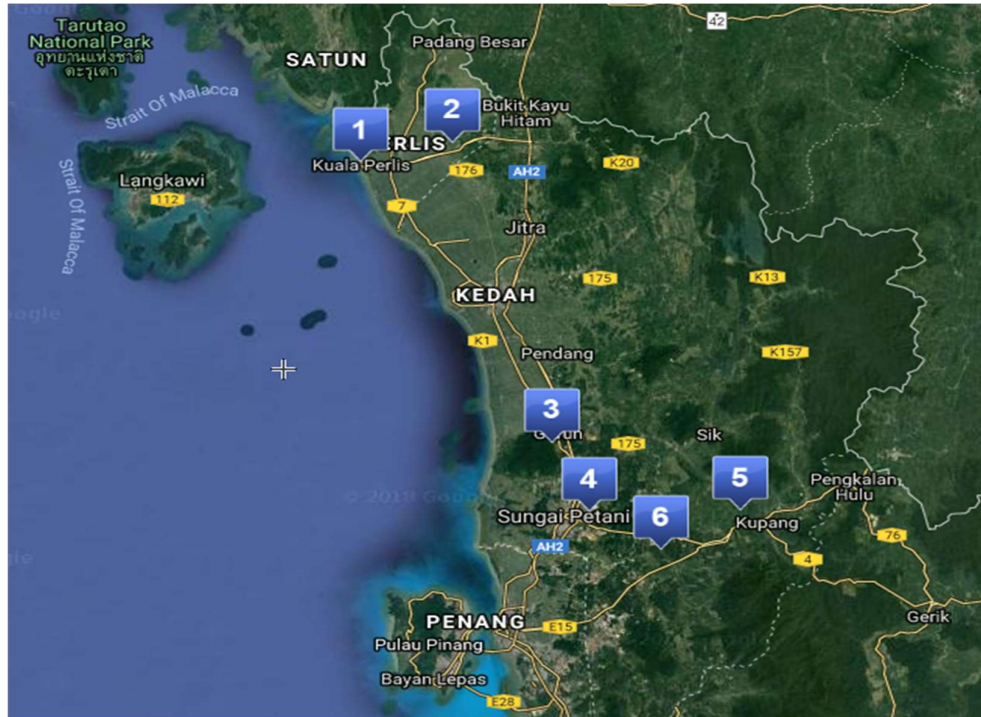


Figure 4.4. Proposed LSS Locations at Kedah & Perlis States.

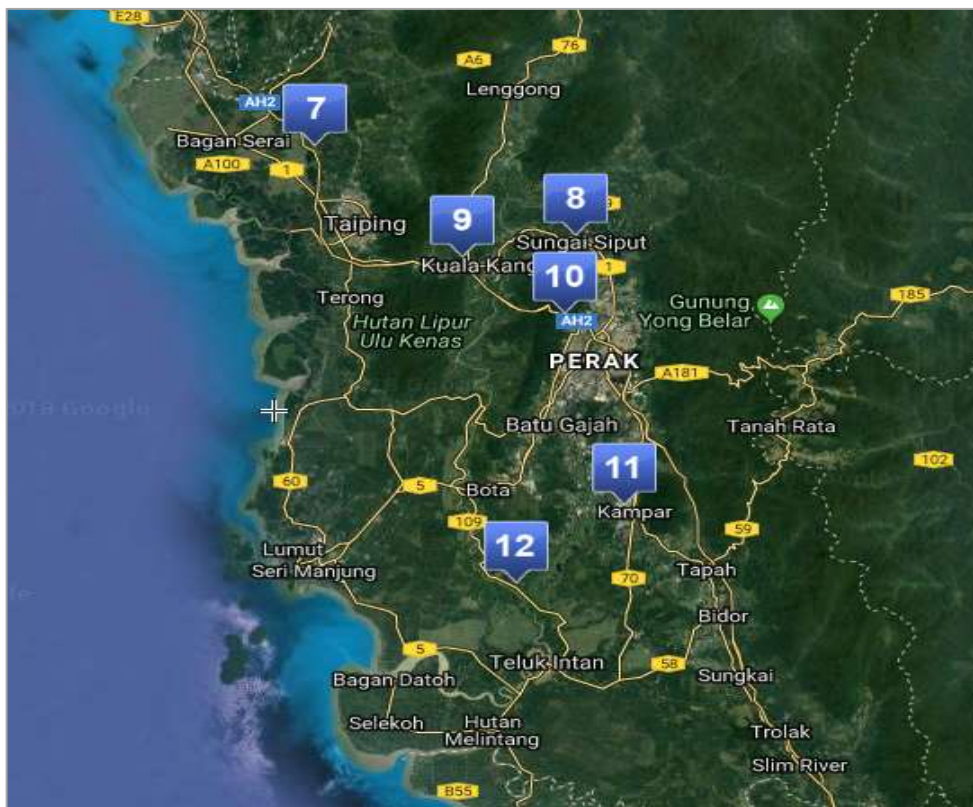


Figure 4.5. Proposed LSS Locations at Perak State.

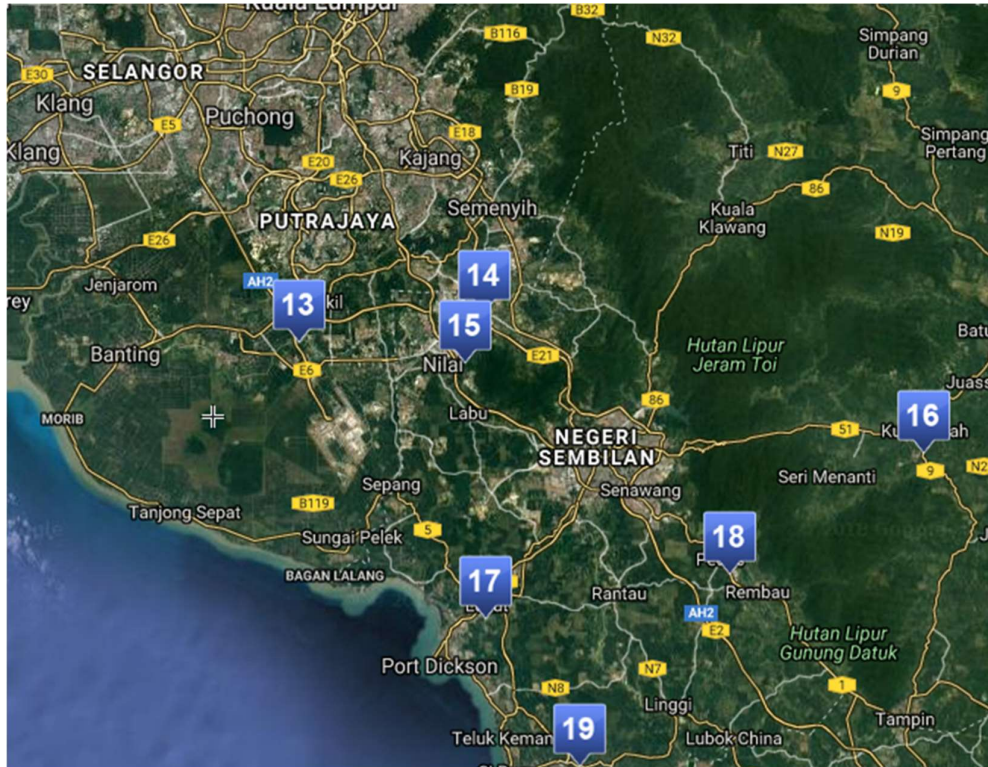


Figure 4.6. Proposed LSS Locations at Negeri Sembilan State.

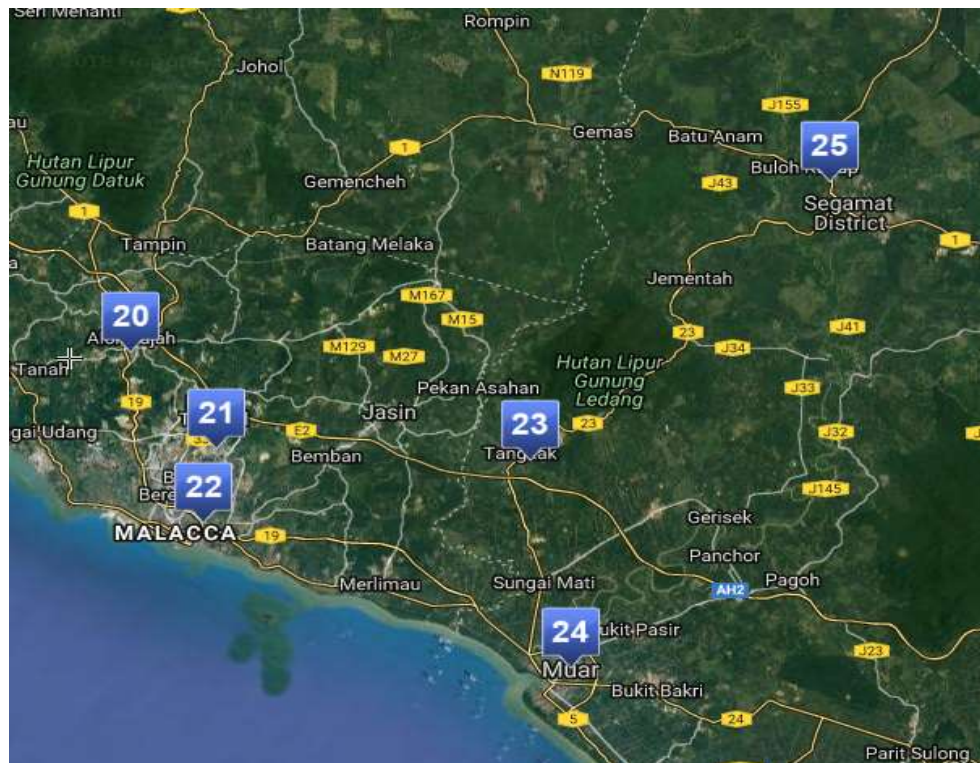


Figure 4.7. Proposed LSS Locations at Malacca & Johor States.

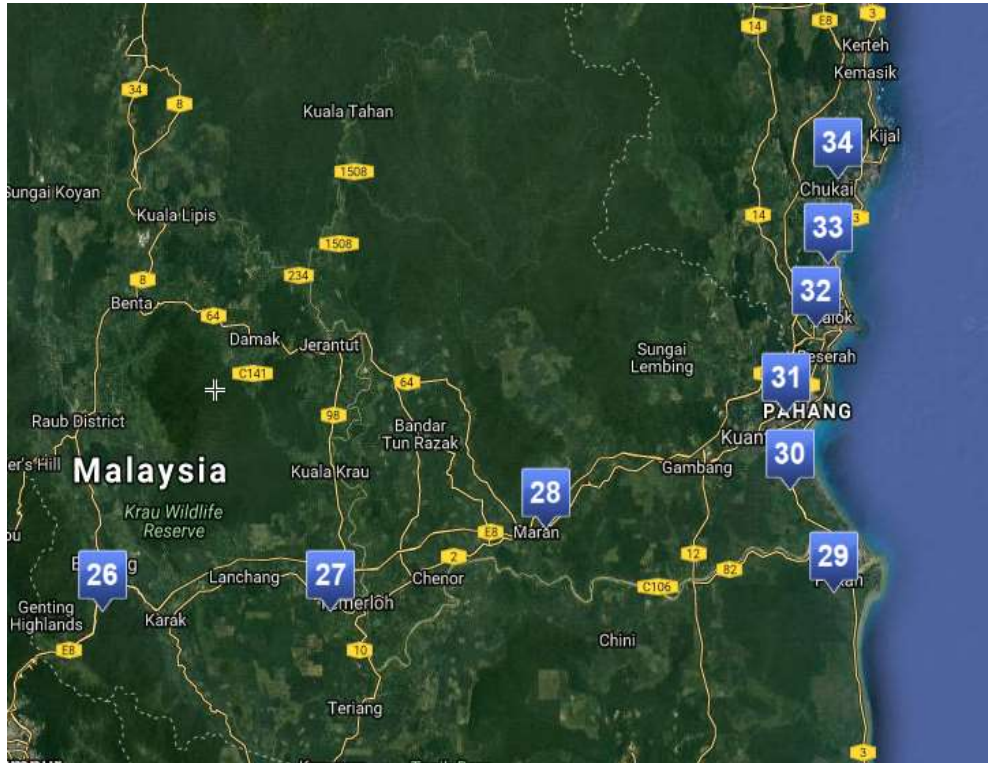


Figure 4.8. Proposed LSS Locations at Pahang State.

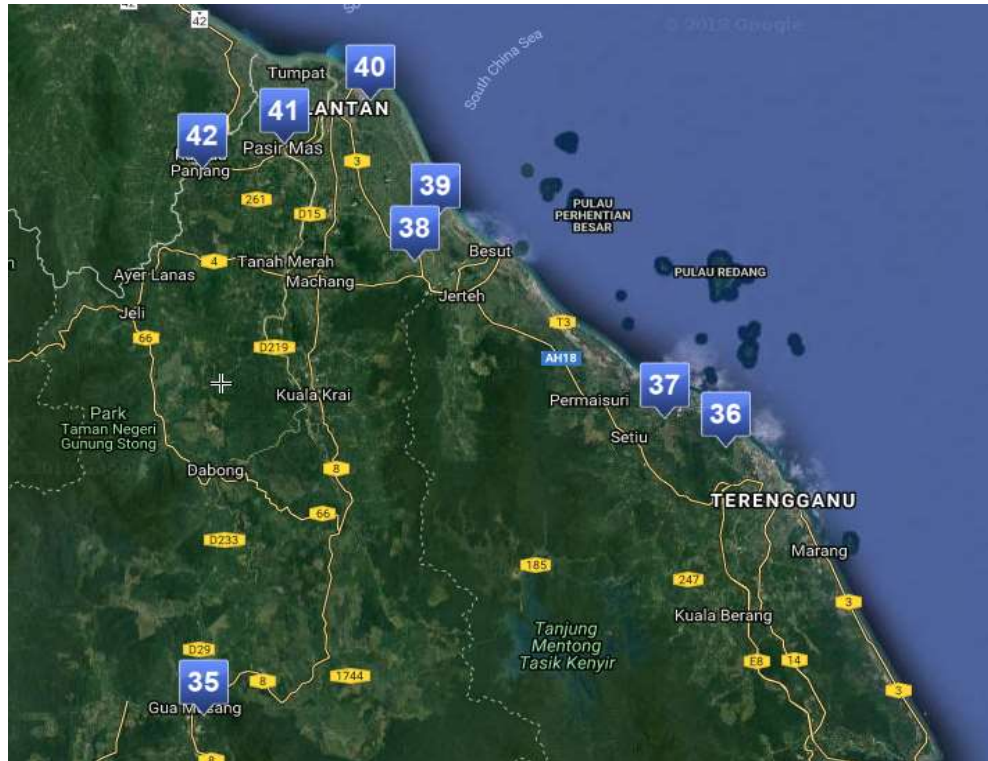


Figure 4.9. Proposed LSS Locations at Kelantan & Terengganu States.

LSS power plants which identified in Figures 4.4 to 4.9 will be connected to the nearest 132 kV transmission substations which had been identified to have double busbar configuration as shown in Table 4.1. The substations are divided into 5 main areas in PSSE, which area Northern, Perak, Central, Southern and Eastern according to the geographical location in Peninsular Malaysia. Whereas, state in each of the areas is listed in Table 4.2.

Table 4.1. List of Identified 132kV Substations for LSS Connection in PSSE.

Substation	State	Area in PSSE
1	Kedah	Northern
2	Kedah	Northern
3	Kedah	Northern
4	Kedah	Northern
5	Kedah	Northern
6	Kedah	Northern
7	Perak	Perak
8	Perak	Perak
9	Perak	Perak
10	Perak	Perak
11	Perak	Perak
12	Perak	Perak
13	Selangor	Central
14	Negeri Sembilan	Southern
15	Negeri Sembilan	Southern
16	Negeri Sembilan	Southern
17	Negeri Sembilan	Southern
18	Negeri Sembilan	Southern
19	Negeri Sembilan	Southern
20	Malacca	Southern
21	Malacca	Southern
22	Malacca	Southern
23	Johor	Southern
24	Johor	Southern
25	Johor	Southern

26	Pahang	Eastern
27	Pahang	Eastern
28	Pahang	Eastern
29	Pahang	Eastern
30	Pahang	Eastern
31	Pahang	Eastern
32	Pahang	Eastern
33	Terengganu	Eastern
34	Terengganu	Eastern
35	Kelantan	Eastern
36	Terengganu	Eastern
37	Terengganu	Eastern
38	Terengganu	Eastern
39	Terengganu	Eastern
40	Kelantan	Eastern
41	Kelantan	Eastern
42	Kelantan	Eastern

4.4 Analysis of Results for Base Case

The transmission grid of Peninsular Malaysia with 20,574 MW system off-peak demand was used as the Base Case for the studies. The study was focused on the off-peak scenario since worst case for high solar PV penetration usually happened during daytime off-peak period. Analysis on the steady state and dynamic simulation studies were carried out for the Base Case.

4.4.1 Overview of Base Case

The total system off-peak demand of the base case is 20,574 MW. With the assumption that the total system off-peak demand is 70% of the total peak demand, the total peak demand value is determined to be 29,391 MW.

Theoretically, the transmission grid in Peninsular Malaysia was split into five main areas, such as Northern, Perak, Central, Southern and Eastern. Table 4.2 shows the

allocated states at each areas according to the geographical location of Peninsular Malaysia by TNB.

Table 4.2. List of Allocated States at Area in Peninsular Malaysia.

Area	Allocated States
Northern	Perlis, Kedah, Penang
Perak	Perak
Central	Kuala Lumpur, Selangor, Putrajaya & Cyberjaya
Southern	Negeri Sembilan, Malacca, Johor
Eastern	Kelantan, Terengganu, Pahang

Each of the areas had difference load levels and the summation of all the loads in the areas resulted in the total system off-peak demand of 20,574 MW. Figure 4.10 showed the total load and generation dispatch at different areas in the Base Case.

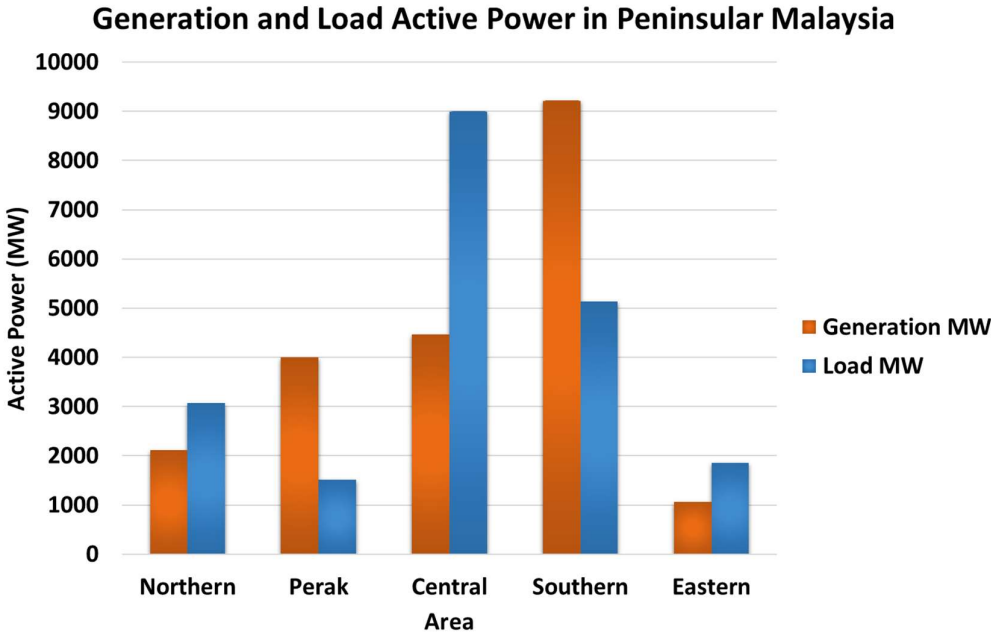


Figure 4.10. Total Generation and Load in the Base Case.

Central area had the highest load level with low generation as compared to its load. Perak and Southern areas have high generation as compared to its load. The demand at Central area was mostly supplied by power from Perak and Southern areas. Figure 4.11

shows the power flows between areas, where high generation area supplied power to high load level area.

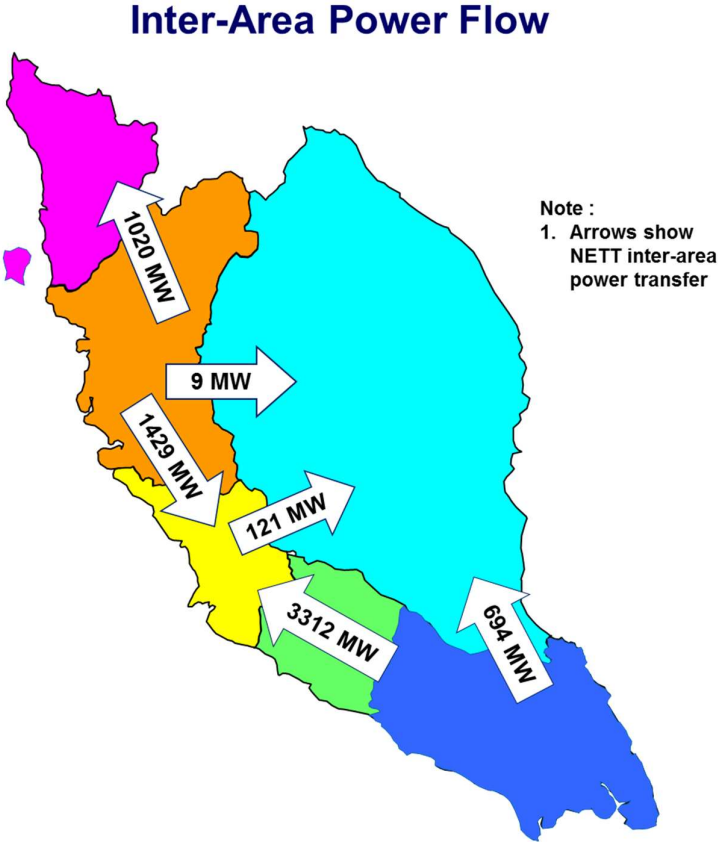


Figure 4.11. Inter-Area Power Flow in the Base Case.

Perak and Southern Areas had more generation than its load level. Northern, Central and Eastern Areas had less generation as compared to its load level. A total of 2,458 MW and 4,006 MW were exported from the Perak and Southern Areas respectively to Northern, Central and Eastern Areas.

Table 4.3. Percentage of Generation Mixed in the Base Case.

Category of Generation	Power Generation (%)
Conventional Power Plant	89.18
Hydro Power Plant	10.55
Solar Power Plant	1.43

Table 4.3 tabulated the percentage contribution of power generation for different generation type. Generations in the Base Case were mostly from coal and gas power

plants, which are also known as conventional power plant. The contribution of the conventional power plant was 89.18% of the total installed generation whereas, hydro power plant occupied 10.55% of the total installed generation and solar power plant in the Base Case was only 1.43%.

4.4.2 Base Case – Steady State Analysis

Steady state analysis on the Base Case will focus on the scope listed below and should comply with the requirements stated in the Transmission System Reliability Standards (TSRS).

- i. Steady state voltage
- ii. Fault level
- iii. No contingency
- iv. N-1 contingency

i. Steady State Voltage

All the 132 kV to 500 kV Substations were within the voltage level of 1.0 pu to 1.05 pu during normal operation. Figure 4.12 to Figure 4.16 shows the voltage profile of Northern, Perak, Central, Southern and Eastern Substations. The substation voltage is regulated by the excitation system of the conventional generation and the reactive power compensation devices such as capacitor bank and shunt reactor in the grid to keep the substation voltage within the range of 1.0 pu to 1.05 pu.

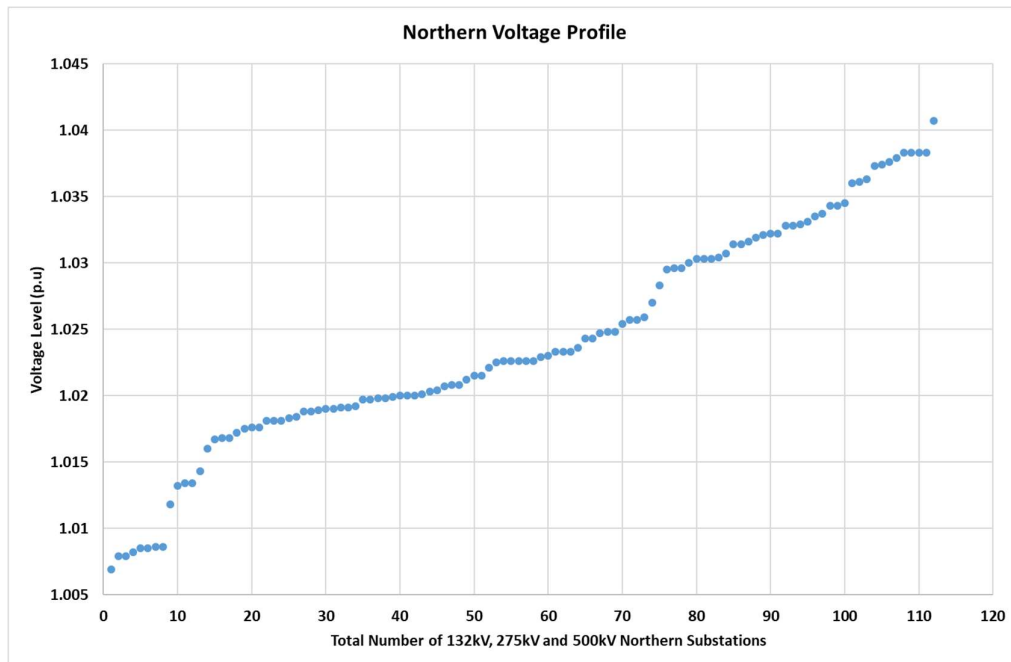


Figure 4.12. Voltage Profile for 132 kV – 500 kV Northern Substations.

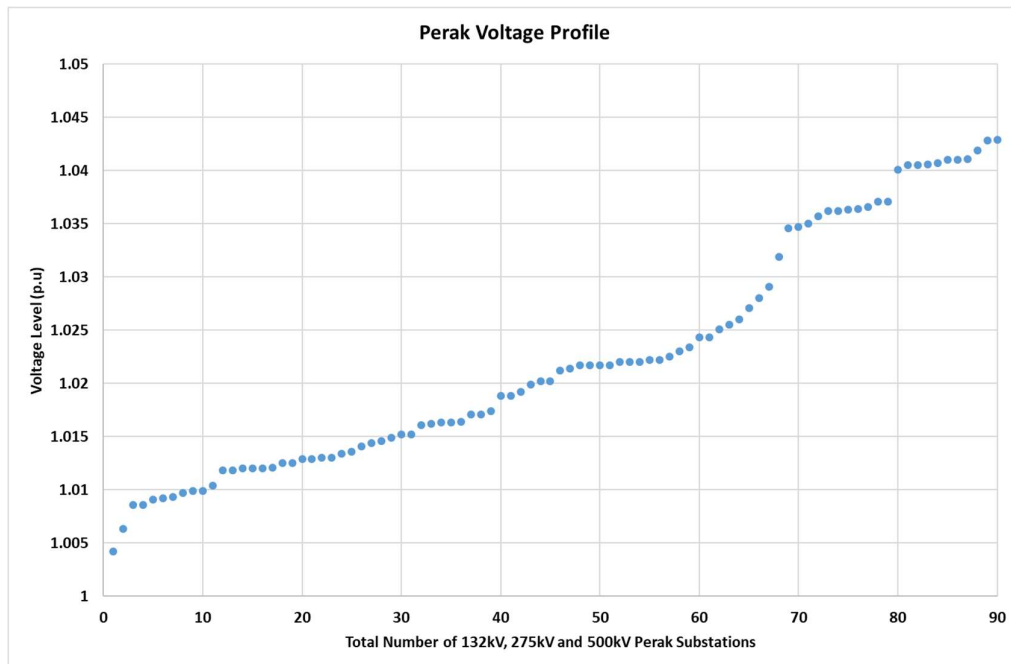


Figure 4.13. Voltage Profile for 132 kV – 500 kV Perak Substations.

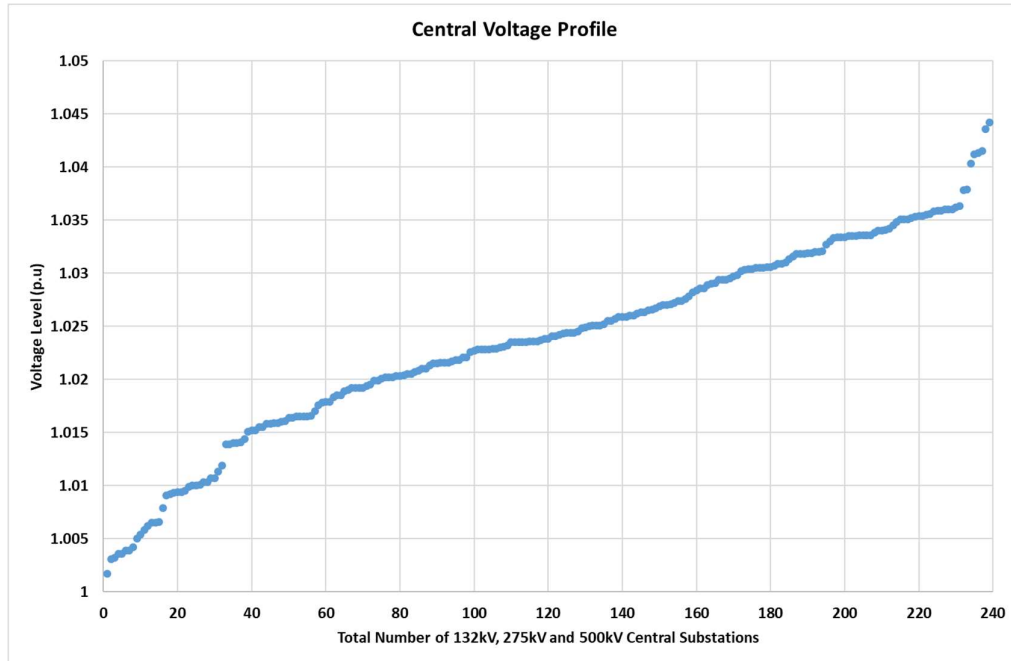


Figure 4.14. Voltage Profile for 132 kV – 500 kV Central Substations.

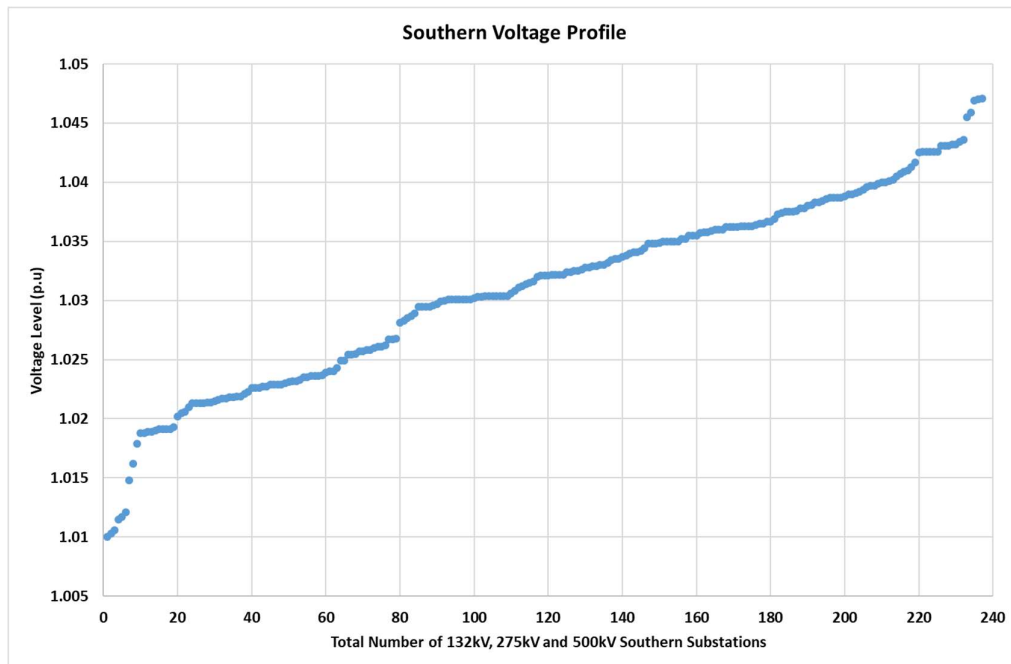


Figure 4.15. Voltage Profile for 132 kV – 500 kV Southern Substations.

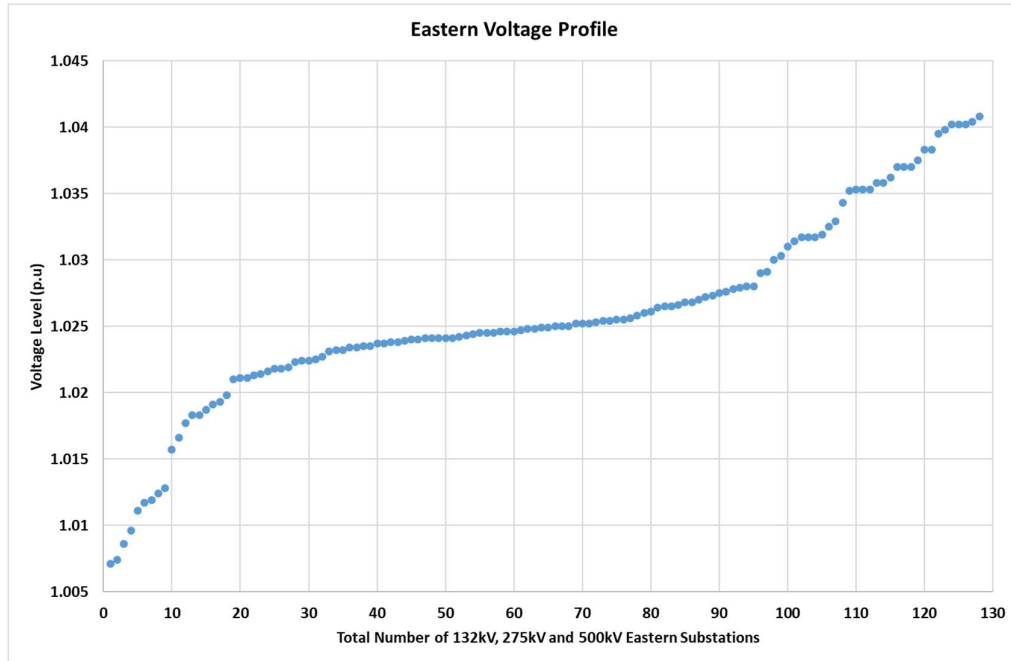


Figure 4.16. Voltage Profile for 132 kV – 500 kV Eastern Substations.

ii. Fault Level

The three (3) phase fault current for the Base Case 132 kV to 500 kV Substations were within the limit of short circuit current rating. Figures 4.17 shows the three phase short circuit currents on the 132 kV substations while Figure 4.18 shows the three phase short circuit currents on the 275 kV Substations which exceed 80 percent of the short circuit rating before the LSS power plant is connected to the system. The high fault current in 275 kV substations are due to the fault current contribution from the conventional generation that mainly connected at the 275 kV grid. Whereas, high fault current at 132 kV substations are due to the mesh configuration of the generic network that directly connect to multiple 275 kV sources.

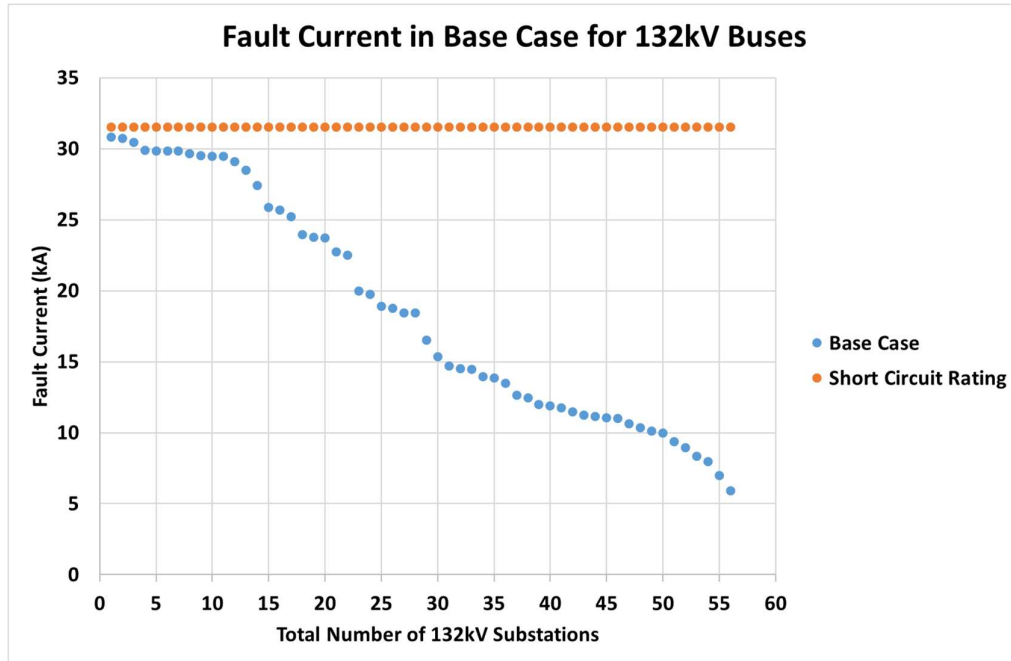


Figure 4.17. Fault Current for 132 kV Substations in Base Case.

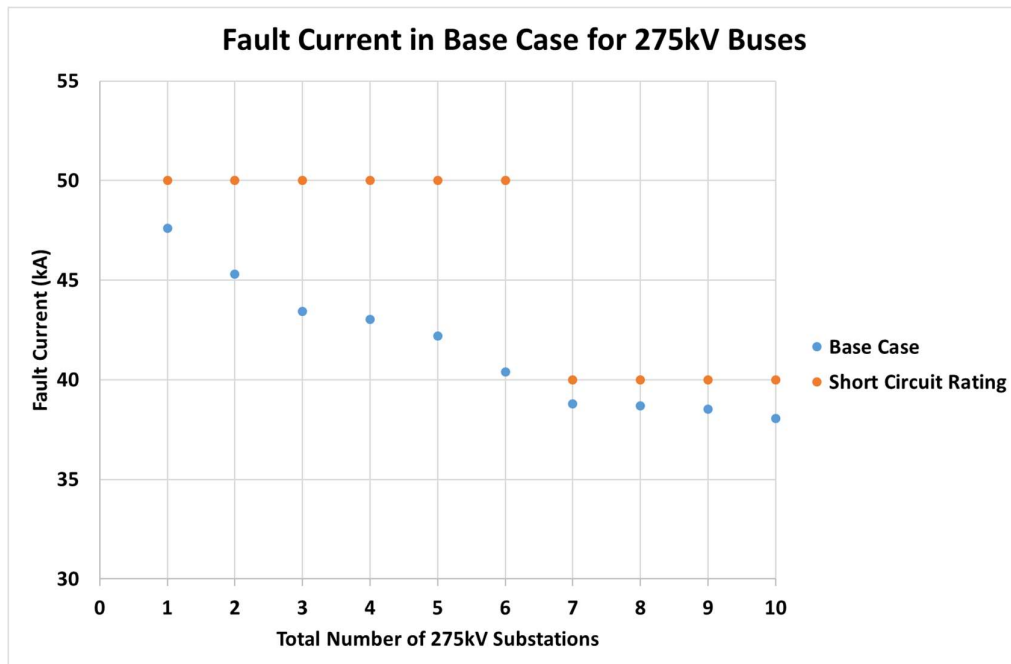


Figure 4.18. Fault Current for 275 kV Substations in Base Case.

iii. No Contingency

Figure 4.19 shows the no contingency analysis results for the Base Case. The no contingency analysis is carried out in PSS/E simulation software. As observed in Figure 4.19, it is clear that during normal operation, without the loss of any transmission element, there is no overloading on the lines and transformers in the Base Case.

```
SUBSYSTEM LOADING CHECK (INCLUDED: LINES; BREAKERS AND SWITCHES; TRANSFORMERS) (EXCLUDED: NONE)
MVA LOADINGS ABOVE 100.0 % OF RATING SET A:

X----- FROM BUS -----X X----- TO BUS -----X
BUS# X-- NAME --X BASKV AREA  BUS# X-- NAME --X BASKV AREA CKT LOADING  RATING PERCENT

* NONE *
```

Figure 4.19. No Contingency Results for Base Case.

iv. N-1 Contingency

N-1 contingency analysis was carried out in the Base Case to study the impact of losing any one of the transmission element in the grid at one moment, which includes line, cable and transformer in the 132 kV to 500 kV generic grid. Results in Figure 4.20 shows that during loss of any one of the line, cable or transformer in the 132 kV to 500 kV generic grid, no overloading is observed in the Base Case. At the same time, no over-voltage and under-voltage issues are observed in the Base Case during N-1 contingency. 'None' in Figure 4.20 below indicates no violation at the substation.

```
Branches loading >100% during contingency:
>Failed contingencies for fictitious buses:
    --- None ---

>Failed contingencies for non-fictitious buses:
<---CONTINGENCY---> <---MONITORED ELEMENT---> <PCTFLOW %> <MVARATING> <MVAFLOW>
    --- None ---

Over voltage violation during contingency of:
> Fictitious buses contingency - Over voltage violation:
    --- None ---

> Non-fictitious buses contingency - Over voltage violation:
    --- None ---

Under voltage violation during contingency of:
> Fictitious buses contingency - Under voltage violation:
    --- None ---

> Non-fictitious buses contingency - Under voltage violation:
    --- None ---
```

Figure 4.20. N-1 Contingency Results for Base Case.

4.4.3 Dynamic Analysis on Base Case

Dynamic analysis on the Base Case is focused on the scope listed below. The results from dynamic analysis shall also comply with the requirements stated in Transmission System Reliability Standards (TSRS).

- i. Critical Fault Clearing Time (CFCT)
- ii. Category A – No Contingency (60 seconds no fault)
- iii. Category B – Loss of Single Element
- iv. Category C – Loss of Two or More Elements
- v. Category D – Loss of a Substation

i. Critical Fault Clearing Times (CFCT)

Critical Fault Clearing Times (CFCT) by definition is the ability of the system to withstand fault within longest fault clearance time until the Main Protection started to operate before the system losing stability.

According to Transmission System Reliability Standards by Tenaga Nasional Berhad [26], the critical fault clearing times of the substations should bound within the limit of maximum fault clearing times of the Main Protection equipment installed in the Transmission System as shown in Table 2.4.

The results of the critical fault clearing times for each generator substations were determined in this section and the results were tabulated in Table 4.4. From the result shown in Table 4.4, the Critical Fault Clearing Times of the generator substations were ascertained higher than the maximum fault clearing times of the Main Protection equipment installed in the Transmission System. Therefore, the system was safe to operate.

Figure 4.21 shows the rotor angle response of four generators, which connected to 500 kV Northern substation. Before 1 second, the machine rotor angles were in steady state condition. However, at 1 second, when fault was applied at the substation for 100 ms, the machine rotor angles started to fluctuate.

Table 4.4. Critical Fault Current Clearing Times for Base Case.

Generator Substation	Critical Fault Clearing Times (ms)	Maximum Fault Clearing Times (ms)
500 kV Northern	≥ 100	≥ 100
500 kV Central	≥ 100	≥ 100
500 kV Southern	≥ 100	≥ 100
275 kV Northern	≥ 100	≥ 100
275 kV Eastern	≥ 100	≥ 100

In operation, total duration for main protection to detect the fault and open the circuit breaker to isolate the fault shall be less than 100 ms [26]. Therefore, fault is injected for 100 ms in the simulation. After 100 ms, the injected fault will be cleared follow by tripping off two 500 kV transmission circuits from the substation.

Figure 4.21 shows that the four unit generators, which connected to the faulted substation. Since Unit 1 and Unit 2 generators are identical and generated same power, thus the rotor angle response for Unit 1 and Unit 2 are similar. All the generators as shown in Figure 4.21 manage to damp to steady state condition after 33 seconds when fault was cleared at 1.1 second. Therefore, the system remain stable and the Critical Fault Clearing Times of the 500 kV Northern Generator Substation was determined to be more than 100ms and complied with the requirements stated in Table 2.4.

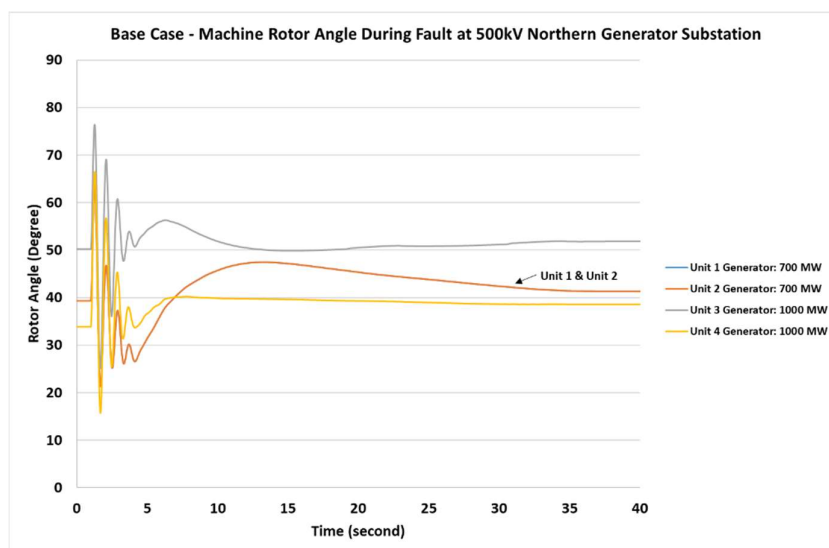


Figure 4.21. Base Case – Machine Rotor Angle Under CFCT Test.

ii. Category A – No Contingency

No contingency analysis was tested on the Base Case by simulated 60 seconds without applying any fault to observe the generator rotor angle during normal condition. The result on the normal condition rotor angle is shown in Figure 4.22. All the generator rotor angles as shown in Figure 4.22 were within 180° , which complied to the requirement stated in TSRS [26]. Therefore, Base Case system had proven to remain stable during normal condition.

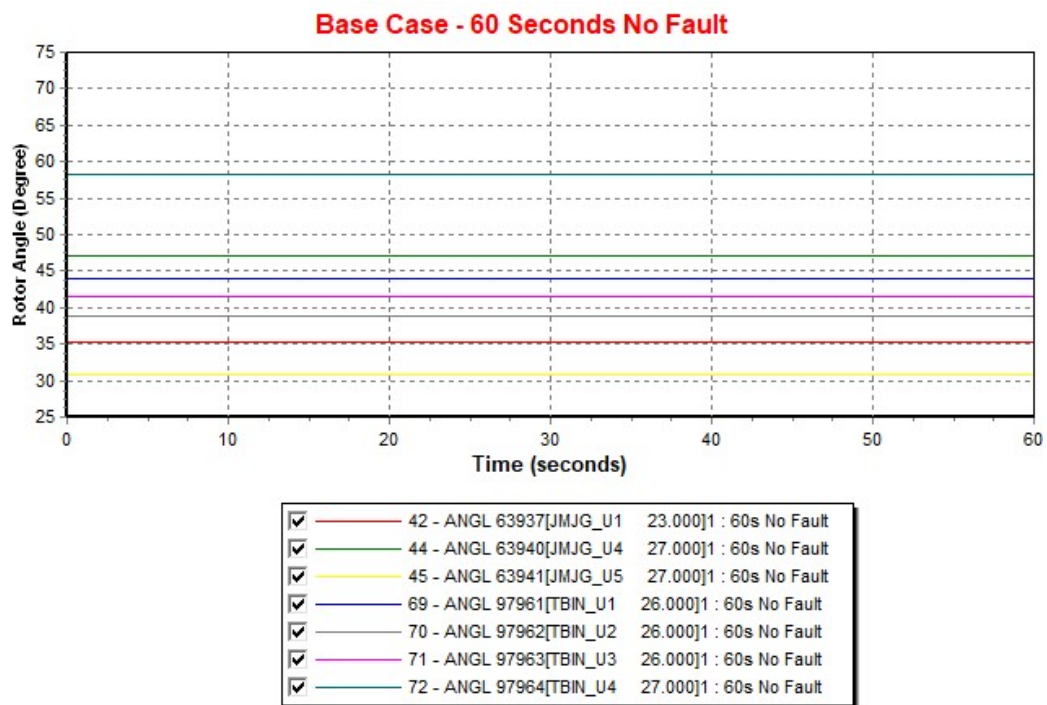


Figure 4.22. Base Case Generator Rotor Angle During 60 Seconds No Fault.

iii. Category B – Loss of Single Largest Element

Category B was tested on the Base Case to observe the response of the system with the loss of a single largest generating unit installed in the system. In this case, the largest generating unit in the generic network is 1000 MW. Therefore, loss of 1000 MW generating unit was studied in this section. Summary of results were tabulated in Table 4.5 and the graphs were shown in Figure 4.23 – 4.25.

Table 4.5. Base Case - Impact of Losing 1000 MW Generating Unit.

System Condition When Loss of 1000 MW Generation Unit	
Spinning Reserve	1208 MW
System stable	Yes
Lowest Frequency	49.504 Hz
Load loss	No load loss
Generator Rotor Angle	Within 180°
Lowest Voltage	0.983 pu

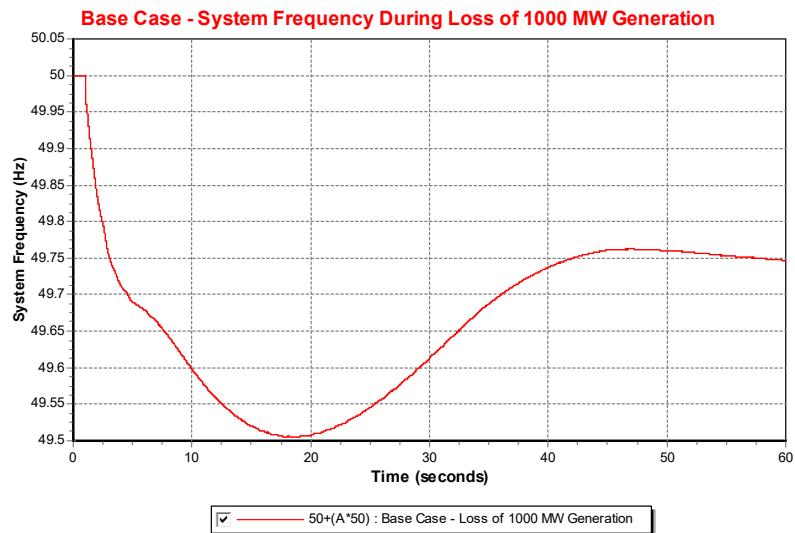


Figure 4.23. Base Case (Loss of 1000 MW Generation) - System Frequency.

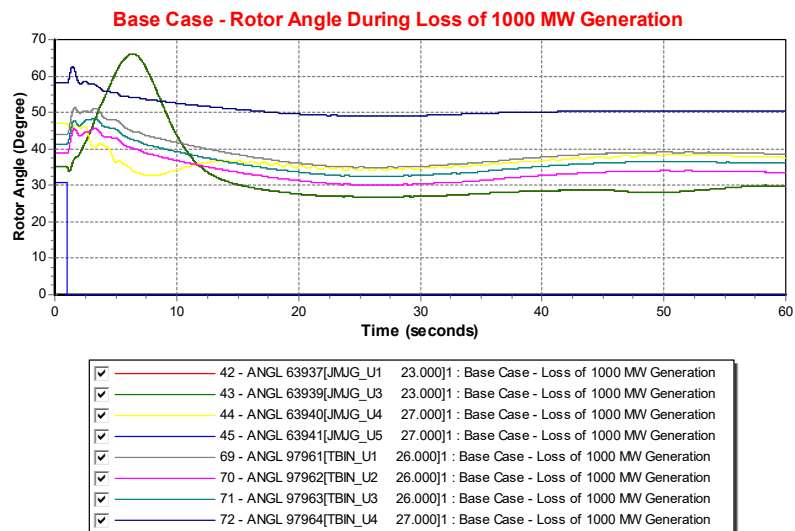


Figure 4.24. Base Case (Loss of 1000 MW Generation) – Rotor Angle.

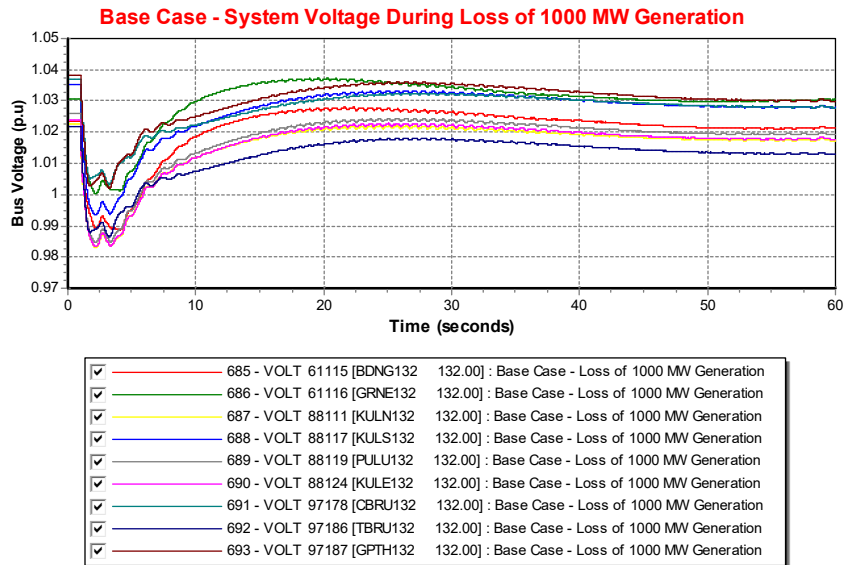


Figure 4.25. Base Case (Loss of 1000 MW Generation) - System Voltage.

Figure 4.23 shows that the system remains stable in the event of losing 1000 MW generation unit. At 1 second, 1000 MW generator, which is JMJG Unit 5 was disconnected from the system, the system frequency started to drop from nominal frequency of 50 Hz down to 49.504 Hz at 17.5 second. However, with the 1208 MW spinning reserve support from the system, the system frequency manage to bring up to 49.75 Hz in less than 60 second without trigger Under Frequency Load Shedding protection scheme which set at 49.3 Hz.

Figure 4.24 shows that the rotor angle for JMJG Unit 5 dropped to zero degree at 1 second as the machine was disconnected from the system. However, rotor angle for JMJG Unit 1, 3 and 4, and TBIN Unit 1, 2, 3 and 4 as shown in Figure 4.24 manage to operate within 180 degrees.

Bus voltage as shown in Figure 4.25 decreased to minimum of 0.983 pu straight after 1000 MW generator disconnected from the system, but went up higher than 1.0 pu after the excitation system of conventional generators started to provide reactive power support to the system. Since steady state bus voltages are within range of 1.0 pu to 1.05 pu, therefore it complied to the requirement stated in the TSRS [26]. Hence, Base Case system had proven stable during loss of largest generation unit.

iv. Category C – Loss of Inter-Area Tie-Line

Category C was tested on the Base Case to study the impact to the system in the event of losing double circuit (DC) transmission lines in the system. In order to study the real impact of this category, loss of DC inter-area tie-lines in the system were studied.

Inter-area tie-line was important to help power transfer from Area to Area in the system. For instance, power was transferred from Perak to Central, Southern to Central and Southern to Eastern through 500 kV and 275 kV transmission lines. Tables 4.6 to 4.8 tabulated the results of losing double circuit (DC) inter-area tie-lines in the Base Case. Results in Table 4.6 to 4.8 showed that the system manage to remain stable after losing DC inter-area tie-lines from Perak to Central, Southern to Central, or Perak to Northern, and system frequency can be kept above 49.9 Hz without activate the Under Frequency Load Shedding protection scheme.

Table 4.6. Base Case - Impact of Losing DC Perak to Central Tie-Lines.

System Condition When Loss of DC Perak to Central Tie-Lines	
Lines	500 kV Perak to Central
System stable	Yes
Lowest Frequency	49.924 Hz
Load loss	No
Generator Rotor Angle	Within 180°
Lines	275 kV Perak to Central
System stable	Yes
Lowest Frequency	49.981 Hz
Load loss	No
Generator Rotor Angle	Within 180°

Table 4.7. Base Case - Impact of Losing DC Southern to Central Tie-Lines.

System Condition When Loss of DC Southern to Central Tie-Lines	
Lines	500 kV Southern to Central
System stable	Yes
Lowest Frequency	49.926 Hz
Load loss	No
Generator Rotor Angle	Within 180°
Lines	275 kV Southern to Central
System stable	Yes
Lowest Frequency	49.931 Hz
Load loss	No
Generator Rotor Angle	Within 180°

Table 4.8. Base Case - Impact of Losing DC Perak to Northern Tie-Lines.

System Condition When Loss of DC Perak to Northern Tie-Lines	
Lines	275 kV Perak to Northern
System stable	Yes
Lowest Frequency	0.969 Hz
Load loss	No
Generator Rotor Angle	Within 180°
Lines	275 kV Perak to Northern
System stable	Yes
Lowest Frequency	49.93 Hz
Load loss	No
Generator Rotor Angle	Within 180°

v. Category D – Loss of a Substation

Category D was tested on the Base Case to study the impact to the system in the event of losing a substation in the system. This category is seen as a severe event to the system. Therefore, as long as the system is able to remain stable, then it is considered to comply with the requirements stated in the Transmission System Reliability Standard (TSRS).

In order to study the impact of this category, event of losing generator substation at Northern, Central and Southern were analysed. Tables 4.9 to 4.11 tabulated the summary for the results of losing a generator substation in the Base Case.

Table 4.9. Base Case - Impact of Losing 500 kV Northern Generator Substation.

System Condition When Loss of 500 kV Northern Generator Substation	
System stable	Yes
Lowest Frequency	48.99 Hz
Load Loss	Load shed 3,762.44 MW started at 49.13 Hz

Table 4.10. Base Case - Impact of Losing 500 kV Central Generator Substation.

System Condition When Loss of 500 kV Central Generator Substation	
System stable	Yes
Lowest Frequency	49.19 Hz
Load Loss	Load shed 1,725.62 MW started at 49.21 Hz

Table 4.11. Base Case - Impact of Losing 500 kV Southern Generator Substation.

System Condition When Loss of 500 kV Southern Generator Substation	
System stable	Yes
Lowest Frequency	49.08 MW
Load Loss	Load shed 2,028.2 MW started at 49.17 Hz

Results in Tables 4.9 to 4.11 show that the Base Case system was stable in the event of losing any 500 kV generator substation in the system. Therefore, the Base Case system was a strong system and thus the installation of Large Scale Solar generation into the system is feasible. However, the amount of total installed LSS generation into the system requires further investigation.

4.5 Scenario Development

The different scenarios for solar penetration level are shown in Table 4.12. This subsection will determine the maximum solar penetration level that the system could take and at the same time, remain stable when subjected to any system disturbances.

Table 4.12 shows the scenarios with difference solar penetration level based upon the total system peak demand of 29,386 MW and system off-peak demand of 20,570 MW. Selection of 22%, 23% and 30% system off-peak solar penetration level in scenario A, B and C was discussed in Chapter 3.2.

After determined 22%, 23% and 30% proposed system off-peak solar penetration level, Equation 3.3 was applied to determine the total solar generation of each scenarios. Then, the total solar generation was divided evenly by 42 LSS locations to determine solar generation for each LSS locations. After getting the total solar generation and total system peak demand, Equation 3.1 was applied to determine system peak solar penetration level. All the scenarios listed in Table 4.12 are studied to determine the maximum solar penetration level and to investigate the impact due to high solar penetration level.

The results for steady state and dynamic study of each scenarios will be compared with the Base Case results. The maximum solar penetration level is determined when the scenario complied with all the requirements listed in Transmission System Reliability Standards [26].

Table 4.12. Solar Penetration Level for Each Scenarios.

Scenario	Solar Penetration Level (%)		Total Solar Generation (MW)	Solar Generation per site (MW)
	System Peak	System Off-Peak		
A	15	22	4525	107.748
B	16	23	4731	112.645
C	21	30	6171	146.930

4.5.1 Scenario Studies – Steady State Analysis

Just like the steady state analysis on the Base Case, steady state analysis for all the scenarios were focused on the Steady State Voltage, Fault Level, No Contingency and N-1 Contingency analysis. All the study results were compared with the Base Case results.

i. Steady State Voltage for Scenario Studies

Steady state voltage for all 132 kV to 500 kV substations in Scenario A, B and C were determined based on the power flow study conducted in PSS/E simulation software by using Full Newton Raphson load flow solution.

Figure 4.26 to Figure 4.30 showed the comparison of voltage graphs for 132 kV to 500 kV Northern, Perak, Central, Southern and Eastern substations in Base Case with Scenario A, B and C. As observed in Figure 4.26 to 4.30, all the voltages for 132 kV to 500 kV substation in Scenario A, B and C were within the voltage limit of 1.0 pu to 1.05 pu in all the areas during normal operation.

Figure 4.26 to Figure 4.30 showed that most of the substations at Northern, Perak, Southern and Eastern regions had higher voltage as compared to the Base Case. This is due to the reason that more LSS were planted up at Northern, Perak, Southern and Eastern. However, voltage at Central substations were slightly reduced due to less LSS planted up at the Central region.

Since LSS power plants behaved like the conventional power plants in the power flow study, where the LSS power plants could provide reactive power support by adjusted the generator terminal voltage of the LSS plant. Thus, LSS power plants could help to improve the system voltage during normal operation and the scattered installation of LSS power plants in the Scenario A, B and C would also had better voltage control as compared to the Base Case.

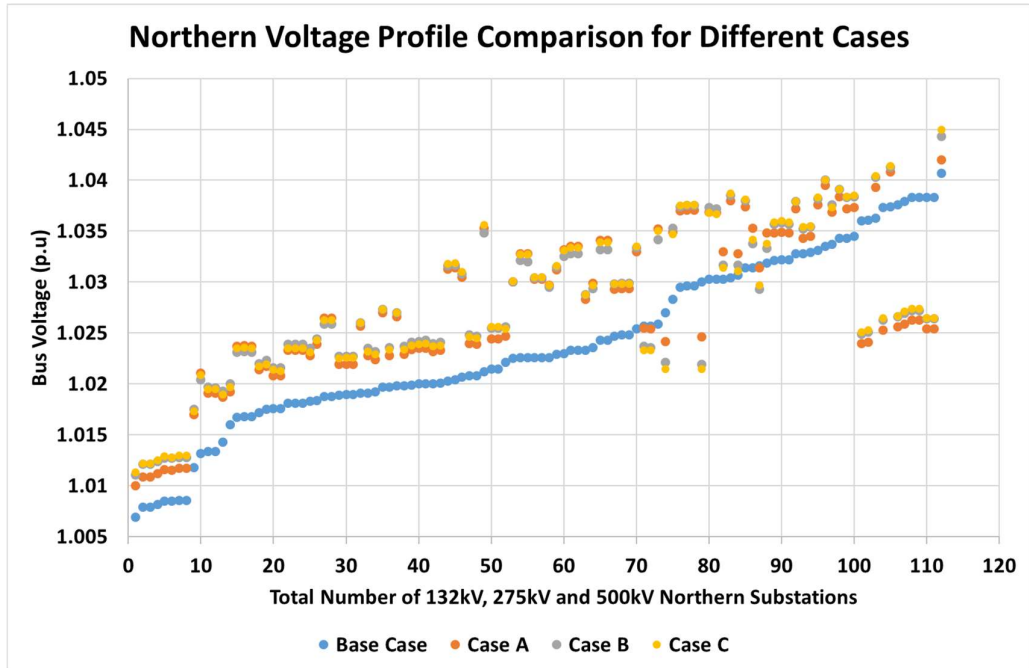


Figure 4.26. Northern Voltage Comparison for 132 kV - 500 kV Substations.

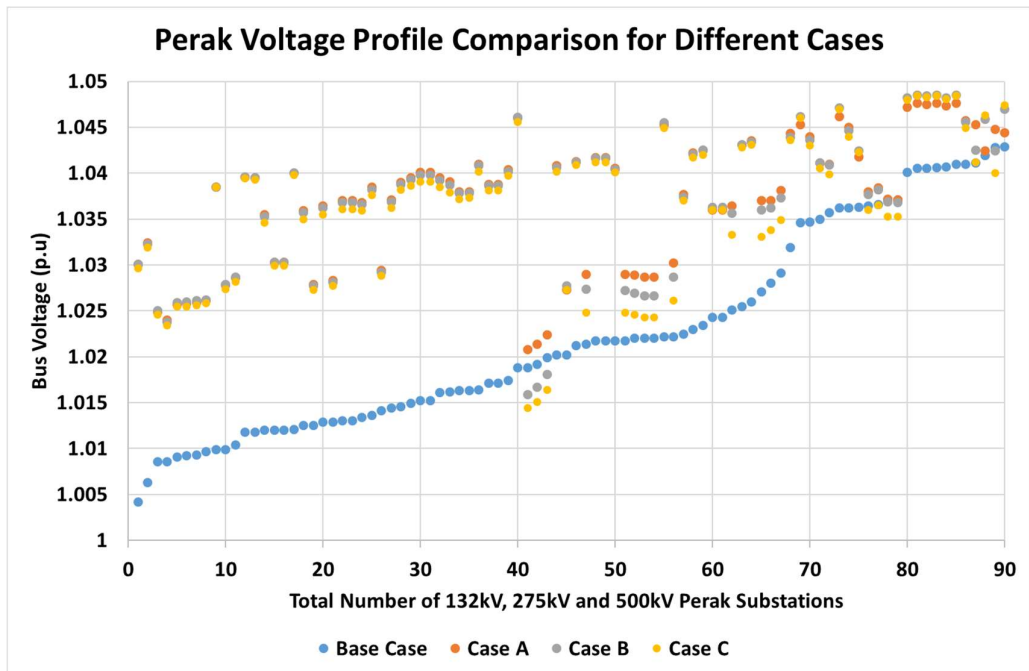


Figure 4.27. Perak Voltage Comparison for 132 kV - 500 kV Substations.

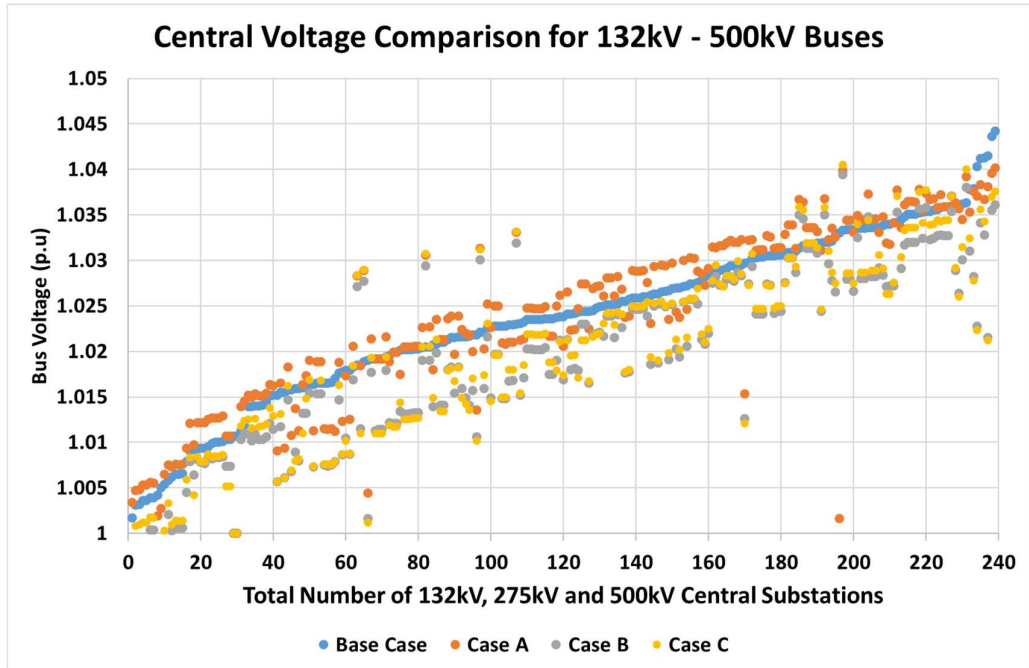


Figure 4.28. Central Voltage Comparison for 132 kV - 500 kV Substations.

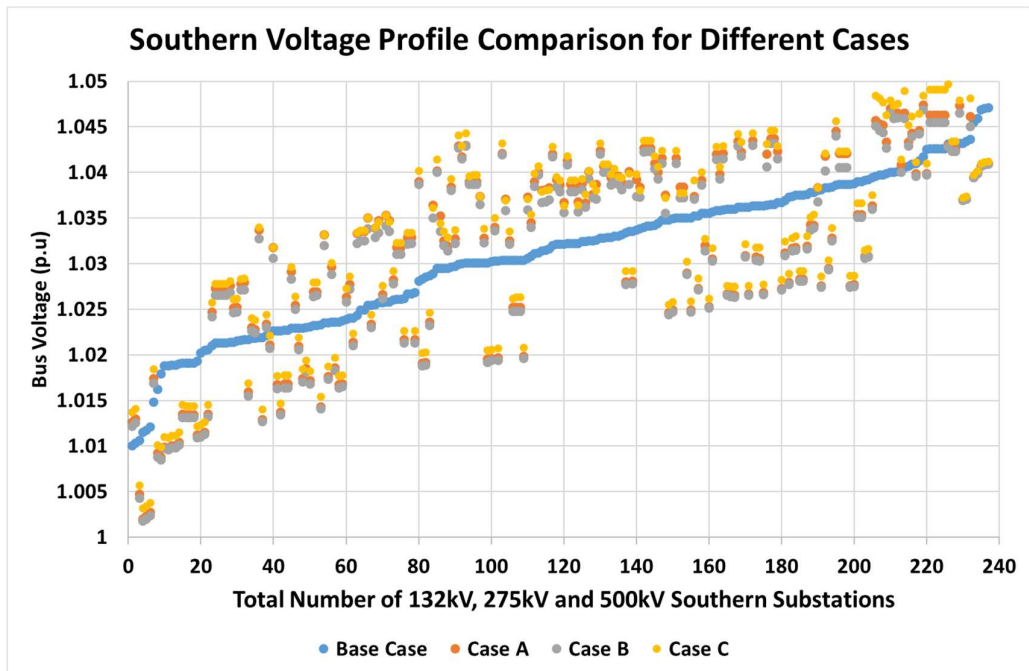


Figure 4.29. Southern Voltage Comparison for 132 kV - 500 kV Substations.

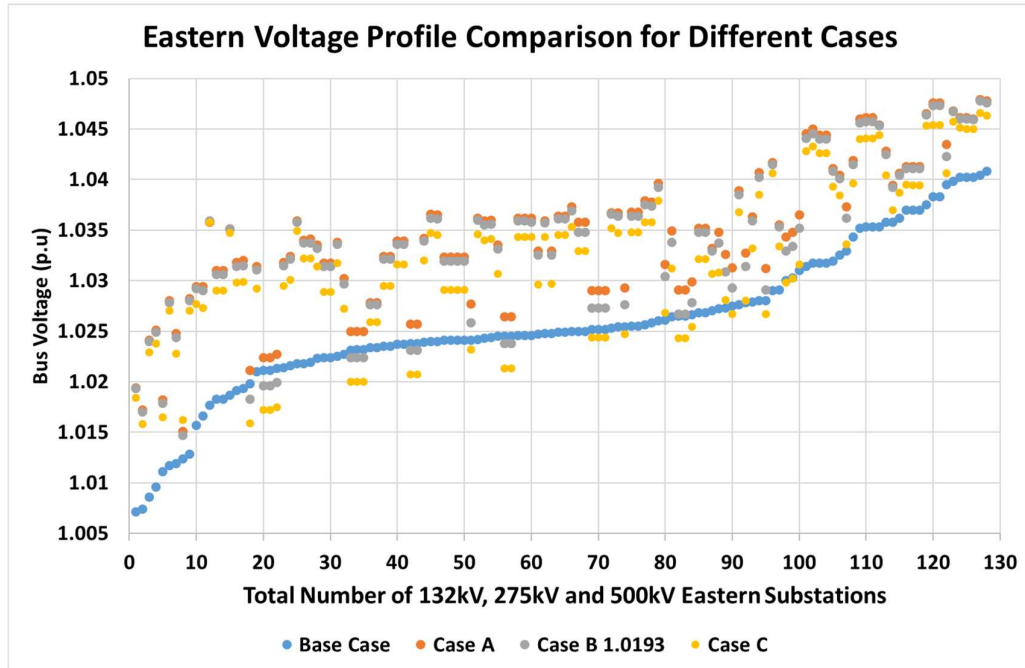


Figure 4.30. Eastern Voltage Comparison for 132 kV - 500 kV Substations.

ii. Fault level

Three phase fault current for all the 132 kV, 275 kV and 500 kV substations in Scenario A, B and C were determined by using IEC 60909 fault calculation method that available in PSS/E simulation software [28].

The new substation fault currents after the installation of LSS power plants in Scenario A, B and C were obtained and were compared with the existing substation fault current that available in the Base Case. The fault current results for 132 kV buses and 275 kV buses were showed in Figure 4.31 to Figure 4.32.

Figure 4.31 showed the fault current value for 132 kV buses in Scenario A, B and C. As observed in the figure, fault current for 132 kV buses in Scenario A, B and C were almost same with the fault current for 132 kV buses in the Base Case. However, there was one 132 kV substation in Scenario C exceeded the substation short circuit rating of 31.5kA. Exceeding the short circuit rating limit of the substation circuit breaker would put the equipment and humans' life at risk as the substation may explode in the event of three-phase fault occurs. Therefore, Scenario C did not comply with the requirement listed in Transmission System Reliability Standards [26].

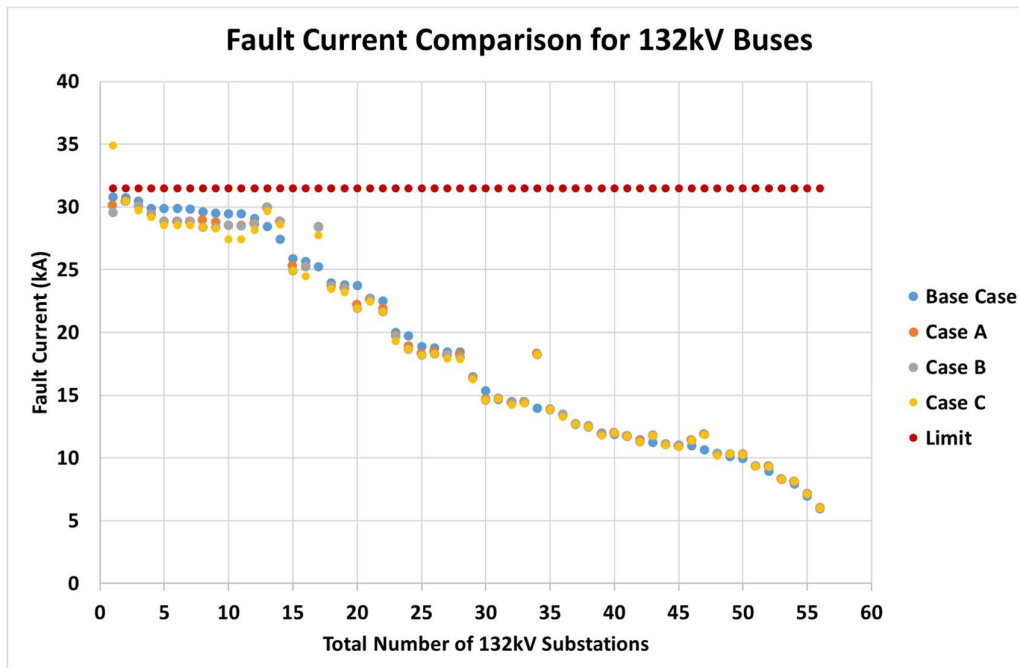


Figure 4.31. Comparison of Fault Current for 132 kV Substations between Base Case and Scenarios.

Whereas, Figure 4.32 showed the fault current value for 275 kV buses in Scenario A, B and C. As observed in the figure, fault current for 275 kV buses in Scenario A, B and C were lower as compared to the fault current for 275 kV buses in the Base Case. The reason was that with high penetration of LSS generation, the conventional generation, which planted up at 275 kV, were turned-off. Therefore, fault current at 275 kV buses were decrease.

In overall, high LSS generation planted up at 132 kV substations would cause fault current slightly increase at 132 kV substations but would reduce fault current at 275 kV substations after turned-off the conventional generations.

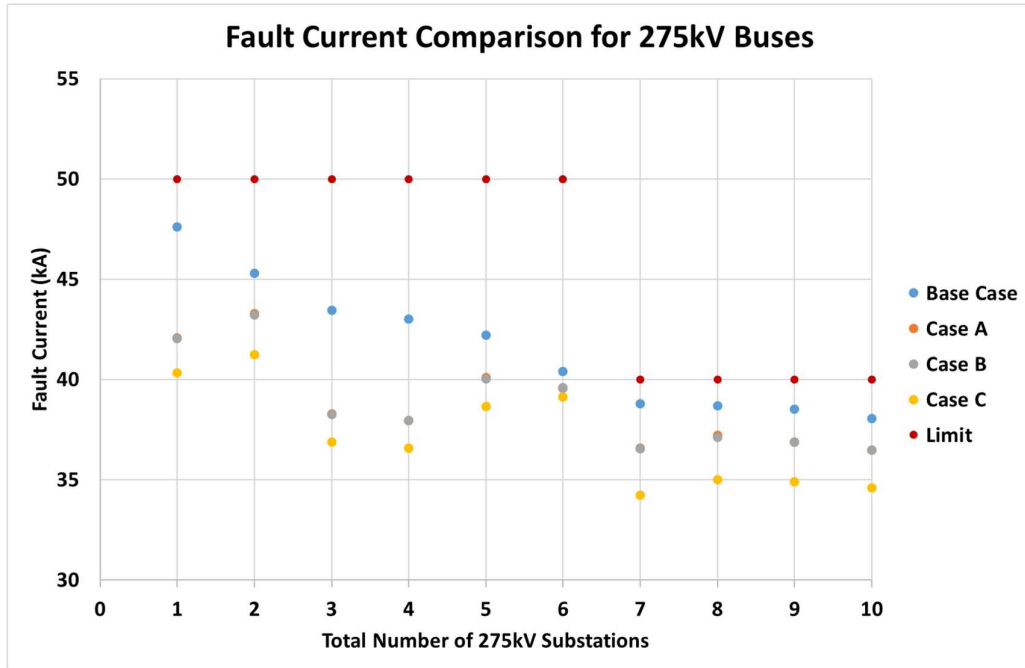


Figure 4.32. Comparison of Fault Current for 275 kV Substations between Base Case and Scenarios.

iii. No contingency

Figure 4.33 showed the No contingency analysis results on the Scenario A, B and C. During normal operation without losing of any transmission element, there is no overloading on the lines and transformers in the Scenario A, B and C. 'None' in Figure 4.33 below showed that there is no overloading violation on the lines and transformers in Scenario A, B and C.

```

SUBSYSTEM LOADING CHECK (INCLUDED: LINES; BREAKERS AND SWITCHES; TRANSFORMERS) (EXCLUDED: NONE)
MVA LOADINGS ABOVE 100.0 % OF RATING SET A:

X----- FROM BUS -----X X----- TO BUS -----X
BUS# X-- NAME --X BASKV AREA  BUS# X-- NAME --X BASKV AREA  CKT LOADING  RATING PERCENT
* NONE *

```

Figure 4.33. Branch / Transformer No Contingency Loading for Scenarios A, B & C.

iv. N-1 contingency

N-1 contingency result in Figure 4.34 showed that during loss of one circuit of 132 kV transmission line at one moment, no overloading on the lines and transformers in the Base Case and Scenario A, where the maximum loading for Scenario A was 100%, which was still acceptable.

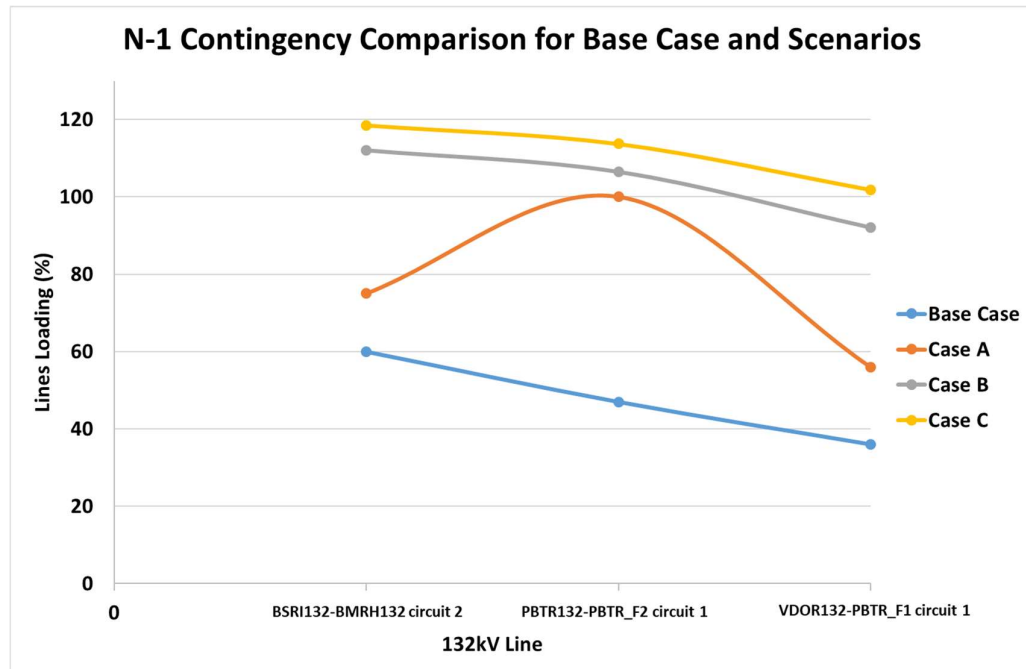


Figure 4.34. Comparison of N-1 Contingency Loading for 132 kV Substation between Base Case and Scenarios.

However, N-1 contingency result in Figure 4.34 showed that in the event of losing one circuit of the transmission line, 132 kV transmission lines in Scenario B and Scenario C overloaded, where the maximum loading for Scenario B and Scenario C in the event of losing line 132kV BSRI-BMRH were 112.12% and 118.54% respectively. Therefore, N-1 contingency test for Scenario B and C had violated the TSRS requirements [26].

4.5.2 Scenario Studies – Dynamic Analysis

Comparable to the dynamic analysis carried out in the Base Case, dynamic stability analysis for Scenarios A, B and C was focused on the below scopes. The stability results for Scenario A, B and C were compared and analysed to determine maximum LSS penetration level.

- i) Critical Fault Clearing Time (CFCT)
- ii) Category A – No Contingency (60 seconds no fault)
- iii) Category B – Loss of Single Element
- iv) Category C – Loss of Two or More Elements
- v) Category D – Loss of a Substation

i) Critical Fault Clearing Times (CFCT)

The results of the critical fault clearing times for each generator substations in each Scenario A, B and C were determined in this section and the results were tabulated in Table 4.13

From the results shown in Table 4.13, the critical fault clearing times of the substations in Scenario A was ascertained higher than maximum fault clearing times of the Main Protection equipment installed in the Transmission System. Therefore, Scenario A system was safe to operate.

However, critical fault clearing times for 500 kV generation substations in Northern and Central were less than 100 ms for Scenario B. Besides, none of the generator substation in Scenario C had more than 100 ms critical fault clearing times. Thus, Scenario B and C failed the requirements stated in TSRS for minimum of 100 ms critical fault clearing times.

Table 4.13. Critical Fault Clearing Times for Base Case and Scenarios.

Generator Substation	Critical Fault Clearing Times (ms)				
	Requirement	Base Case	Scenario	Scenario	Scenario
			A	B	C
500 kV Northern	≥ 100	≥ 100	≥ 100	Failed	Failed
500 kV Central	≥ 100	≥ 100	≥ 100	Failed	Failed
500 kV Southern	≥ 100	≥ 100	≥ 100	≥ 100	Failed
275 kV Northern	≥ 100	≥ 100	≥ 100	≥ 100	Failed
275 kV Eastern	≥ 100	≥ 100	≥ 100	≥ 100	Failed

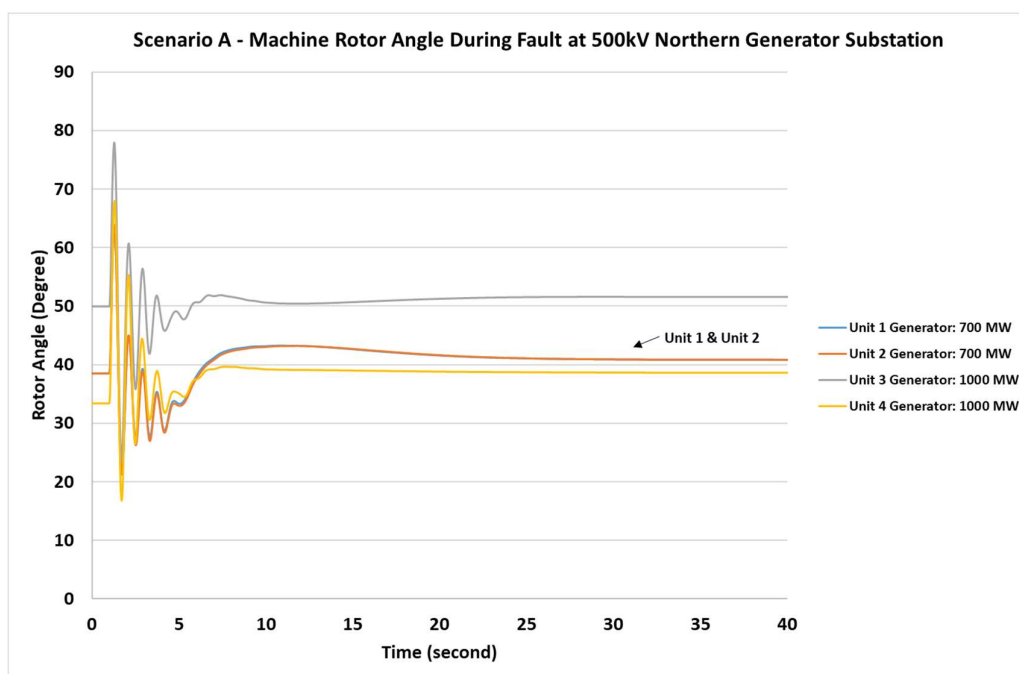


Figure 4.35. Scenario A – 1000 MW Machine Rotor Angle During the Fault.

Figure 4.35 showed the rotor angle response of four generators, which connected to 500 kV Northern substation in Scenario A. Since Unit 1 and Unit 2 generators are identical and generated same power, thus the rotor angle response for Unit 1 and Unit 2 are similar. Before 1 second, the machine rotor angles were in steady state condition. However, at 1 second, when fault was applied at the substation for 100 ms, the machine rotor angles started to fluctuate.

In operation, total duration for main protection to detect the fault and open the circuit breaker to isolate the fault shall be less than 100 ms [26]. Therefore, fault is injected for 100 ms in the simulation. After 100 ms, the injected fault will be cleared follow by tripping off two 500 kV transmission circuits from the substation.

Once the fault was cleared at 1.1 seconds followed with loss of two circuits from the generator substation, the rotor angles manage to damp and restore back to the steady state condition after 25 seconds. Therefore, Scenario A system had proven remain stable after subjected to the fault and compliance with TSRS requirements.

ii) Category A – No Contingency

No contingency, which was also known as Category A – No contingency analysis was tested on Scenario A, B and C by simulated 60 seconds without apply any fault to observe the generator rotor angle response.

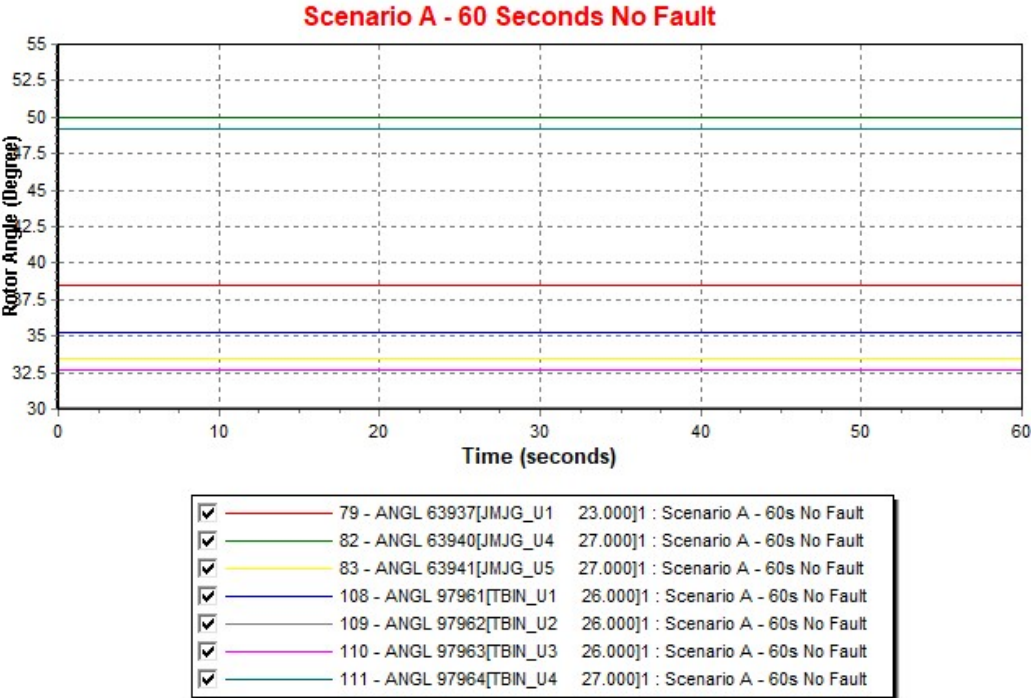


Figure 4.36. Scenario A – Generator Rotor Angle During 60 Seconds No Fault.

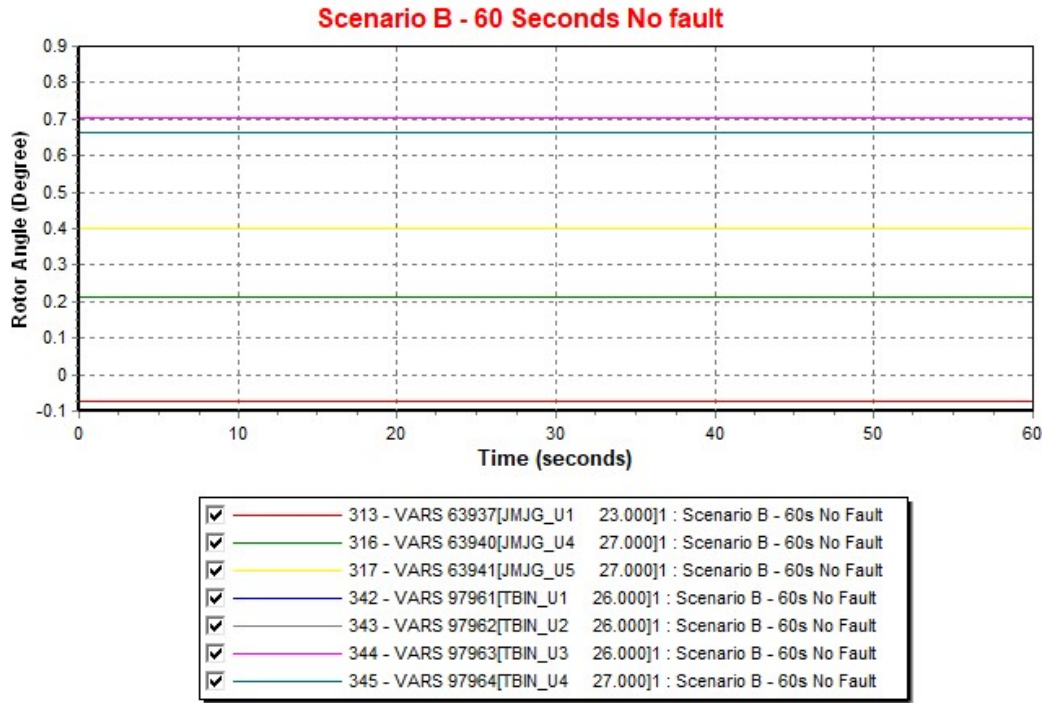


Figure 4.37. Scenario B – Generator Rotor Angle During 60 Seconds No Fault.

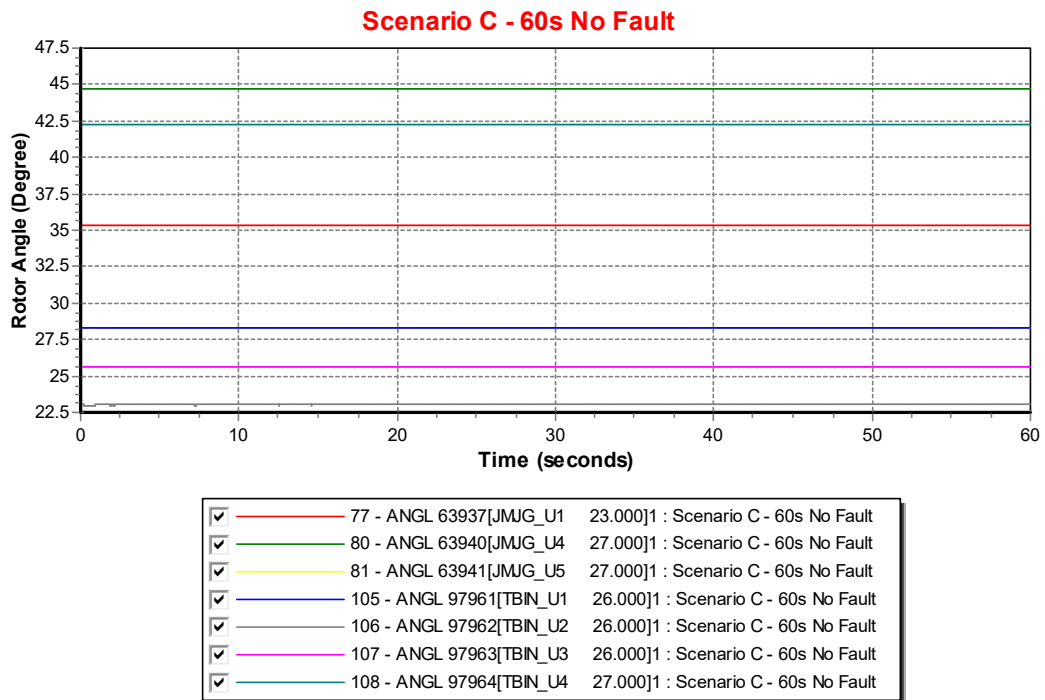


Figure 4.38. Scenario C – Generator Rotor Angle During 60 Seconds No Fault.

No contingency analysis was tested on Scenario A to C by simulated 60 seconds without applying any fault to observe the generator rotor angle during normal condition. The response of generators rotor angles during 60 seconds no fault for Scenario A, B and C were showed in Figure 4.36 to 4.38. During 60 seconds no fault, the generator rotor angles in Scenario A, B and C were within 180 degrees. Therefore, Scenario A, B and C systems had proven remained stable during normal condition.

iii) Category B – Loss of Single Largest Element

Category B was tested on Scenario A, B and C to study the response of the system towards tripping of a single largest generation unit. The installed capacity of a single largest generation unit in the system was found to be 1000 MW. Since the spinning reserve in each of the scenarios was set to 1,220 MW. Therefore, it is important for the system to remain stable without shedding the load in this category of study.

Table 4.14 showed the study results for Scenario A and B in the event of losing 1000 MW generation from the system. Both Scenario A and B managed to remain stable after the generation tripping and keep the machine rotor angle within 180 degrees. Scenario A able to restore the system frequency back to above 49.75 Hz after 25 second without triggered the Under Frequency Load Shedding (UFLS) protection scheme. Therefore, there is no load loss in Scenario A under Category B test.

However, system frequency in Scenario B went down to 49.18 Hz in less than 10 second when 1000 MW generation was tripped off from the system. As the UFLS load shedding scheme was set at 49.2 Hz, total of 1719.27 MW loads were tripped off by the UFLS protection scheme when system frequency dropped down to 49.18 Hz. Hence, Scenario B could not meet the TSRS requirement while Scenario A able to meet the TSRS requirement for Category B test [26].

The different in system frequency response for Scenario A and B was due to the difference in the system inertia. With 1% higher in solar penetration level, system inertia in Scenario B was slightly lower than Scenario A. When 1000 MW generation unit was lose from the system, lower system inertia in Scenario B caused greater frequency drop

in the system. Thus, the lowest frequency in Scenario B was 49.18 Hz, which was about 0.1 Hz lower than Scenario A.

Table 4.14 also showed the comparison between Scenarios A and B with the Base Case results. The lowest system frequency in Base Case was slightly higher than Scenario A and B due to higher system inertia in the system. Figure 4.39 to Figure 4.44 showed the graphs of system frequency, machine rotor angle and system voltage response in the event of losing 1000 MW generation unit for Scenario A and B.

Table 4.14. Scenario A & B - Impact of Losing 1000 MW Generating Units.

System Condition When Loss of 1000 MW Generation Unit			
	Base Case	Scenario A	Scenario B
Spinning Reserve	1208 MW	1220 MW	1214 MW
System Stable	Yes	Yes	Yes
Lowest Frequency	49.504 Hz	49.289 Hz	49.18 Hz
Load Loss	No load loss	No Load Loss	Load shed 1719.27 MW started at 49.18 Hz.
Generator Rotor Angle	Within 180°	Within 180°	Within 180°
Lowest Voltage	0.983 pu	0.976 pu	0.975 pu

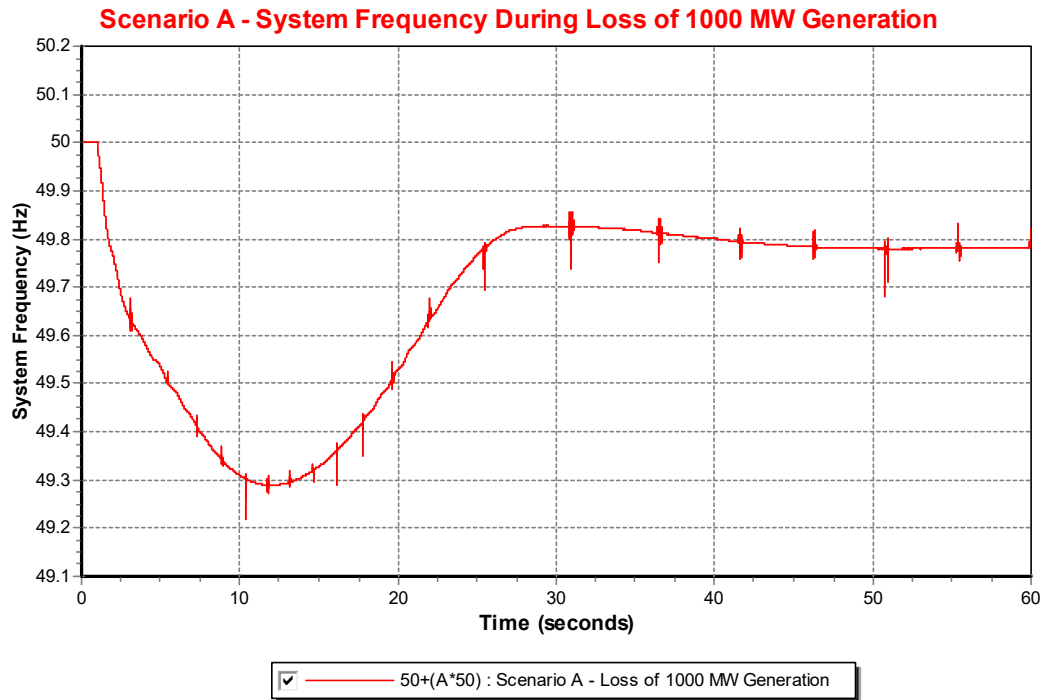


Figure 4.39. Scenario A – System Frequency during Loss of 1000 MW Generation

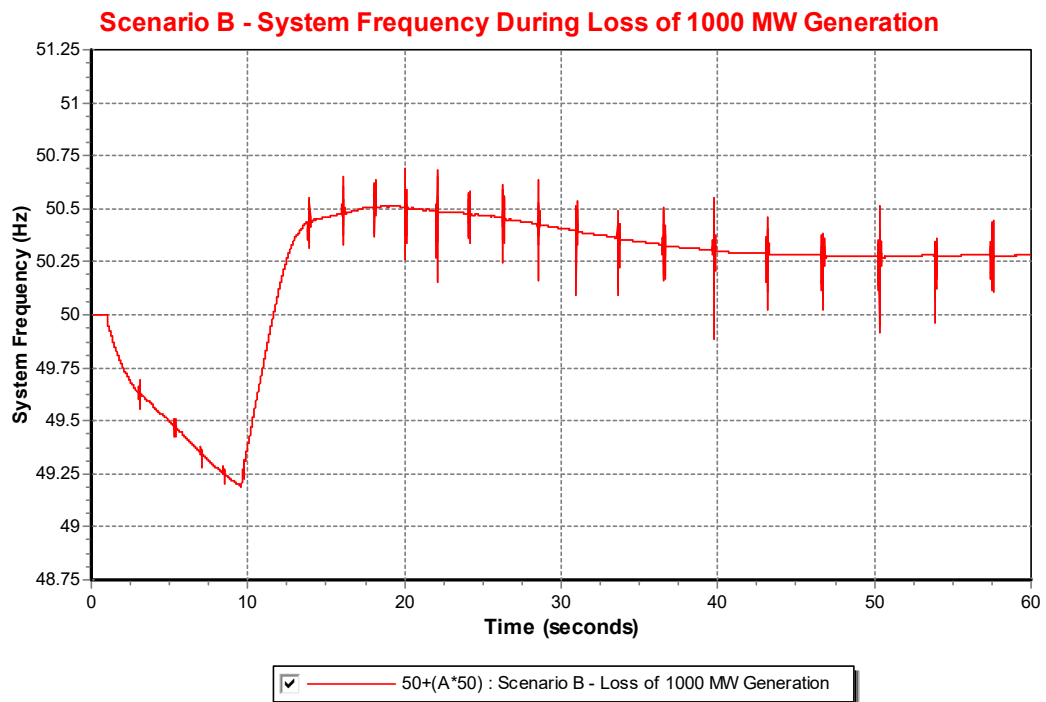


Figure 4.40. Scenario B – System Frequency during Loss of 1000 MW Generation.

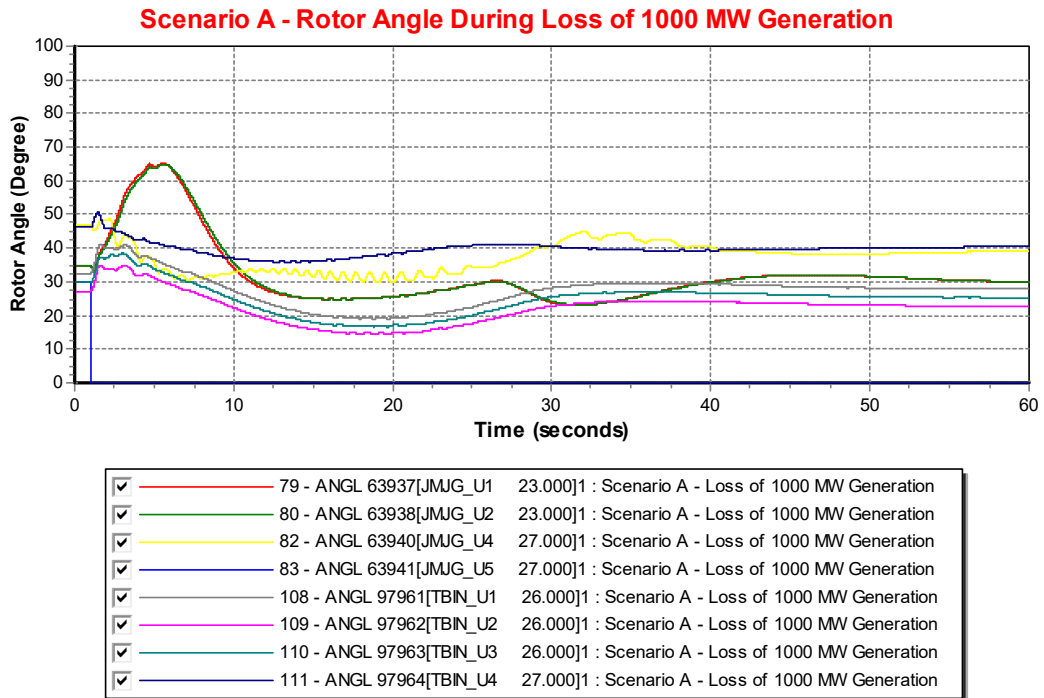


Figure 4.41. Scenario A – Rotor Angle during Loss of 1000 MW Generation.

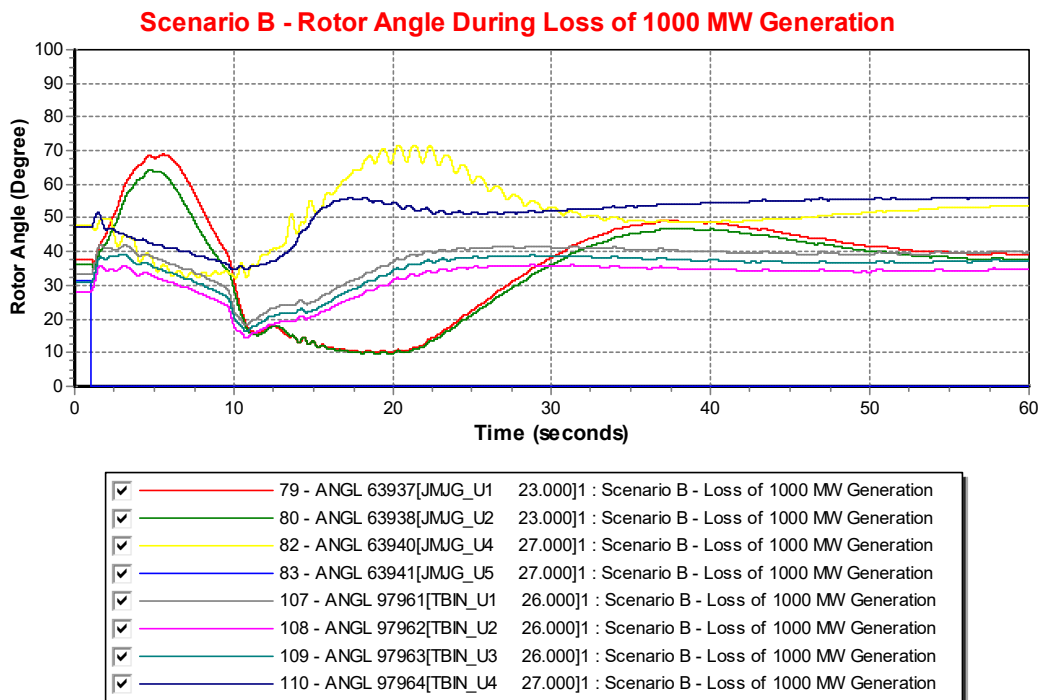


Figure 4.42. Scenario B – Rotor Angle during Loss of 1000 MW Generation.

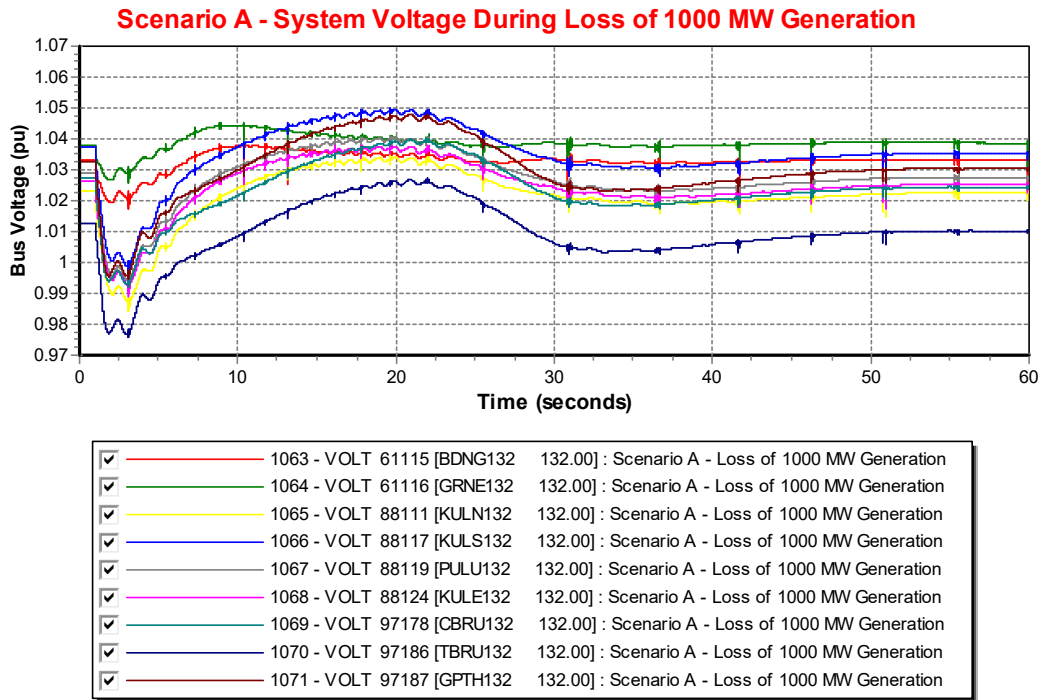


Figure 4.43. Scenario A – System Voltage during Loss of 1000 MW Generation.

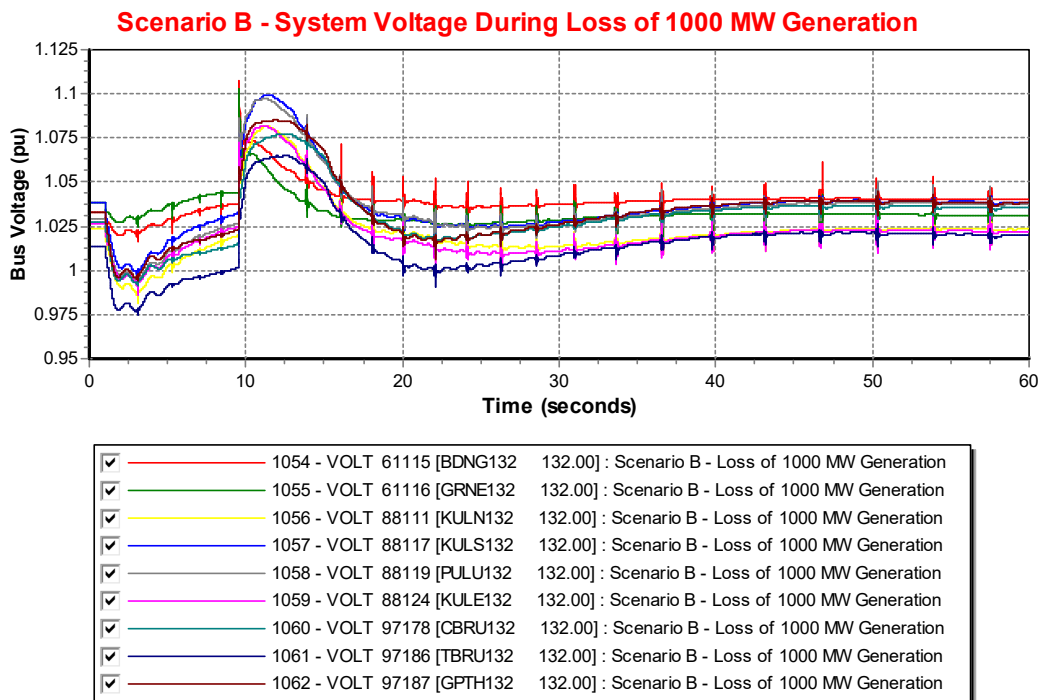


Figure 4.44. Scenario B – System Voltage during Loss of 1000 MW Generation.

On the other hand, Table 4.15 showed results for Scenario C in the event of losing 1000 MW Generation unit. Similar to Scenarios A and B, the spinning reserve in Scenario C was also set to 1220 MW. However, unlike Scenarios A and B, Scenario C was unable to remain system stability after losing of 1000 MW generation from the system.

In 2.375 seconds, out-of-step happened at LSS connected buses as shown in Table 4.15. The out-of-step LSS buses were found at areas of Pahang and Terengganu. With high LSS penetration level in Scenario C, numbers of conventional plants had to shut down or turn-off in order to dispatch the “must-run” solar generation.

With less conventional generation unit that available in the system, system inertia reduced tremendously and cannot support the system frequency when 1000 MW generation unit was loss from the system. As a fallout, system frequency dropped continuously and the system went out-of-step before the conventional generation had enough response time to boost up the system frequency. Therefore, solar penetration level as proposed in Scenario C may not suitable to be installed in the system.

Table 4.15. Scenario C - Impact of Losing 1000 MW Generating Units.

Scenario C – System Condition During Losing 1000 MW Generation Unit	
Spinning Reserve	1220 MW
System stable	No
Out of Step	At time 2.3750 seconds

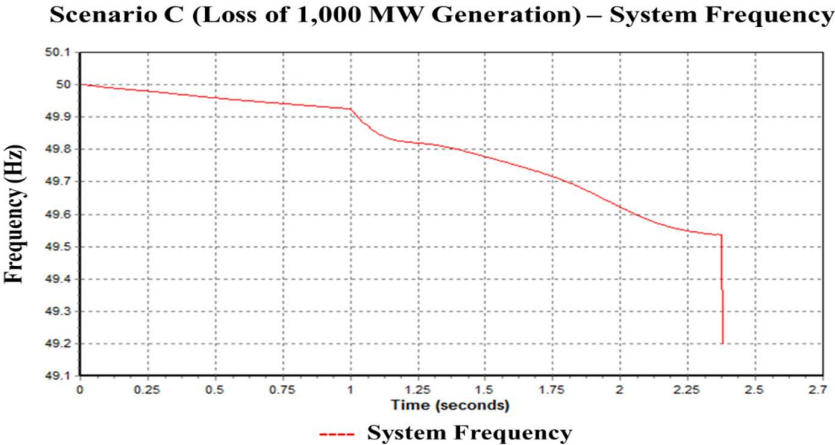


Figure 4.45. Scenario C – System Frequency during Loss of 1000 MW Generation.

iv) Category C – Loss of Inter-Area Tie-Line

Category C was tested on the Scenarios A, B and C to study the impact of losing double circuit (DC) transmission lines to the system. In order to study the severe impact of this category, similar to the Base Case study, losing of DC inter-area tie-lines in the system were studied.

The 500 kV and 275 kV DC inter-area tie-lines from Perak to Central and Southern to Central were studied in this Category C. Table 4.16 to 4.19 summarized the results of losing DC inter-area tie-lines in the Scenarios A, B and C. As observed in Table 4.16 to 4.19, Scenario A and B systems were stable in the event of losing any 275 kV and 500 kV DC inter-area tie-lines. System frequency for Scenario B dropped slightly greater than Scenario A due to the lower system inertia in Scenario B as compared to Scenario A.

Besides, Table 4.16 to 4.19 also summarized the results for Scenario C. However, Scenario C was unable to remain stable in the event of losing inter-area tie-lines. The LSS buses went out-of-step after the lines tripped. The fastest Scenario C system that went out-of-step was 5.8268 seconds, which was during the tripping of 275 kV DC inter-area tie-lines from Southern to Central as shown in Table 4.19. Since Scenario C could not remain stable for any of the events in Category C. Hence, solar penetration level in Scenario C was conclude as a reason that caused system unstable.

Table 4.16. Impact of Losing DC 500 kV Perak – Central Inter-Area Tie-Lines.

Scenario	System Condition	
A	System stable	Yes
	Lowest Frequency	49.885 Hz
	Load loss	No
	Generator Rotor Angle	Within 180°
B	System stable	Yes
	Lowest Frequency	49.883 Hz
	Load loss	No
	Generator Rotor Angle	Within 180°

C	System stable	No
	Out of Step	Yes, at time 6.5857 seconds

Table 4.17. Impact of Losing DC 275 kV Perak – Central Inter-Area Tie-Lines.

Scenario	System Condition	
A	System stable	Yes
	Lowest Frequency	49.884 Hz
	Load loss	No
	Generator Rotor Angle	Within 180°
B	System stable	Yes
	Lowest Frequency	49.881 Hz
	Load loss	No
	Generator Rotor Angle	Within 180°
C	System stable	No
	Out of Step	Yes, at time 13.7579 seconds

Table 4.18. Impact of Losing DC 500 kV Southern – Central Inter-Area Tie-Lines.

Scenario	System Condition	
A	System stable	Yes
	Lowest Frequency	49.884 Hz
	Load loss	No
	Generator Rotor Angle	Within 180°
B	System stable	Yes
	Lowest Frequency	49.884 Hz
	Load loss	No
	Generator Rotor Angle	Within 180°
C	System stable	No
	Out of Step	Yes, at time 6.4947 seconds

Table 4.19. Impact of Losing DC 275 kV Southern – Central Inter-Area Tie-Lines.

Scenario	System Condition	
A	System stable	Yes
	Lowest Frequency	49.887 Hz
	Load loss	No
	Generator Rotor Angle	Within 180°
B	System stable	Yes
	Lowest Frequency	49.885 Hz
	Load loss	No
	Generator Rotor Angle	Within 180°
C	System stable	No
	Out of Step	Yes, at time 5.8268 seconds

v) Category D – Loss of a Substation

Category D was tested on Scenarios A, B and C to study the impact of losing a substation to the system. Table 4.20 to Table 4.22 summarized the results of losing 500 kV generator substations at Central, Southern and Perak.

In the event of losing 500 kV Central and Southern generator substation one at a time as shown in Table 4.20 and Table 4.21, Scenarios A and B managed to remain stable at lowest system frequency of 49.20 Hz for losing Central generator substation, and 49.10 Hz for losing Southern generator substation. Both Scenario A and B have about the same lowest system frequency with 1% different in solar penetration level. Besides, the lowest system voltage for Scenario A and B were 0.96 pu and 0.97 pu Scenario B was observed to have better voltage control as compared to Scenario A.

On the other hand, when loss 500 kV Perak generator substation as shown in Table 4.22, Scenario B system was unstable. Out-of-step happened at time 1.7290 seconds at LSS buses. Even though Scenario B was able to remain stable in the event of losing of 500 kV Central and Southern generator substations, Scenario B was considered

exceeds the stability limit in the case of losing 500 kV Perak generation. Therefore, solar penetration level that used in Scenario B should not be applied in the healthy system.

As shown in Table 4.20 to Table 4.22, Scenario C system was unstable when lose of any generator substation in the system. The out-of-step condition happened at the LSS buses at the fastest time of 1.6330 seconds. Which was less than 1 second after substation tripped. This condition was bad to the system as it could cause the whole system blackout. Therefore, solar penetration level in Scenario C was considered had exceeded the system stability limit and violated the TSRS requirements.

Table 4.20. Scenario A, B & C - Impact of Losing 500 kV Central Generator Substation.

Scenario	System Condition	
A	Spinning Reserve	1220 MW
	Loss of Generation	1400 MW
	System stable	Yes
	Lowest Frequency	49.20 Hz
	Load loss	Load shed 1719.6 MW started at 49.18 Hz.
	Generator Rotor Angle	Within 180°
	Lowest Voltage	0.96 pu
B	Spinning Reserve	1220 MW
	Loss of Generation	1400 MW
	System stable	Yes
	Lowest Frequency	49.20 Hz
	Load loss	Load shed 1719.27 MW started at 49.16 Hz.
	Generator Rotor Angle	Within 180°
	Lowest Voltage	0.97 pu
C	Spinning Reserve	1220 MW
	Loss of Generation	1400 MW
	System stable	No
	Out-of-Step	Yes, at 2.2040 seconds

Scenario A - System Frequency During Loss of 500kV Central Generator Substation

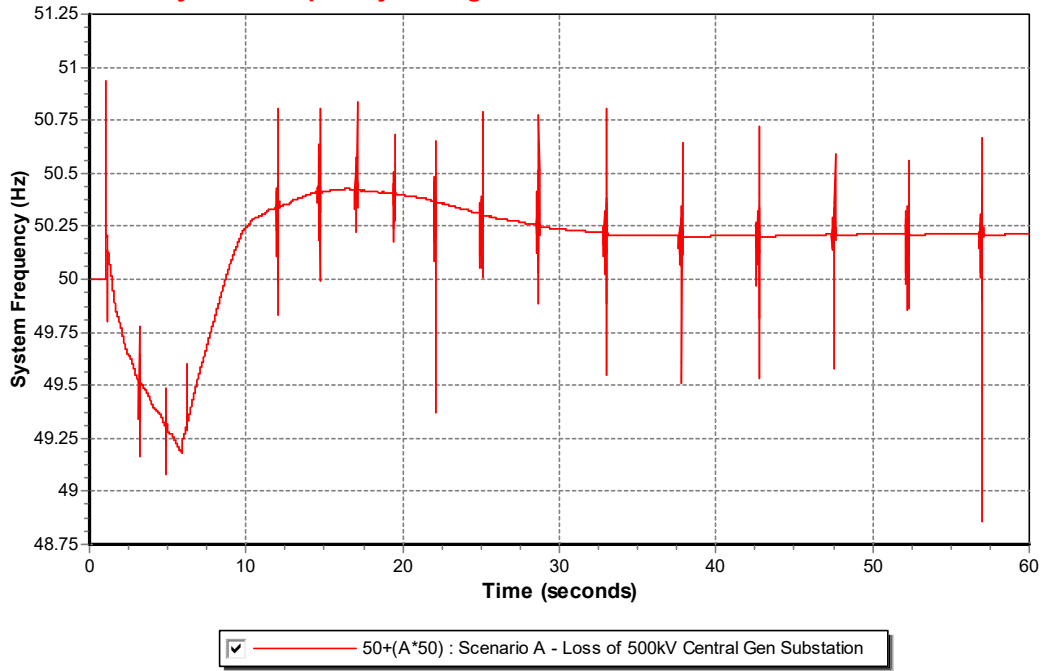


Figure 4.46. Scenario A – System Frequency during Loss of 500 kV Central Generator Substation.

Scenario B - System Frequency During Loss of 500kV Central Generator Substation

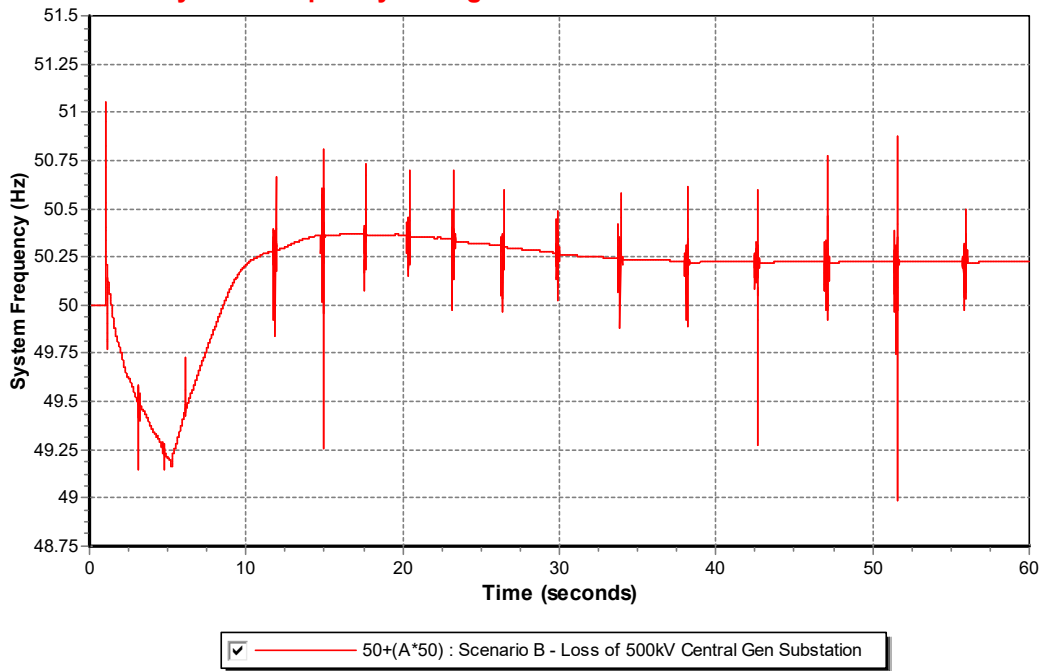


Figure 4.47. Scenario B – System Frequency during Loss of 500 kV Central Generator Substation.

Scenario A - Rotor Angle During Loss of 500kV Central Generator Substation

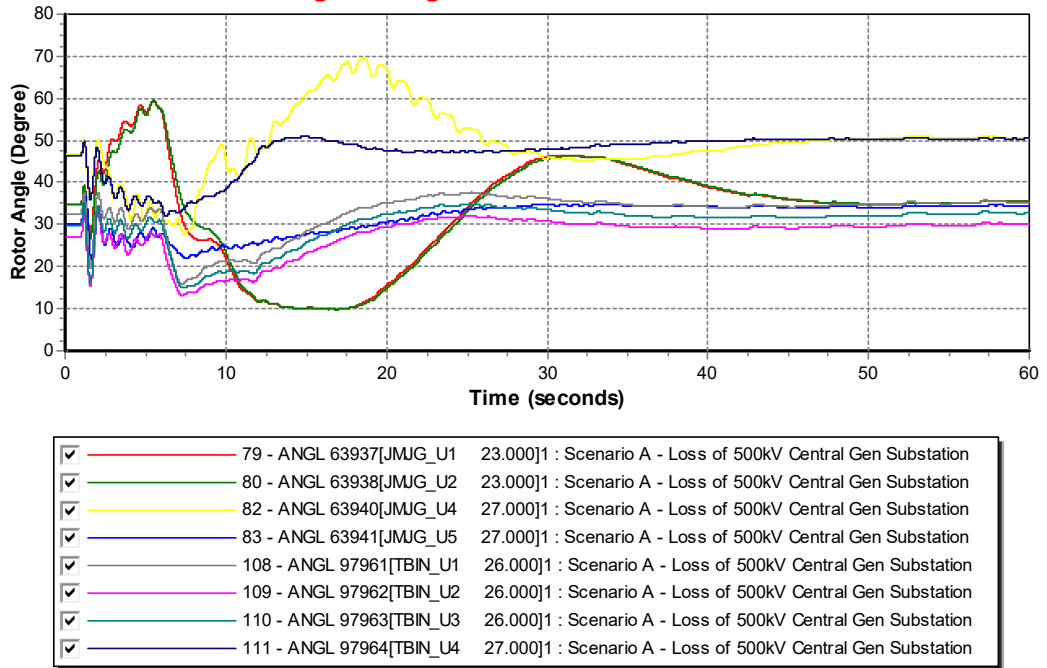


Figure 4.48. Scenario A – Rotor Angle during Loss of 500 kV Central Generator Substation.

Scenario B - Rotor Angle During Loss of 500kV Central Generator Substation

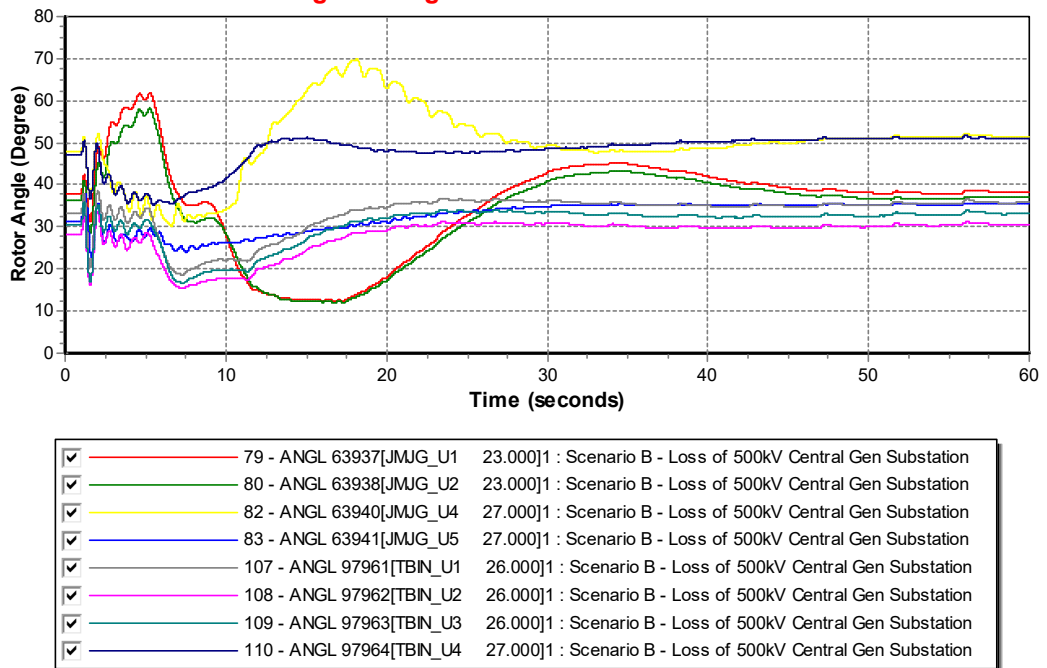


Figure 4.49. Scenario B – Rotor Angle during Loss of 500 kV Central Generator Substation.

Scenario A - System Voltage During Loss of 500kV Central Generator Substation

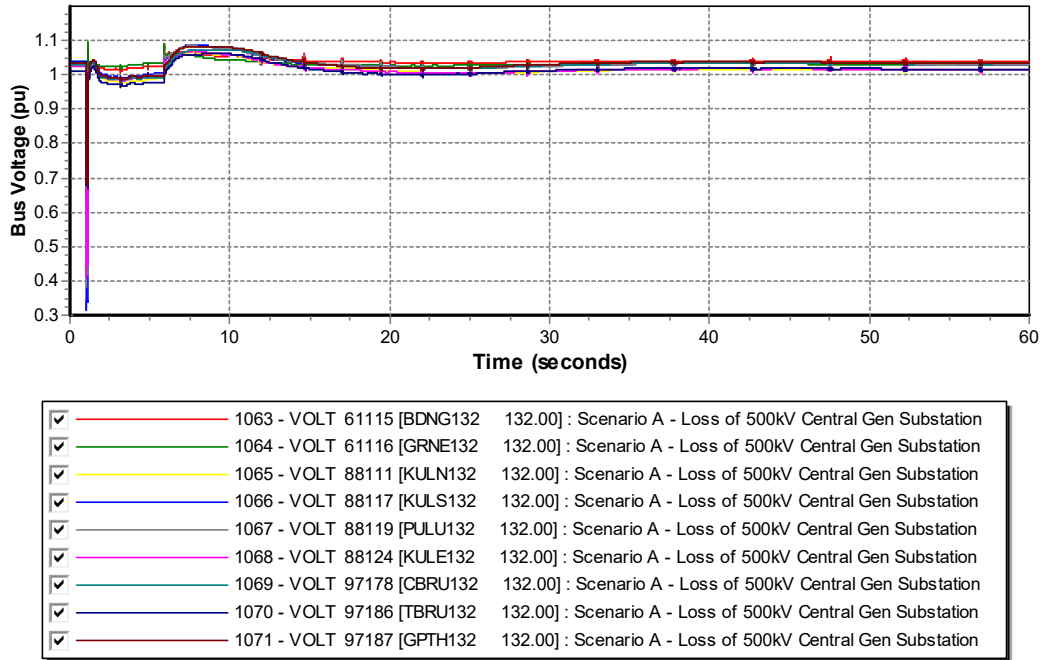


Figure 4.50. Scenario A – System Voltage during Loss of 500 kV Central Generator Substation.

Scenario B - System Voltage During Loss of 500kV Central Generator Substation

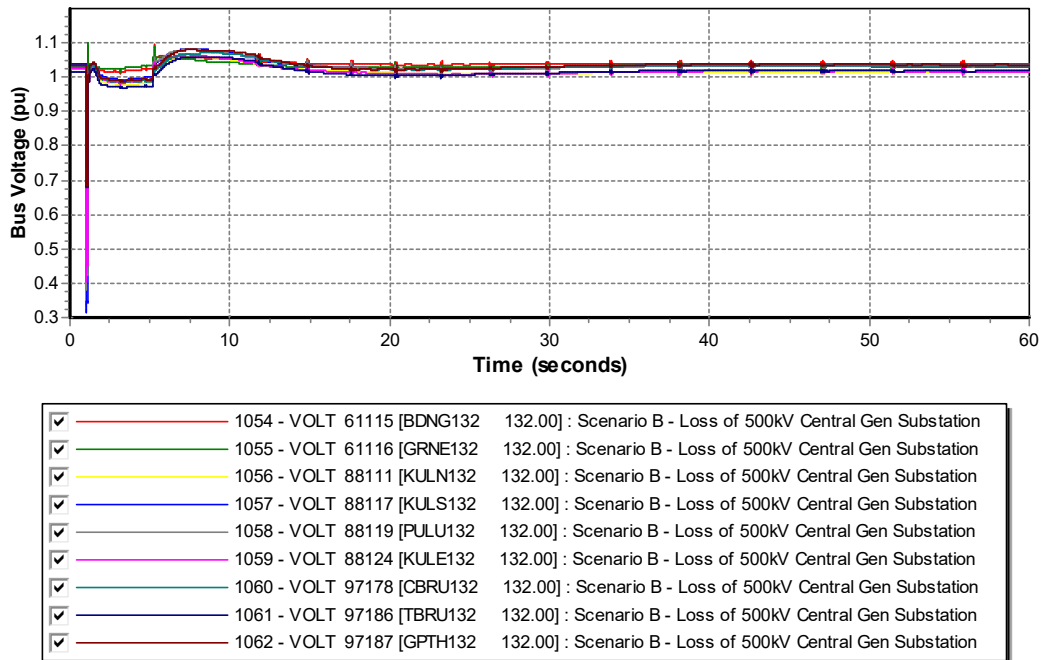


Figure 4.51. Scenario B – System Voltage during Loss of 500 kV Central Generator Substation.

Table 4.21. Scenario A, B & C - Impact of Losing 500 kV Southern Generator Substation.

Scenario		System Condition
A	Spinning Reserve	1220 MW
	Loss of Generation	3100 MW
	System stable	Yes
	Lowest Frequency	49.10 Hz
	Load loss	Load shed 2,559.98 MW started at 49.07 Hz.
	Generator Rotor Angle	Within 180°
	Lowest Voltage	0.96 pu
B	Spinning Reserve	1220 MW
	Loss of Generation	3100 MW
	System stable	Yes
	Lowest Frequency	49.10 Hz
	Load loss	Load shed 2805.95 MW started at 49.05 Hz.
	Generator Rotor Angle	Within 180°
	Lowest Voltage	0.96 pu
C	Spinning Reserve	1220 MW
	Loss of Generation	3100 MW
	System stable	No
	Out-of-Step	Yes, at 3.1270 seconds

Scenario A - System Frequency During Loss of 500kV Southern Gen Substation

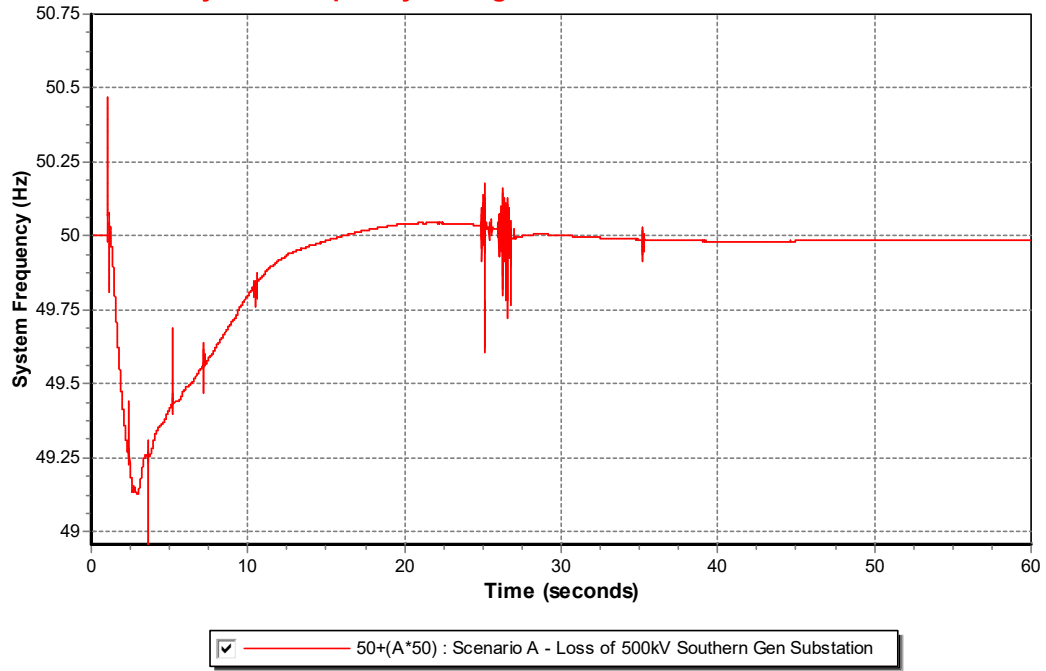


Figure 4.52. Scenario A – System Frequency during Loss of 500 kV Southern Generator Substation.

Scenario B - System Frequency During Loss of 500kV Southern Gen Substation

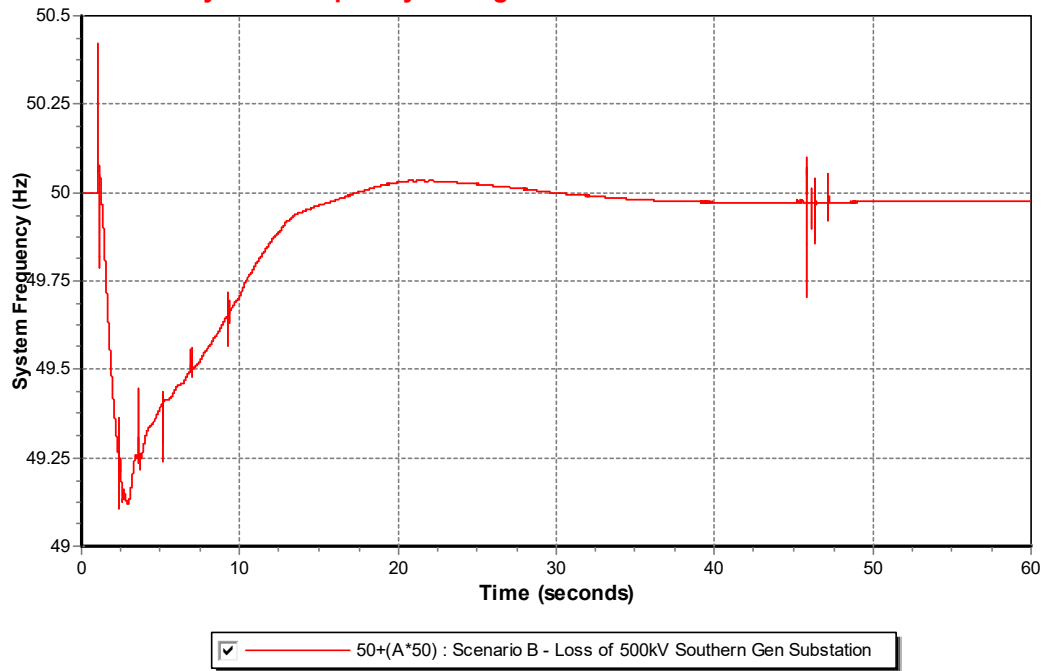


Figure 4.53. Scenario B – System Frequency during Loss of 500 kV Southern Generator Substation.

Scenario A - Rotor Angle During Loss of 500kV Southern Generator Substation

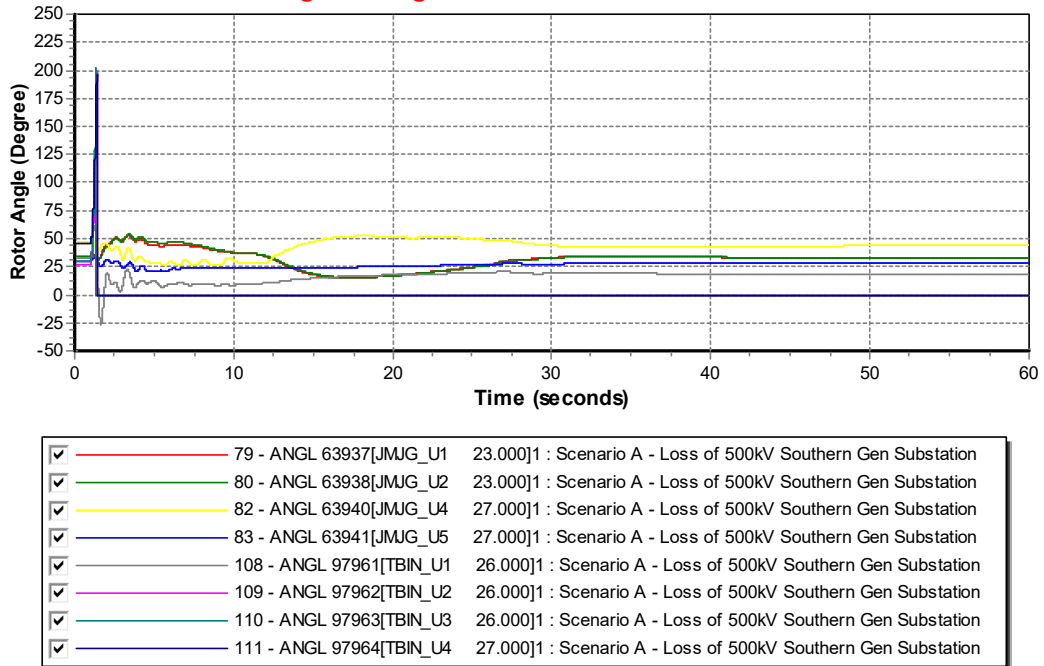


Figure 4.54. Scenario A – Rotor Angle during Loss of 500 kV Southern Generator Substation.

Scenario B - Rotor Angle During Loss of 500kV Southern Generator Substation

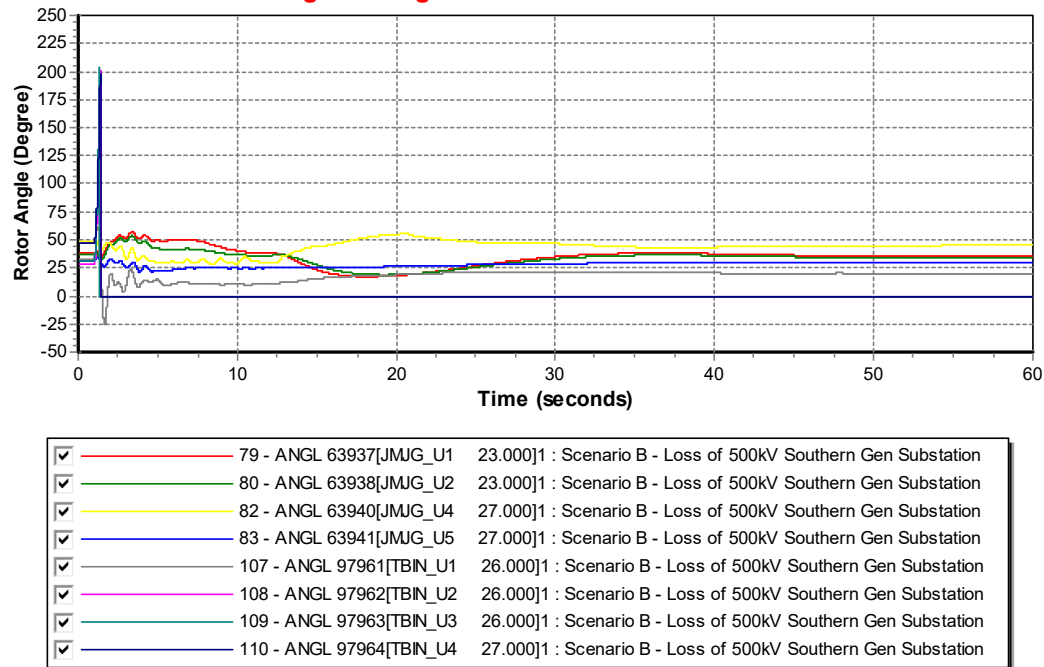
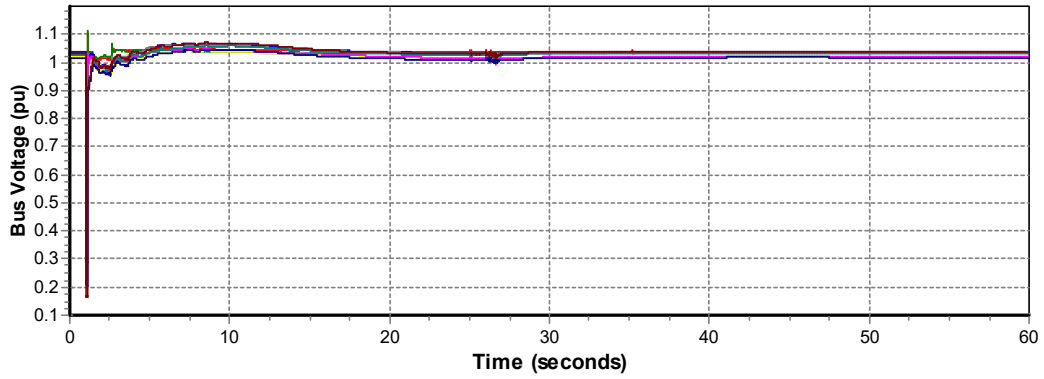


Figure 4.55. Scenario B – Rotor Angle during Loss of 500 kV Southern Generator Substation.

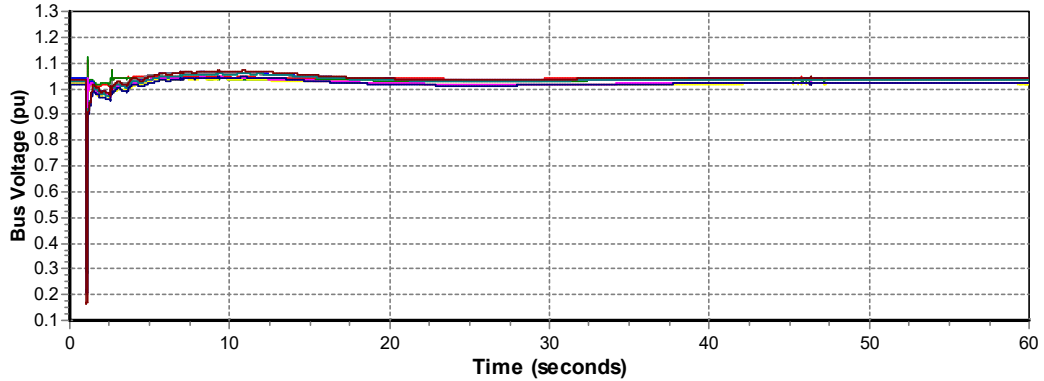
Scenario A - System Voltage During Loss of 500kV Southern Gen Substation



<input checked="" type="checkbox"/>	1063 - VOLT 61115 [BDNG132 132.00] : Scenario A - Loss of 500kV Southern Gen Substation
<input checked="" type="checkbox"/>	1064 - VOLT 61116 [GRNE132 132.00] : Scenario A - Loss of 500kV Southern Gen Substation
<input checked="" type="checkbox"/>	1065 - VOLT 88111 [KULN132 132.00] : Scenario A - Loss of 500kV Southern Gen Substation
<input checked="" type="checkbox"/>	1066 - VOLT 88117 [KULS132 132.00] : Scenario A - Loss of 500kV Southern Gen Substation
<input checked="" type="checkbox"/>	1067 - VOLT 88119 [PULU132 132.00] : Scenario A - Loss of 500kV Southern Gen Substation
<input checked="" type="checkbox"/>	1068 - VOLT 88124 [KULE132 132.00] : Scenario A - Loss of 500kV Southern Gen Substation
<input checked="" type="checkbox"/>	1069 - VOLT 97178 [CBRU132 132.00] : Scenario A - Loss of 500kV Southern Gen Substation
<input checked="" type="checkbox"/>	1070 - VOLT 97186 [TBRU132 132.00] : Scenario A - Loss of 500kV Southern Gen Substation
<input checked="" type="checkbox"/>	1071 - VOLT 97187 [GPTH132 132.00] : Scenario A - Loss of 500kV Southern Gen Substation

Figure 4.56. Scenario A – System Voltage during Loss of 500 kV Southern Generator Substation.

Scenario B - System Voltage During Loss of 500kV Southern Generator Substation



<input checked="" type="checkbox"/>	1054 - VOLT 61115 [BDNG132 132.00] : Scenario B - Loss of 500kV Southern Gen Substation
<input checked="" type="checkbox"/>	1055 - VOLT 61116 [GRNE132 132.00] : Scenario B - Loss of 500kV Southern Gen Substation
<input checked="" type="checkbox"/>	1056 - VOLT 88111 [KULN132 132.00] : Scenario B - Loss of 500kV Southern Gen Substation
<input checked="" type="checkbox"/>	1057 - VOLT 88117 [KULS132 132.00] : Scenario B - Loss of 500kV Southern Gen Substation
<input checked="" type="checkbox"/>	1058 - VOLT 88119 [PULU132 132.00] : Scenario B - Loss of 500kV Southern Gen Substation
<input checked="" type="checkbox"/>	1059 - VOLT 88124 [KULE132 132.00] : Scenario B - Loss of 500kV Southern Gen Substation
<input checked="" type="checkbox"/>	1060 - VOLT 97178 [CBRU132 132.00] : Scenario B - Loss of 500kV Southern Gen Substation
<input checked="" type="checkbox"/>	1061 - VOLT 97186 [TBRU132 132.00] : Scenario B - Loss of 500kV Southern Gen Substation
<input checked="" type="checkbox"/>	1062 - VOLT 97187 [GPTH132 132.00] : Scenario B - Loss of 500kV Southern Gen Substation

Figure 4.57. Scenario B – System Voltage during Loss of 500 kV Southern Generator Substation.

Table 4.22. Scenario A, B & C - Impact of Losing 500 kV Perak Generator Substation.

Scenario	System Condition	
A	Spinning Reserve	1220 MW
	Loss of Generation	4100 MW
	System stable	Yes
	Lowest Frequency	48.70 Hz
	Load loss	Load shed 4838.17 MW started at 48.31 Hz.
	Generator Rotor Angle	Within 180°
	Lowest Voltage	0.94 pu
B	Spinning Reserve	1220 MW
	Loss of Generation	4100 MW
	System stable	No
	Out-of-Step	Yes, at 1.7290 second
C	Spinning Reserve	1220 MW
	Loss of Generation	4100 MW
	System stable	No
	Out-of-Step	Yes, at 1.6330 second

Scenario A - System Frequency During Loss of 500kV Perak Generator Substation

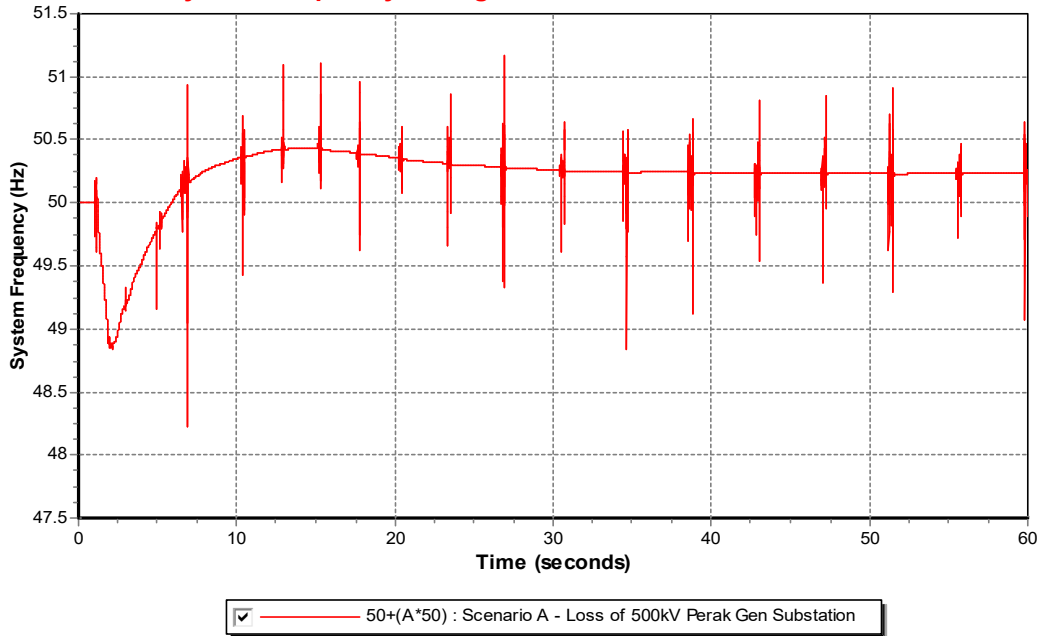


Figure 4.58. Scenario A – System Frequency during Loss of 500 kV Perak Generator Substation.

Scenario A - Rotor Angle During Loss of 500kV Perak Generator Substation

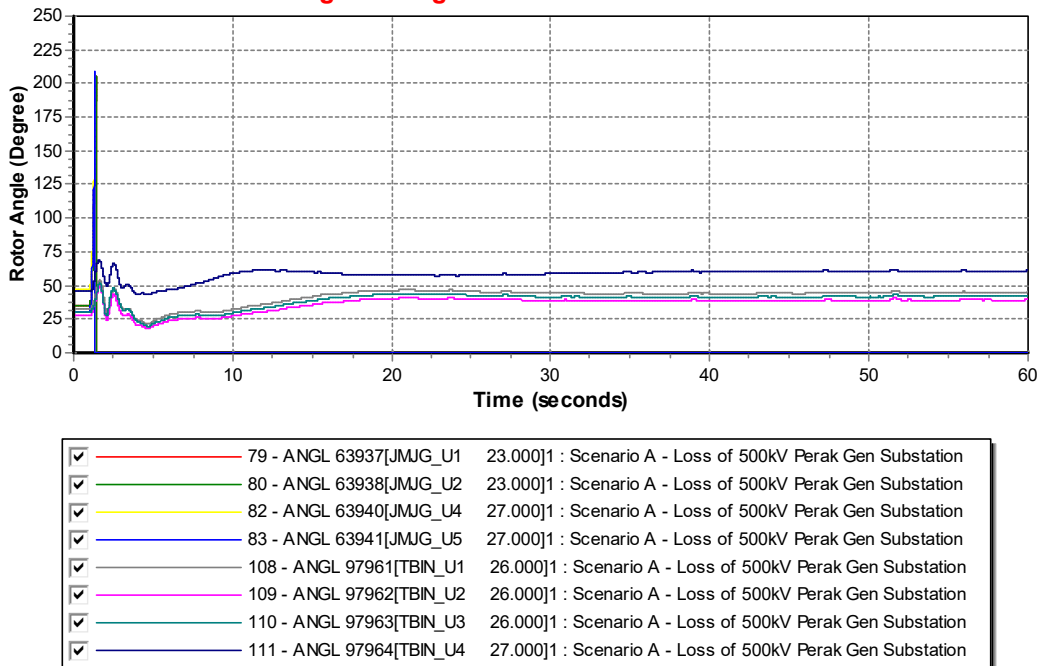


Figure 4.59. Scenario A – Rotor during Loss of 500 kV Perak Generator Substation.

Scenario A - System Voltage During Loss of 500kV Perak Generator Substation

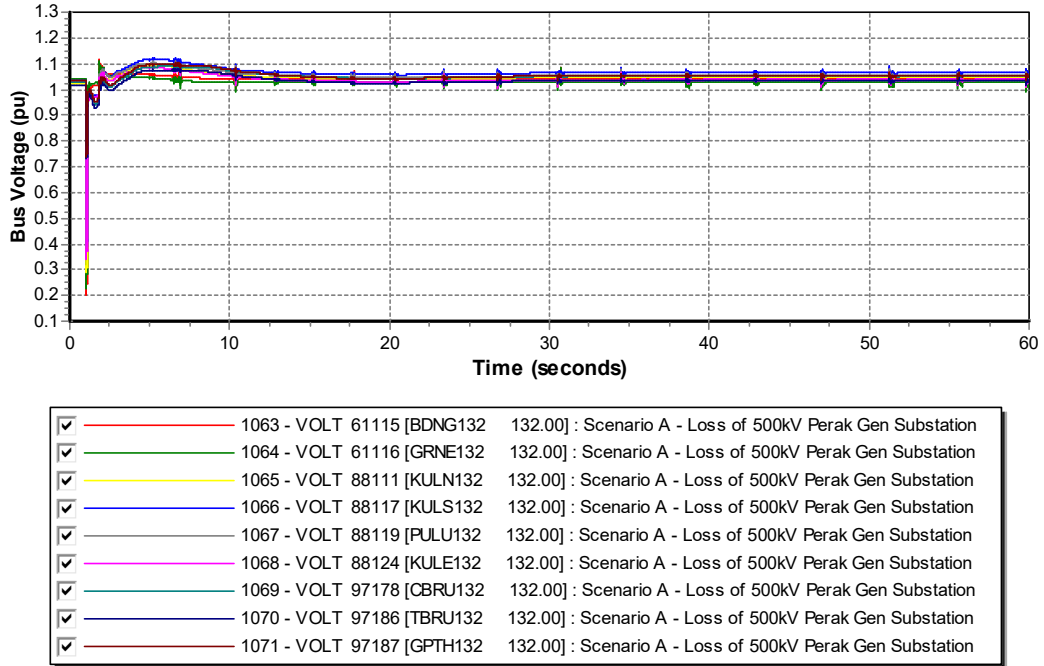


Figure 4.60. Scenario A – System Voltage during Loss of 500 kV Perak Generator Substation.

4.6 Discussion of Results

Table 4.23 and 4.24 summarized all the results on the steady state and dynamic stability study for Base Case, Scenarios A, B and C. The results in Table 4.23 and 4.24 were based on the criteria stated in the Transmission System Reliability Standards (TSRS). The scenario that complied with TSRS requirements would be selected as maximum solar penetration level that the grid system can take before it breached the system stability limit.

According to Table 4.23 and 4.24, Scenario B failed on the N-1 contingency in steady state study as well as Fault Clearing Time, Category B and Category D in dynamic stability study. Whereas, Scenario C failed on the fault level and N-1 contingency in steady state study, CFCT and Category B to D in dynamic stability study. Therefore, solar penetration level in Scenario B and C were not suitable to be implemented in the power system.

On the other hand, Scenario A passed for all the scopes in steady state and dynamic stability study, meaning that Scenario A managed to comply with the TSRS requirements. Therefore, 4525 MW solar generation that installed in Scenario A, which was equivalent to 22% solar penetration based on off-peak demand or 15% solar penetration based on system peak demand had been identified to be the maximum solar penetration level for generic Peninsular Malaysia network. Any solar installation that more than the 15% solar penetration based on peak demand is not advisable, as it will cause system unstable.

Table 4.23. Summary of Steady State Results for Base Case and Scenarios A, B and C.

	Steady State Power Flow Studies			
	Base Case	Scenario A	Scenario B	Scenario C
Steady State Voltage	Passed	Passed	Passed	Passed
Fault Level	Passed	Passed	Passed	Failed
No Contingency	Passed	Passed	Passed	Passed
N-1 Contingency	Passed	Passed	Failed	Failed

Table 4.24. Summary of Dynamic Results for Base Case and Scenarios A, B and C.

Category	Dynamic Studies			
	Base Case	Scenario A	Scenario B	Scenario C
CFCT	Passed	Passed	Failed	Failed
Category A	Passed	Passed	Passed	Passed
Category B	Passed	Passed	Failed	Failed
Category C	Passed	Passed	Passed	Failed
Category D	Passed	Passed	Failed	Failed

4.7 Summary of Chapter 4

In summary, Scenario A, which is 22% LSS penetration based on system off-peak demand, was determined to be the optimal LSS penetration level as the system manage to remain stable under all the contingencies during steady state and dynamic stability studies.

However, with more than 22% LSS penetration level, the system started to be unstable during system disturbances. When higher LSS penetration level is installed in the system, mitigation shall be taken to reinforce the system such as upgrading lines, building new lines, partially dispatch conventional generators or installing battery storage system, which will increase more generation cost to the power utility company. Thus, installing more than 22% LSS penetration level will be not optimal to the power utility to dispatch economic generation.

CHAPTER 5

CONCLUSION AND RECOMMENDATIONS FOR FUTURE WORK

5.1 Introduction

In general, installing the LSS power plants into the grid system will enhance the performance of the power system network. LSS plants that are connected at 132 kV buses could provide power directly to the load and thus reduce the active power transferred and release the capacity loading on the transmission lines. Following that, losses in transmission lines could be reduced and thus prolonging the lifetime of the transmission lines.

On the other hand, LSS power plants that behaved like the conventional plants in steady state by providing reactive power will help to improve the system voltage profile. The reduced usage of capacitor bank and reactors in the system could prolonged lifetime of the equipment. Overall, the installation of LSS power plants at 132 kV system will enhance the system steady state performance.

However, with more solar power plants in the system, the existing conventional power plants had to be turned-off. Conventional generation such as coal-fired thermal plants, combine cycle power plants and hydro plants which have rotating synchronous generator and contribute to the system rotational inertia with their stored kinetic energy had to shut down in order to fully dispatch the must-run solar power plants.

It is critically important to maintain the system frequency within an acceptable range to maintain stable power system. With the electro-mechanical coupling that are made available in the conventional plants, generator's rotating mass provides kinetic energy to the system to minimize the rate of change of system frequency when grid frequency deviates. Hence, the rotational inertia helps to increase additional response time for the governor to react to the faulted events to maintain grid frequency.

With less conventional generation and more inverter-connected solar power plants, rotational inertia in the grid system will become lower. This will have implication

on the dynamic frequency of the power system during faulted events. The rate of frequency change in a low rotational inertia system is too fast and lead to the situation where the governor control is too slow to respond, to support the grid frequency. Hence, if the issue is prolonged, it will lead to frequency and power system instability. Therefore, it is essential to identify the maximum solar penetration level in the system so that power system instability caused by excessive solar generation can be avoided.

In conclusion, the objective 1 had been addressed, where impact of increased LSS penetration level to the power system had been studied with steady state and dynamic simulation and discussed in detailed in Chapter 4. Besides, objective 2 in determining the optimal solar penetration level for generic electrical grid of Peninsular Malaysia was identified to be 22% based on system off-peak demand. Both objectives of the project had been achieved throughout the studies.

5.2 Significant Contribution of project

The main contribution of this project to the power utility was the design of a methodology that considers the overall process flow to conduct a successful study, with the main objective to determine the maximum solar penetration level in a power system. The calculation for the solar penetration level that is based on system peak demand and off-peak demand were used in the study. This shall be a reference for people to identify the penetration level easily with any available load data.

Various scenarios that represent different solar penetration level had been developed to assess the impact of different solar penetration level on the power system stability. Lastly, the benefit and impact of high solar penetration to the power system were studied and as the outcome of the study, maximum solar penetration level for generic Peninsular Malaysia network was determined.

5.3 Recommendation for Future Work

This study was based on the trough case with maximum solar generation output, which was the worst case for system with high solar penetration level. As the study was for one snapshot data, it was not possible to determine if overloading happened for different loads, different solar irradiations and generation scheduling patterns. Therefore, future enhancement can be done to verify the adequacy of the transmission system by conducting multiple snap-shot study at multiple load, multiple solar irradiation and generation scheduling patterns. One of the simulation methods that can be used for the study is the Quasi-dynamic simulations.

Another recommendation for future study is to include battery storage system into the study network. With battery storage installed together with the LSS power plants, the system inertia can be improved with the virtual inertia provided by the battery storage system. Hence, the frequency and power system stability can be improved. Thus, higher solar penetration level can be installed in the power system.

REFERENCES

- [1] K. K. Ajit, M. P. Selvan, and K. Rajapandiyan. (2017). Grid Stability Analysis for High Penetration Solar Photovoltaics. *Semantic Scholar*. [Online]. pp. 1-8. Available: <https://www.semanticscholar.org/paper/Grid-Stability-Analysis-for-High-Penetration-Solar-Kumar-Selvan/add09457912ab7537bc16db905f4f6b163cbd252>
- [2] O. H. Abdalla, R. Al-Badwawi, H. Al-Hadi, H. Al-Riyami, and A. Al-Nadabi, "Impact of a 200 MW concentrated receiver solar power plant on steady-state and transient performances of Oman transmission system," *2012 IEEE Int. Power Eng. Optim. Conf. PEOCO 2012 - Conf. Proc.*, no. June 2012, pp. 401–406, 2012.
- [3] K. Komoto, E. Cunow, C. Breyer, D. Faiman, K. Megherbi, and P. Van Der Vleuten, "IEA PVPS Task8: Study on very large scale photovoltaic (VLS-PV) systems," *Conf. Rec. IEEE Photovolt. Spec. Conf.*, pp. 1778–1782, 2012.
- [4] S. Azzam, E. Feilat, and A. Al-Salaymeh, "Impact of connecting renewable energy plants on the capacity and voltage stability of the national grid of Jordan," *2017 8th Int. Renew. Energy Congr. IREC 2017*, no. Irec, 2017.
- [5] EWEA, "Wind energy scenarios for 2030," *Ewea*, no. August, pp. 1–8, 2015.
- [6] W. Chen, "Solar PV: Policy, Market & Industry in Malaysia: Electricity Generation Mix," *4th International Sustainable Energy Summit (ISES)*, 2018.
- [7] J. von Appen, M. Braun, T. Stetz, K. Diwold, and D. Geibel, "Time in the Sun: The Challenge of High PV Penetration in the German Electric Grid," *IEEE Power Energy Mag.*, no. February, pp. 55–64, 2013.
- [8] A. Ulbig, T. S. Borsche, and G. Andersson, "Impact of low rotational inertia on power system stability and operation," *IFAC Proc. Vol.*, vol. 19, no. August 2014, pp. 7290–7297, 2014.
- [9] Y. T. Tan and D. S. Kirschen, "Impact on the power system of a large penetration of photovoltaic generation," *2007 IEEE Power Eng. Soc. Gen. Meet. PES*, pp. 1–8, 2007.
- [10] S. Eftekharnjad, V. Vittal, B. Keel, and J. Loehr, "Impact of increased penetration of photovoltaic generation on power systems," *IEEE Trans. Power Syst.*, vol. 28, no. 2, pp. 893–901, 2013.
- [11] A. S. Brouwer, M. Van Den Broek, A. Seebregts, and A. Faaij, "Impacts of large-

- scale Intermittent Renewable Energy Sources on electricity systems, and how these can be modeled,” *Renew. Sustain. Energy Rev.*, vol. 33, no. December 2017, pp. 443–466, 2014.
- [12] W. Yang, X. Zhou, and F. Xue, “Impacts of large scale and high voltage level photovoltaic penetration on the security and stability of power system,” *Asia-Pacific Power Energy Eng. Conf. APPEEC*, 2010.
- [13] J. H. R. Enslin, “Network impacts of high penetration of photovoltaic solar power systems,” *IEEE PES Gen. Meet.*, pp. 1–5, 2010.
- [14] J. Zhao, C. Wan, Z. Xu and J. Li, "Impacts of large-scale photovoltaic generation penetration on power system spinning reserve allocation," *2016 IEEE Power and Energy Society General Meeting (PESGM)*, Boston, MA, 2016, pp. 1-5.
- [15] H. Liu, L. Jin, D. Le and A. A. Chowdhury, "Impact of high penetration of solar photovoltaic generation on power system small signal stability," *2010 International Conference on Power System Technology*, Hangzhou, 2010, pp. 1-7.
- [16] D. Remon, A. M. Cantarellas, J. M. Mauricio and P. Rodriguez, "Power system stability analysis under increasing penetration of photovoltaic power plants with synchronous power controllers," in *IET Renewable Power Generation*, vol. 11, no. 6, pp. 733-741, 2017.
- [17] M. S. ElNozahy, and M. M. A. Salama. (2013). Technical Impacts of Grid-Connected Photovoltaic Systems on Electrical Networks—A Review. *Journal of Renewable and Sustainable Energy*. [Online]. 5 (032702), pp. 1-11. Available: <https://aip.scitation.org/doi/10.1063/1.4808264>
- [18] A. Zahedi, “Maximizing solar PV energy penetration using energy storage technology,” *Renew. Sustain. Energy Rev.*, vol. 15, no. 1, pp. 866–870, 2011.
- [19] S. Achilles, S. Schramm, and J. Bebic, “Transmission system performance analysis for high-penetration photovoltaics,” *Renew. Energy Grid Integr. Tech. Perform. Requir.*, no. February, pp. 1–56, 2011.
- [20] K. Kawabe and K. Tanaka, “Impact of Dynamic Behavior of Photovoltaic Power Generation Systems on Short-Term Voltage Stability,” vol. 30, no. 6, pp. 1–9, 2015.
- [21] J. Bank, B. Mather, J. Keller, and M. Coddington, “High Penetration Photovoltaic Case Study Report,” Rep. Nrel/Tp-5500-54742, Jan. 2013.
- [22] A. Cabrera-Tobar and O. Gomis-Bellmunt, "Dynamic study of a photovoltaic power plant interconnected with the grid," *2016 IEEE PES Innovative Smart Grid*

- Technologies Conference Europe (ISGT-Europe)*, Ljubljana, 2016, pp. 1-6.
- [23] A. Cabrera-Tobar, E. Bullich-Massagué, M. Aragüés-Peñalba, and O. Gomis-Bellmunt, "Capability curve analysis of photovoltaic generation systems," *Sol. Energy*, vol. 140, pp. 255–264, 2016.
- [24] L. Ma, H. Liao, J. Li, X. Yang, and K. Tschegodajew, "Analysis of Chinese photovoltaic generation system low voltage ride through characters," *IEEE 7th Int. Power Electron. Motion Control Conf.*, pp. 1178–1182, 2012.
- [25] S. Eftekharnejad, G. T. Heydt, and V. Vittal, "Optimal Generation Dispatch With High Penetration of Photovoltaic Generation," *IEEE Trans. Sustain. Energy*, vol. 6, no. 3, pp. 1013–1020, 2015.
- [26] *Transmission System Reliability Standards*, Tenaga Nasional Berhad, Malaysia, 2006.
- [27] *Grid Code for Peninsular Malaysia*, Code/ST/No. K0002/2016, 2016.
- [28] *PSS® E 32.0 Volume I Program Application Guide*, Siemens Power Technologies International, vol. I, June, 2009.
- [29] *PSS® E 32.0 Volume II Program Application Guide*, Siemens Power Technologies International, vol. II, October, 2010.
- [30] B. Belcher, B. J. Petry, T. Davis and K. Hatipoglu, "The effects of major solar integration on a 21-Bus system: Technology review and PSAT simulations," *SoutheastCon 2017*, Charlotte, NC, 2017, pp. 1-8.
- [31] N. Dhlamini and S. P. Daniel Chowdhury, "Solar Photovoltaic Generation and its Integration Impact on the Existing Power Grid," *2018 IEEE PES/IAS PowerAfrica*, Cape Town, 2018, pp. 710-715.
- [32] A. Guwaeder, H. Sarhan and I. Aldaouab, "A study of the penetration of photovoltaic generation into the Libyan power system," *2017 International Energy and Sustainability Conference (IESC)*, Farmingdale, NY, 2017, pp. 1-5.
- [33] S. RajaMohamed, P. A. Jeyanthi and D. Devaraj, "Novel control of grid-tied solar PV for enhancing transient stability limit at zero and high penetration levels," *2017 International Conference on Intelligent Computing, Instrumentation and Control Technologies (ICICT)*, Kannur, 2017, pp. 132-137.
- [34] J. H. R. Enslin, "Network impacts of high penetration of photovoltaic solar power systems," *IEEE PES General Meeting*, Providence, RI, 2010, pp. 1-5.
- [35] J. Bank, B. Mather, J. Keller, and M. Coddington, "High Penetration Photovoltaic Case Study Report High Penetration Photovoltaic Case Study Report," National

- Renewable Energy Laboratory, New York, Tech. Rep. NREL/TP-5500-54742, Jan. 2013.
- [36] J. Bebic, "Power System Planning: Emerging Practices Suitable for Evaluating the Impact of High-Penetration Photovoltaics," National Renewable Energy Laboratory, New York, Tech. Rep. NREL/SR-581-42297, Feb. 2008.
- [37] D. McPhail, B. Croker and B. Harvey, "A study of solar PV saturation limits for representative low voltage networks," *2016 Australasian Universities Power Engineering Conference (AUPEC)*, Brisbane, QLD, 2016, pp. 1-6.
- [38] A. Anzalchi, A. Sundararajan, A. Moghadasi and A. Sarwat, "Power quality and voltage profile analyses of high penetration grid-tied photovoltaics: A case study," *2017 IEEE Industry Applications Society Annual Meeting*, Cincinnati, OH, 2017, pp. 1-8.
- [39] A. Anzalchi, M. M. Pour and A. Sarwat, "A combinatorial approach for addressing intermittency and providing inertial response in a grid-connected photovoltaic system," *2016 IEEE Power and Energy Society General Meeting (PESGM)*, Boston, MA, 2016, pp. 1-5.
- [40] A. I. Sarwat, A. Sundararajan, I. Parvez, M. Moghaddami, A. Moghadasi, "Toward a Smart City of Interdependent Critical Infrastructure Networks," *Sustainable Interdependent Networks*, Springer, Berlin, Germany, 2018, pp. 21-45.
- [41] A. I. Sarwat, A. Sundararajan, I. Parvez, "Trends and Future Directions of Research for Smart Grid IoT Sensor Networks," *Sustainable Interdependent Networks*, Springer, Berlin, Germany, 2017, pp. 45-61.
- [42] D. S. Terzi, B. Arslan and S. Sagiroglu, "Smart grid security evaluation with a big data use case," *2018 IEEE 12th International Conference on Compatibility, Power Electronics and Power Engineering (CPE-POWERENG 2018)*, Doha, 2018, pp. 1-6.
- [43] S. V. Nandury and B. A. Begum, "Big data for smart grid operation in smart cities," *2017 International Conference on Wireless Communications, Signal Processing and Networking (WiSPNET)*, Chennai, 2017, pp. 1507-1511.
- [44] A. Bagheri, M. H. J. Bollen and I. Y. H. Gu, "Big data from smart grids," *2017 IEEE PES Innovative Smart Grid Technologies Conference Europe (ISGT-Europe)*, Torino, 2017, pp. 1-5.
- [45] K. Wang *et al.*, "A Survey on Energy Internet: Architecture, Approach, and Emerging Technologies," in *IEEE Systems Journal*, vol. 12, no. 3, pp. 2403-2416,

Sept. 2018.

- [46] W. Chin, W. Li and H. Chen, "Energy Big Data Security Threats in IoT-Based Smart Grid Communications," in *IEEE Communications Magazine*, vol. 55, no. 10, pp. 70-75, Oct. 2017.
- [47] R. Ma, H. Chen, Y. Huang and W. Meng, "Smart Grid Communication: Its Challenges and Opportunities," in *IEEE Transactions on Smart Grid*, vol. 4, no. 1, pp. 36-46, March 2013.
- [48] Z. Fan *et al.*, "Smart Grid Communications: Overview of Research Challenges, Solutions, and Standardization Activities," in *IEEE Communications Surveys & Tutorials*, vol. 15, no. 1, pp. 21-38, First Quarter 2013.
- [49] U. Ozgur, H. T. Nair, A. Sundararajan, K. Akkaya and A. I. Sarwat, "An efficient MQTT framework for control and protection of networked cyber-physical systems," *2017 IEEE Conference on Communications and Network Security (CNS)*, Las Vegas, NV, 2017, pp. 421-426.
- [50] A. Sundararajan, T. Khan, H. Aburub, A. I. Sarwat and S. Rahman, "A Tri-Modular Human-on-the-Loop Framework for Intelligent Smart Grid Cyber-Attack Visualization," *SoutheastCon 2018*, St. Petersburg, FL, 2018, pp. 1-8.
- [51] A. W. Miranda and S. Goldsmith, "Cyber-physical risk management for PV photovoltaic plants," *2017 International Carnahan Conference on Security Technology (ICCST)*, Madrid, 2017, pp. 1-8.
- [52] X. Liu, M. Shahidehpour, Y. Cao, L. Wu, W. Wei and X. Liu, "Microgrid Risk Analysis Considering the Impact of Cyber Attacks on Solar PV and ESS Control Systems," in *IEEE Transactions on Smart Grid*, vol. 8, no. 3, pp. 1330-1339, May 2017.
- [53] X. Zhong, I. Jayawardene, G. K. Venayagamoorthy and R. Brooks, "Denial of Service Attack on Tie-Line Bias Control in a Power System With PV Plant," in *IEEE Transactions on Emerging Topics in Computational Intelligence*, vol. 1, no. 5, pp. 375-390, Oct. 2017.
- [54] Coddington, Michael, Miller, Mackay, Katz, "Grid-Integrated Distributed Solar: Addressing Challenges for Operations and Planning, Greening the Grid," United States, <https://www.osti.gov/servlets/purl/1244310>, 2016.
- [55] B. Belcher, B. J. Petry, T. Davis and K. Hatipoglu, "The effects of major solar integration on a 21-Bus system: Technology review and PSAT simulations," *SoutheastCon 2017*, Charlotte, NC, 2017, pp. 1-8.

- [56] E. Mulenga, "Impacts of Integrating Solar PV Power to An Existing Grid Case Studies of Molndal and Orust Energy Distribution (10/0.4 kV and 130/10 kV) Grids," M.S. thesis, Department of Energy and Environment, Chalmers University of Technology, 2015.
- [57] O. Temitayo, A. Sundararajan, M. Moghaddami, and S. Arif. (2018, July). Future Challenges and Mitigation Methods for High Photovoltaic Penetration: A Survey. *Energies*. [Online]. *11(1782)*, pp. 1-20. Available: https://www.researchgate.net/publication/326242449_Future_Challenges_and_Mitigation_Methods_for_High_Photovoltaic_Penetration_A_Survey
- [58] N. Dhlamini and S. P. Daniel Chowdhury, "Solar Photovoltaic Generation and its Integration Impact on the Existing Power Grid," *2018 IEEE PES/IAS PowerAfrica*, Cape Town, 2018, pp. 710-715.
- [59] *Guidelines On Large Scale Solar Photovoltaic Plant For Connection To Electricity Networks*, GP/ST/No. 1/2016, 2016.

Appendix A: Dynamic Data for PVGU1 – Generator / Converter Module

Con Value	Con Description
0.02	TIQCmd, Converter time constant for IQcmd, second
0.02	TLpCmd, Converter time constant for IPcmd, second
0.40	VLVPL1 – Low Voltage Power Logic (LVPL), Voltage 1 (pu)
0.90	VLVPL2 – LVPL Voltage 2 (pu)
1.11	GLVPL – LVPL gain
1.20	High Voltage Reactive Current (HVRC) Logic, Voltage (pu)
2.00	CURHVRCR – HVRC Logic, Current (pu)
2.00	Rlp_LVPL, Rate of active current change
0.02	T_LVPL, Voltage sensor for LVPL, second

Appendix B: Dynamic Data for PANELU1 – Mechanical Module

Con Value	Con Description
0.16	P200, PDCmax at 200 W/m ² , pu
0.38	P400, PDCmax at 400 W/m ² , pu
0.59	P600, PDCmax at 600 W/m ² , pu
0.85	P800, PDCmax at 800 W/m ² , pu
1.00	P1000, PDCmax at 1000 W/m ² , pu

Appendix C: Dynamic Data for PVEU1 – Electrical Control Module

Con Value	Con Description
0.15	Tfv – V-regulator filter
18.00	Kpv – V-regulator proportional gain
5.00	Kiv – V-regulator integrator gain
0.05	Kpp – T-regulator proportional gain
0.10	Kip – T-regulator integrator gain
0.00	Kf – Rate feedback gain
0.08	Tf – Rate feedback time constant
0.47	QMX – V-regulator max limit
-0.47	QMN – V-regulator min limit
1.10	IPMAX – Max active current limit
0.00	TRV – V-sensor
0.50	dPMX – Max limit in power PI controller (pu)
-0.50	dPMN – Min limit in power PI controller (pu)
0.05	T_POWER – Power filter time constant
0.10	KQi – MVAR/Volt gain
0.90	VMINCL
1.10	VMAXCL
120.00	KVi – Volt/MAR gain
0.05	Tv – Lag time constant in WindVar controller

0.05	T_p – Pelec filter in fast PF controller
1.70	I_{maxTD} – Converter current limit
1.11	I_{phl} – Hard active current limit
1.11	L_{qhl} – Hard active current limit
100	PMAX of PV plant

Appendix D: Dynamic Data for IRRADU1 – Pitch Module

Con Value	Con Description
60.00	T1, Time of the first data point, second
1000.00	I1, Irradiance at first data point, W/m ²
0.00	T2, Time of the second data point, second
0.00	I2, Irradiance at second data point, W/m ²
0.00	T3, Time of the third data point, second
0.00	I3, Irradiance at third data point, W/m ²
0.00	T4, Time of the fourth data point, second
0.00	I4, Irradiance at fourth data point, W/m ²
0.00	T5, Time of the fifth data point, second
0.00	I5, Irradiance at fifth data point, W/m ²
0.00	T6, Time of the sixth data point, second
0.00	I6, Irradiance at sixth data point, W/m ²
0.00	T7, Time of the seventh data point, second
0.00	I7, Irradiance at seventh data point, W/m ²
0.00	T8, Time of the eighth data point, second
0.00	I8, Irradiance at eighth data point, W/m ²
0.00	T9, Time of the ninth data point, second
0.00	I9, Irradiance at ninth data point, W/m ²
0.00	T10, Time of the tenth data point, second

0.00

I10, Irradiance at tenth data point, W/m²
